

JOSIP JURAJ STROSSMAYER UNIVERSITY OF OSIJEK
UNIVERSITY OF DUBROVNIK
RUĐER BOŠKOVIĆ INSTITUTE

UNIVERSITY POSTGRADUATE INTERDISCIPLINARY DOCTORAL
STUDY OF MOLECULAR BIOSCIENCES

Petar Ozretić

Functional Analysis of the 5' Untranslated Region
of the *PTCH1* Gene, Transcript Variant 1b

PhD THESIS

Zagreb, 2013

JOSIP JURAJ STROSSMAYER UNIVERSITY OF OSIJEK
UNIVERSITY OF DUBROVNIK
RUĐER BOŠKOVIĆ INSTITUTE

UNIVERSITY POSTGRADUATE INTERDISCIPLINARY DOCTORAL
STUDY OF MOLECULAR BIOSCIENCES

Petar Ozretić

Functional Analysis of the 5' Untranslated Region
of the *PTCH1* Gene, Transcript Variant 1b

PhD Thesis proposed to the University Council for Postgraduate
Interdisciplinary Doctoral Studies in order to achieve academic PhD Degree at
the University Postgraduate Interdisciplinary Doctoral Study of Molecular
biosciences - module bioinformatics

Zagreb, 2013

TEMELJNA DOKUMENTACIJSKA KARTICA

Sveučilište Josipa Jurja Strossmayera u Osijeku
Sveučilište u Dubrovniku
Institut Ruđer Bošković
Sveučilišni poslijediplomski interdisciplinarni
doktorski studij Molekularne bioznanosti

Doktorski rad

Znanstveno područje: Biomedicina i zdravstvo
Znanstveno polje: Temeljne medicinske znanosti

Funkcionalna analiza 5' netranslatirane regije transkripta 1b gena *PTCH1*

Petar Ozretić

Rad je izrađen u: Laboratoriju za nasljedni rak Zavoda za molekularnu medicinu Instituta Ruđer Bošković u Zagrebu, Hrvatska i Laboratoriju za transkripcijske mreže Centra za integrativnu biologiju Sveučilišta u Trentu, Trento, Italija

Mentori: Prof. dr. sc. *Sonja Levanat* i Prof. dr. sc. *Alberto Inga*

Kratki sažetak doktorskog rada:

Gen *PTCH1* jedan od glavnih članova signalnog puta Hedgehog-Gli. U 5' netranslatiranoj regiji (5' UTR) transkripta 1b gena *PTCH1*, pronađen je različiti broj CGG ponavljanja blizu mjesta inicijacije translacije. Kako je poznata općenita uloga 5' UTR u regulaciji translacije, ovim radom željeli smo detaljno istražiti sve regulatorne elemente prisutne u 5' UTR gena *PTCH1b*. Upotreba luciferaznih reporterskih konstrukta u testovima sa trajnim humanim staničnim linijama pokazala je da broj CGG ponavljanja nema značajniji utjecaj na izražaj reporterskog gena. Dužina 5' UTR pokazala se kao potencijalno značajan čimbenik u regulaciji izražaja gena *PTCH1* jer uzvodni otvoreni okviri čitanja prisutni samo u dužim 5' UTR mogu dovesti do smanjenja količine proteina Ptch1. Postojanje unutarnjeg mjesta vezanja ribosoma omogućava sintezu proteina Ptch1 i u uvjetima kada je generalna razina sinteze proteina snižena, kao npr. u stanjima snižene količine kisika (hipoksije). Sve to ukazuje na izuzetno kompleksnu i do sada neistraženu ulogu 5' UTR u regulaciji izražaja gena *PTCH1*.

Broj stranica: 120

Broj slika: 53

Broj tablica: 4

Broj literaturnih navoda: 201

Jezik izvornika: engleski

Ključne riječi: signalni put Hedgehog-Gli, gen *PTCH1*, 5' netranslatirana regija, CGG ponavljanja, uzvodni otvoreni okviri čitanja, unutarnje mjesto vezanja ribosoma

Datum obrane: 28. svibnja 2013.

Stručno povjerenstvo za obranu:

1. Prof. dr. sc. *Vera Cesar*, izvanredna profesorica
2. Prof. dr. sc. *Sonja Levanat*, znanstvena savjetnica u trajnom zvanju
3. Prof. dr. sc. *Alberto Inga*, izvanredni profesor
4. Prof. dr. sc. *Ljubica Glavaš Obrovac*, redovita profesorica
5. Dr. sc. *Vesna Musani*, znanstvena suradnica
6. Dr. sc. *Maja Herak Bosnar*, viša znanstvena suradnica (zamjena)

Rad je pohranjen u: Gradskoj i sveučilišnoj knjižnici Osijek, Europska avenija 24, Osijek; Sveučilištu Josipa Jurja Strossmayera u Osijeku, Trg sv. Trojstva 3, Osijek

BASIC DOCUMENTATION CARD

Josip Juraj Strossmayer University of Osijek
University of Dubrovnik
Ruđer Bošković Institute
University Postgraduate Interdisciplinary Doctoral Study of
Molecular biosciences

PhD thesis

Scientific Area: Biomedicine and Health
Scientific Field: Basic Medical Sciences

Functional Analysis of the 5' Untranslated Region of the *PTCH1* Gene, Transcript Variant 1b

Petar Ozretić

Thesis performed at: Laboratory for Hereditary Cancer, Division of Molecular Medicine, Ruđer Bošković Institute, Zagreb, Croatia and at Laboratory of Transcriptional Networks, Centre for Integrative Biology (CIBIO), University of Trento, Trento, Italy

Supervisors: Prof. *Sonja Levanat*, PhD and Prof. *Alberto Inga*, PhD

Short abstract:

PTCH1 gene is one of the main members of the Hedgehog-Gli signaling pathway. In the 5' untranslated region (5' UTR) of *PTCH1* transcript 1b, a CGG-repeat polymorphism was found close to the translation initiation site. Given the role of 5' UTRs in the regulation of translation, our aim was to thoroughly explore all the regulatory elements present in the 5' UTR of *PTCH1b*. Using luciferase reporter constructs in tests with human cell lines it was shown that the number of CGG repeats has no significant impact on reporter gene expression. The length of 5' UTR was shown to be potentially an important factor in the regulation of *PTCH1* expression, for the reason that upstream open reading frames present only in longer 5' UTRs may reduce the amount of Ptch1 protein. The existence of an internal ribosome entry site enables Ptch1 protein synthesis under conditions when the general level of protein synthesis is decreased, such as in low oxygen levels, i.e., hypoxia. All these results point to the exceptionally complex and so far unexplored role of 5' UTR in the regulation of *PTCH1* expression.

Number of pages: 120

Number of figures: 53

Number of tables: 4

Number of references: 201

Original in: English

Key words: Hedgehog-Gli signaling pathway, *PTCH1* gene, 5' untranslated region, CGG repeats, upstream open reading frames, internal ribosome entry site

Date of the thesis defense: May 28, 2013

Reviewers:

1. Prof. *Vera Cesar*, PhD
2. Prof. *Sonja Levanat*, PhD
3. Prof. *Alberto Inga*, PhD
4. Prof. *Ljubica Glavaš Obrovac*, PhD
5. *Vesna Musani*, PhD
6. *Maja Herak Bosnar*, PhD (substitute)

Thesis deposited in: City and University Library of Osijek, Europska avenija 24, Osijek; Josip Juraj Strossmayer University of Osijek, Trg sv. Trojstva 3, Osijek

This Thesis was performed in the Laboratory for Hereditary Cancer, Division of Molecular Medicine, Ruđer Bošković Institute, Zagreb, Croatia, and in the Laboratory of Transcriptional Networks, Centre for Integrative Biology (CIBIO), University of Trento, Trento, Italy, under the supervision of Prof. Sonja Levanat, PhD and Prof. Alberto Inga, PhD as a part of University Postgraduate Interdisciplinary Doctoral Study of Molecular biosciences.

This work was supported by the Croatian Ministry of Science, Education and Sport (grant number 098-0982464-2461), EACR Travel Fellowship, FEBS Collaborative Experimental Scholarships for Central & Eastern Europe, and Croatian Science Foundation's Fellowship for Doctoral Students (project number 03.01/214).

Acknowledgments

First of all, THE BIGGEST THANKS for all the support, help and stimulation go to both of my mentors: my boss Prof. Sonja Levanat and Prof. Alberto Inga!

I sincerely thank Alessandra Bisio for teaching me the most of the “Methods” chapter!

I heartily thank my precious colleagues from the Laboratory for Hereditary Cancer: Vesna Musani, Maja Sabol, Diana Car; and Mirela Levačić Cvok from the Ruđer Medikal Diagnostics!

For 10 (un)forgettable months in Trento, I thank all “permanent” and “temporary” members of the Laboratory of Transcriptional Networks: Yari Ciribilli, Sara Zaccara Dassi, Mattia Lion, Anna Estevan Barber, Rae... and Anissa!

In addition, I would like to thank all other colleagues from the Division of Molecular Medicine, from the Ruđer Bošković Institute, and from all other institutions, with whom I have been collaborating in the past years.

I would also like to acknowledge all the Committee members for their help and suggestions.

Finally, I need to thank the European Association for Cancer Research, the Federation of the Societies of Biochemistry and Molecular Biology, and the Croatian Science Foundation for providing me a financial support indispensable for my stay in Trento.

At the end, last but not least, I would like to thank my mom & dad, my brother, my friends... and all other “grieving” family members!

Abbreviations

60S	eukaryotic large ribosomal subunit
80S	mature eukaryotic ribosome
aa	amino acid
Amp ^R	ampicillin-resistance gene
ANOVA	ANalysis Of VAriance
AUG	adenine-uracil-guanine (start codon)
B2M	beta-2-microglobulin gene
BAG1	BCL2-associated athanogene
BCC	Basal Cell Carcinoma
Bcl2	apoptosis regulator Bcl-2 protein
BCL2	B-cell CLL/lymphoma 2 gene
BCNS	Basal Cell Nevus Syndrome
BEN	binding factor for early enhancer
BLAST	Basic Local Alignment Search Tool
bp	base pair
BRCA1	breast cancer 1, early onset gene
Brca1	breast cancer type 1 susceptibility protein
BRCA1a	BRCA1 trascript variant 1b
BRCA1b	BRCA1 trascript variant 1a
CAAC	cytosine-adenine-adenine-cytosine
cap	7-methylguanosine (m ⁷ G)
CDK1	cyclin-dependent kinase 1 protein
cDNA	complementary DNA
CGG	cytosine-guanine-guanine
c-Myc	v-myc myelocytomatosis viral oncogene homolog (avian)
Ct	cycle threshold
DHH	desert hedgehog gene
DLR	Dual-Luciferase Reporter Assay
DMEM	Dulbecco's Modified Eagle's Medium
DNA	deoxyribonucleic acid
dNTP	deoxyribonucleotide triphosphate
dsDNA	double-stranded DNA
<i>E. coli</i>	<i>Escherichia coli</i>
EDTA	ethylenediaminetetraacetic acid
eIF	eukaryotic initiation factor
EMCV	encephalomyocarditis virus
ETF	EGFR-specific transcription factor
FBS	Fetal Bovine Serum
FMR1	fragile X mental retardation 1 gene

<i>g</i>	gravity, centrifugal force
GAPDH	glyceraldehyde 3-phosphate dehydrogenase gene
GC	guanine-cytosine
GLI	GLI family zinc finger gene
Gli	zinc finger protein GLI
GTP	guanosine-5'-triphosphate
HBOC	Hereditary Breast and Ovarian Cancer
HCT116	human colon cancer cell line
HEK 293T	Human Embryonic Kidney 293 cells transformed with large T antigen from SV40 virus
Hh	hedgehog protein
Hh-Gli	Hedgehog-Gli signaling pathway
Hhip	Hedgehog interacting protein
HMG-CoA	3-hydroxy-3-methylglutaryl-coenzyme A
HNSCC	Head and Neck Squamous Cell Carcinoma
HuR	Hu antigen R protein
IHH	indian hedgehog gene
IRE	Iron Response Element
IRES	Internal Ribosome Entry Site
IRP	Iron-responsive element-binding protein
ITAF	IRES <i>Trans</i> -Acting Factor
JUN	jun proto-oncogene
LB	Luria-Bertani / lysogeny broth
LUC	firefly luciferase
<i>luc</i> ⁺	firefly luciferase cDNA
MB	medulloblastoma
MCF-7	human breast adenocarcinoma cell line
<i>Mcr</i> BC	methylation-dependent endonuclease
Met-tRNAi	initiator methionyl-transfer RNA
MFE	Minimum Free Energy
midiprep	plasmid midi-preparation method
miniprep	plasmid mini-preparation method
MPF	M-phase Promoting Factor
mRNA	messenger RNA
mTOR	mechanistic target of rapamycin (serine/threonine kinase)
Musashi1	Musashi homolog 1 protein
MYC	v-myc myelocytomatosis viral oncogene homolog (avian)
NBCCS	Nevoid Basal Cell Carcinoma Syndrome
NCBI	National Center for Biotechnology Information
ncRNA	non-coding RNA
NPC1	Niemann-Pick C1 protein
nt	nucleotide

ODC1	ornithine decarboxylase 1 gene
ORF	Open Reading Frame
p16	cyclin-dependent kinase inhibitor 2A
PABP	polyA-binding protein
PBS	Phosphate Buffered Saline buffer
PCR	Polymerase Chain Reaction
pGL3-P	pGL3-Promoter luciferase reporter vector
PLB	Passive Lysis Buffer
Ptch1	Protein patched homolog 1
PTCH1	patched 1 gene
PTCH1b	patched 1 gene, transcript variant 1b
PV	poliovirus
qPCR	Quantitative Real-Time Polymerase Chain Reaction
RBP	Ribosome Binding Protein
refSNP	reference Single Nucleotide Polymorphism
REN	<i>Renilla reniformis</i> luciferase
RLU	Relative Luciferase Unit
Rluc	<i>Renilla reniformis</i> luciferase cDNA
RNA	ribonucleic acid
RNase	ribonuclease
RND	resistance-nodulation-cell division family of prokaryotic permeases
RPMI	Roswell Park Memorial Institute medium
rRNA	ribosomal RNA
SCC	Squamous Cell Carcinoma
SD	standard deviation
SDM	site-directed mutagenesis
SHH	sonic hedgehog gene
Smo	Smoothened homolog protein
SSD	sterol-sensing domain
Stop	translation termination site
SuFu	Suppressor of fused homolog protein
SV40	Simian vacuolating virus 40
TAE	Tris-acetate-EDTA buffer
TGA	thymine-guanine-adenine (stop codone)
TIS	Translation Initiation Site
TSS	Transcription Start Site
uAUG	upstream AUG codon
UniProt	Universal Protein Resource
uORF	upstream Open Reading Frame
VEGF	vascular endothelial growth factor
ZF5	zinc finger protein 5 homolog

Table of Contents

1. Introduction	1
1.1. The Hedgehog-Gli Signaling Pathway.....	1
1.1.1. The Components of the Hedgehog-Gli Signaling Pathway and Mechanism of Action.....	1
1.1.2. Human <i>PTCHI</i> Gene and Ptch1 Protein.....	3
1.1.3. The Role of Ptch1 and Mechanisms of <i>PTCHI</i> Inactivation	6
1.1.4. A CGG-repeat Polymorphism in Five Prime Untranslated Region of <i>PTCHI</i> Transcript Variant 1b.....	7
1.2. The Five Prime Untranslated Regions of mRNA Molecules.....	8
1.2.1. A 7-methylguanosine Cap and Cap-dependent Initiation of Translation.....	8
1.2.2. Internal Ribosome Entry Sites and Cap-independent Initiation of Translation	11
1.2.3. The Elements of 5' UTRs Involved in the Regulation of Gene Expression	12
1.2.3.1. Secondary Structure	13
1.2.3.2. Upstream Open Reading Frames and Upstream AUG Codons	14
1.2.3.3. Length of 5' UTRs and Alternative 5' UTRs.....	15
1.2.3.4. <i>Trans</i> -acting Factors.....	16
1.2.4. The Role of 5' UTRs in Human Diseases	17
2. Aims	19
3. Materials and Methods	21
3.1. Materials.....	21
3.2. Methods.....	22
3.2.1. Construction of Monocistronic Luciferase Reporter Vectors	22
3.2.1.1. Polymerase Chain Reaction (PCR)	23
3.2.1.2. Digestion by Restriction Endonucleases.....	26
3.2.1.3. DNA Ligation	26
3.2.1.4. Transformation of DH5 α Competent <i>E. coli</i> Strain	27
3.2.1.5. Plasmid Preparations.....	27
3.2.2. Agarose Gel Electrophoresis.....	30
3.2.3. Site-directed Mutagenesis	30
3.2.4. DNA Sequencing by Sanger Method.....	33
3.2.5. Construction of Bicistronic Dual-luciferase Reporter Vectors	33
3.2.5.1. Precise Localization of Putative IRES Motif within the <i>PTCH1b</i> 5' UTR.....	36
3.2.5.2. Alternative Splicing of pRuF-based Plasmid mRNA	39
3.2.6. Transient Transfection of Human Cells	40
3.2.6.1. Transfection for Luciferase Assay	41

3.2.6.2. Transfection for RNA/DNA Extraction	42
3.2.6.3. Transfection for Hedgehog-Gli Signaling Pathway Activation	42
3.2.6.4. Treatment of Transfected Cells with Hypoxia and Rapamycin	43
3.2.7. Dual-Luciferase Reporter Assays	45
3.2.7.1. Dual-Luciferase Reporter Assay Protocol.....	46
3.2.7.2. Luciferase Assays Data Analysis	47
3.2.8. Total RNA and Genomic DNA Extraction	47
3.2.9. Quantification of Luciferase mRNA and <i>PTCH1b</i> 5' UTR Expression by Quantitative Real-Time PCR.....	49
3.2.9.1. First Strand cDNA Synthesis	50
3.2.9.2. Quantitative Real-Time Polymerase Chain Reaction (qPCR)	50
3.2.9.3. qPCR Data Analysis.....	53
3.2.10. <i>In Silico</i> Analysis of <i>PTCH1b</i> 5' UTR	54
3.2.11. Statistical Analysis	55
4. Results	56
4.1. Monocistronic Luciferase Reporter Vectors with Cloned <i>PTCH1b</i> 5' UTR	56
4.2. Impact of Different <i>PTCH1b</i> 5' UTR Size and CGG-repeat Number on Translation or Transcription of Luciferase Reporter Gene.....	58
4.2.1. Results of Dual-Luciferase Reporter Assay in HCT116 ^{p53+/+} Cell Line.....	58
4.2.2. Results of Firefly Luciferase mRNA Quantification in HCT116 ^{p53+/+} Cell Line	59
4.2.3. Results of Dual-Luciferase Reporter Assay in MCF-7 Cell Line	60
4.2.4. Results of Firefly Luciferase mRNA Quantification in MCF-7 Cell Line.....	61
4.2.5. Results of Dual-Luciferase Reporter Assay in HEK 293T Cell Line	62
4.2.6. Results of Firefly Luciferase mRNA Quantification in HEK 293T Cell Line.....	63
4.3. Upstream Open Reading Frames and Upstream AUG Codon in <i>PTCH1b</i> 5' UTR	64
4.3.1 Site-directed Mutagenesis of Two Upstream AUG Codons in pGL3-P PTCH1 300/7 Plasmid	65
4.4. Impact of Mutated pGL3-P PTCH1 300/7 Plasmid, 6 CGG Repeats and 372-nucleotide-long <i>PTCH1b</i> 5' UTR on Translation or Transcription of Luciferase Reporter Gene.....	66
4.4.1. Results of Dual-Luciferase Reporter Assay in MCF-7 Cell Line	66
4.4.2 Results of Firefly Luciferase mRNA Quantification in MCF-7 Cell Line.....	67
4.4.3. Results of Dual-Luciferase Reporter Assay in HEK 293T Cell Line	68
4.4.4. Results of Firefly Luciferase mRNA Quantification in HEK 293T Cell Line.....	69
4.5. Expression Patterns of 188- and 300-nucleotide-Long <i>PTCH1b</i> 5' UTRs in Cancer Cells under Basal and Endogenously Activated Hedgehog-Gli Signaling Pathway	70
4.6. Prediction of Secondary Structure of <i>PTCH1b</i> 5' UTR.....	71
4.6.1. Prediction of Secondary Structure of 188-nucleotide-long <i>PTCH1b</i> 5' UTR	71

4.6.2. Prediction of Secondary Structure of 300-nucleotide-long <i>PTCH1b</i> 5' UTR	72
4.7. Bicistronic Dual-luciferase Reporter Vectors with Cloned <i>PTCH1b</i> 5' UTR	73
4.8. Impact of Different <i>PTCH1b</i> 5' UTR Size and CGG-repeat Number on Cap-independent Translation of Firefly Luciferase Gene	74
4.8.1. Results of Dual-Luciferase Reporter Assay in MCF-7 Cell Line	74
4.8.2. Results of Dual-Luciferase Reporter Assay in HEK 293T Cell Line	75
4.9. Ruling-out the Presence of Cryptic Promoter within <i>PTCH1b</i> 5' UTR.....	76
4.9.1. Results of Firefly and <i>Renilla</i> Luciferase mRNA Quantification in MCF-7 Cell Line	76
4.9.2. Results of Firefly and <i>Renilla</i> Luciferase mRNA Quantification in HEK 293T Cell Line	77
4.10. Precise Localization of IRES Motif within <i>PTCH1b</i> 5' UTR.....	78
4.11. Impact of Putative <i>PTCH1b</i> IRES Motif on Cap-independent Translation of Firefly Luciferase Gene	79
4.11.1. Results of Dual-Luciferase Reporter Assay in MCF-7 Cell Line	79
4.11.2. Results of Dual-Luciferase Reporter Assay in HEK 293T Cell Line	80
4.12. Ruling-out the Presence of Cryptic Promoter within Putative <i>PTCH1b</i> IRES Motif	81
4.12.1. Results of Firefly and <i>Renilla</i> Luciferase mRNA Quantification in MCF-7 Cell Line	81
4.12.2. Results of Firefly and <i>Renilla</i> Luciferase mRNA Quantification in HEK 293T Cell Line ..	82
4.13. Ruling-out an Alternative Splicing of pRuF Bicistronic mRNAs with Different Cloned Fragments.....	83
4.14. Effects of Hypoxia and Rapamycin Treatment on Cap-independent Translation of Firefly Luciferase Gene	84
4.14.1. Results of Dual-Luciferase Reporter Assay in MCF-7 Cell Line after Treatment with Hypoxia and Rapamycin	84
4.14.2. Results of Dual-Luciferase Reporter Assay in HEK 293T Cell Line after Treatment with Hypoxia and Rapamycin.....	85
4.15. Evolutionary Conservation of <i>Cis</i> -regulatory Elements Found in 5' UTR of <i>PTCH1b</i> Gene.	86
5. Discussion	87
6. Conclusions	95
7. References	97
8. Summary	114
9. Sažetak	116
10. Biography	118

1. Introduction

1.1. The Hedgehog-Gli Signaling Pathway

The Hedgehog-Gli (Hh-Gli) signaling pathway is a highly conserved cellular mechanism for transducing the signals from the cell surface into the nucleus for stimulating expression of many genes that results in an appropriate physiological response to changes in the cellular environment (Fosset, 2013). Since the Hedgehog (Hh) was discovered in 1980 as a segment polarity gene in the fruit fly *Drosophila melanogaster* (Nusslein-Volhard and Wieschaus, 1980), a great interest has been focused on elucidating its role in embryonic development of many multicellular organisms, throughout the animal kingdom (Ingham and McMahon, 2001; Huangfu and Anderson, 2006). Other cellular processes associated with the pathway include cell proliferation and migration, stem/progenitor cell renewal, and tissue regeneration and repair (Beachy et al, 2004). Because of its important role in many developmental processes, several human syndromes, involving congenital malformations, are caused by genetic alterations of Hh-Gli pathway genes (Nieuwenhuis and Hui, 2005). In the last decades, the greatest interest of both scientific research and pharmaceutical industry, is on exploration of Hh-Gli pathway's connection with cancerogenesis of an increasing number of different tumor types (Gould and Missailidis, 2011; Kiesslich and Neureiter, 2012).

1.1.1. The Components of the Hedgehog-Gli Signaling Pathway and Mechanism of Action

Although many aspects of the *Drosophila* Hh-Gli pathway are conserved through the evolution (Ryan and Chiang, 2012), many mechanistic differences in vertebrates have emerged and our study is primarily focused on the structure and functioning of the Hh-Gli pathway in mammals, more precisely in humans.

The basic members of Hh-Gli signaling pathway (Figure 1) include the Hh family of three ligands coded by Sonic (*SHH*), Indian (*IHH*) and Desert (*DHH*) Hedgehog genes (Bürglin, 2008). Hedgehog proteins are secreted from different tissues at various developmental stages and all three trigger a signaling cascade in target cells by binding the Hh receptor Protein patched homolog 1 (Ptch1) (Marigo et al, 1996), which relieves its catalytic inhibition of the G-protein-coupled receptor-like signal transducer Smoothed homolog (Smo) (Ayers and Théron, 2010). De-repression of Smo triggers a cascade of downstream events in primary

cilia (Wilson and Stainier, 2010), which ends in the activation of glioma-associated oncogene family of zinc finger transcription factors Gli1, Gli2 and Gli3 (Lipinski et al, 2006), which initiate transcription of Hh-Gli target genes (Katoh and Katoh, 2009). Transcription is repressed by Suppressor of fused homolog (SuFu) protein which binds directly to the Gli transcription factors, thus affecting their nuclear entry and ability to transcribe DNA (Cheng and Yue, 2006). One of the Hh-Gli target gene is *GLI1* itself, which further amplifies the initial signal and thus acts as a positive feedback loop (Lai et al, 2004). Other Hh-Gli target genes code for Ptch1 and Hedgehog interacting protein (Hhip) (Bak et al, 2001) that can also bind Hh, mediating a negative feedback loop by limiting the quantity of available unbound ligand required for pathway activation (Lai et al, 2004; Ribes and Briscoe, 2009).

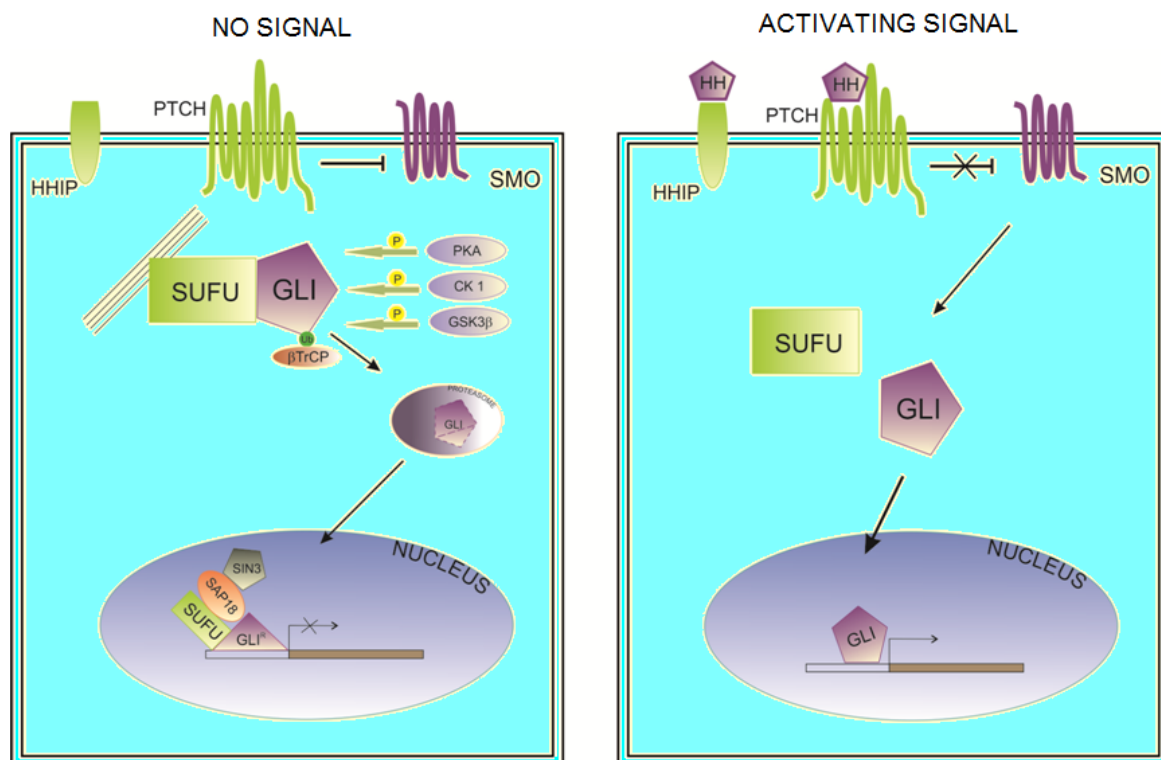


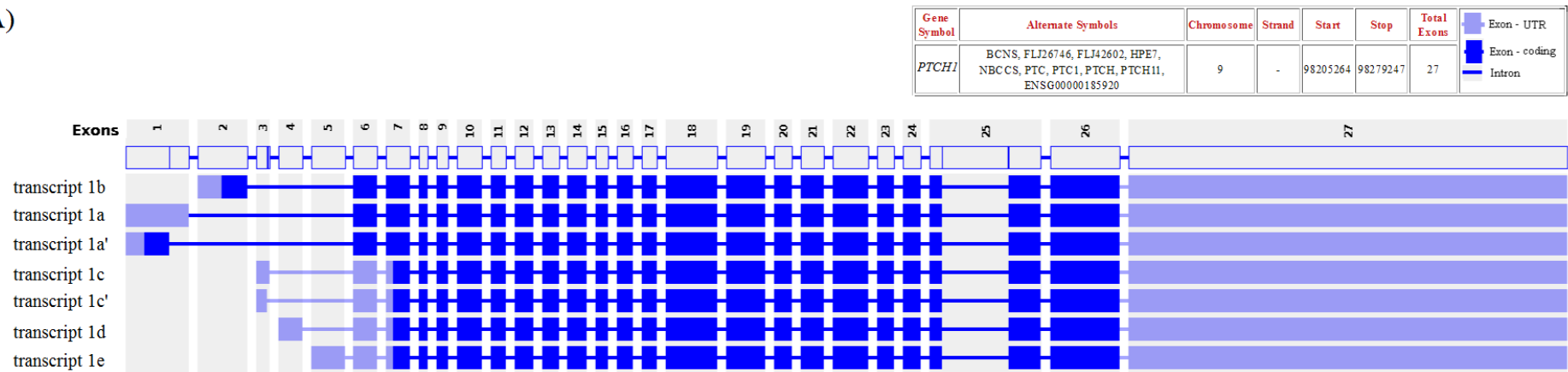
Figure 1. A schematic representation of Hedgehog-Gli signaling pathway in mammals. In the absence of Hh ligand, Ptch represses Smo and downstream signal transduction is blocked. SuFu sequesters Gli to the cytoplasm and inhibits Gli-mediated transcription by recruiting a histone deacetylase complex to Gli target genes (Cheng and Bishop, 2002). In the presence of Hh ligand, Hh binds to Ptch, which derepresses Smo and activates a signal transduction which leads to target gene expression. Hedgehog-interacting protein (Hhip) also binds Hh and regulates ligand availability. Only basic components of pathway are illustrated. (figure from: Car et al, 2010)

The outcome of activated Hh-Gli signaling depends on the signal-receiving cell type, but it can include overexpression of a variety of cell-specific transcription factors which mediate different developmental fate responses (McMahon et al, 2003): expression of D-type cyclins results in cell proliferation (Duman-Scheel et al, 2002); expression of anti-apoptotic proteins such as B-cell lymphoma 2 (Bcl2) mediates cell survival (Bigelow et al, 2003); production of vascular endothelial growth factor (VEGF) and angiopoietins regulate angiogenesis (Pola et al, 2001), and transcription of Snail family of zinc-finger transcription factors initiates the epithelial-to-mesenchymal transition in metastasis (Talbot et al, 2012). In consequence, it is not surprising that deregulation of Hh-Gli signaling leads to a variety of cancers (Scales and de Sauvage, 2009).

1.1.2. Human *PTCH1* Gene and Ptc1 Protein

Human *PTCH1* gene (MIM 601309) is located on chromosome 9q22.32 and spans around 74 kilobases (NCBI RefSeqGene ID NG_007664.1) (Hahn et al, 1996). There exist at least 7 major *PTCH1* transcript variants: 1a, 1a', 1b, 1c, 1c', 1d, and 1e. Each variant has 24 exons, of which 23 are coding and the first exon is specific for each variant (Kogerman et al, 2002; Shimokawa et al, 2004; Shimokawa et al, 2007) (Figure 2A). Since transcripts differ in the first exon, their protein products have different N-terminal region. These 7 transcripts code for 4 different Ptc1 protein isoforms: isoform L (coded by transcript 1b, has 1,447 amino acids and weight of 161 kDa), isoform L' (transcript 1a', 1,446 aa, 161 kDa), isoform M (transcript 1a, 1,381 aa, 154 kDa), and isoform S (transcripts 1c, 1c', 1d, and 1e, 1,296 aa, 144 kDa) (Figure 2B). Functional analyses have revealed that *PTCH1* alternative first exons affect protein isoform stability, expression pattern, as well as their capacity to inhibit Hh-Gli1 signaling pathway (Kogerman et al, 2002; Nagao et al, 2005b; Shimokawa et al, 2004; Shimokawa et al, 2007). Transcript 1b and transcript 1c harbor in their promoter one active Gli-consensus binding site, which upon Hh stimulation affects their specific expression (Agren et al, 2004). Transcript 1b and its protein product are considered as the “canonical” forms, since the isoform L is the largest form of Ptc1 protein, with the highest repressing activity on Smo. Furthermore, the expression of the exon 1b is specifically induced in nodular basal cell carcinoma (BCC) (Kogerman et al, 2002; Suzuki et al, 2012). It was recently discovered that except alternative first exon there exists alternative exon 12b, which is expressed in heart and brain tissue (Nagao et al, 2005a; Uchikawa et al, 2006).

A)



B)

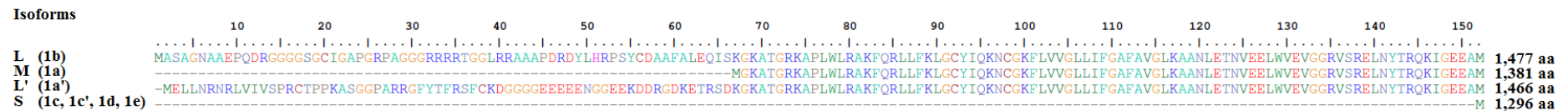


Figure 2. Transcript variants of human *PTCH1* gene (NCBI RefSeqGene ID NG_007664.1). **A)** There are 7 major transcript variants consisted of 23 coding exons and each variant has alternative first exon. **B)** Seven *PTCH1* transcript variants code for 4 different Ptch1 protein isoforms which differ in first 151 amino acid residues in the N-terminal region. Transcript variant 1b and protein isoform L are considered as the “canonical” forms of *PTCH1* gene and Ptch1 protein.

Ptch1 protein is a cell membrane receptor, predicted to have 12 transmembrane domains, 2 big extracellular loops where Hh ligand binding occurs, and a large intracellular loops (Figure 3) (Marigo et al, 1996). Part of the Ptch1 protein from amino acid residue 438 to 598 shows high similarity to the sterol-sensing domain (SSD) of Niemann-Pick disease protein C1 (NPC1) and HMG-CoA reductase, which play a role in cholesterol homeostasis and in intracellular trafficking (Loftus et al, 1997; Incardona and Eaton, 2000). It is therefore assumed that with this domain Ptch1 interacts with cholesterol molecule attached to the Hh (Ingham, 2000; Martin et al, 2001). Structurally, Ptch1 is also similar to the resistance-nodulation-cell division (RND) family of prokaryotic permeases that transport small molecules across membranes (Ryan and Chiang, 2012). It has been therefore proposed that Ptch1 can function as a transporter of a small molecule which can act as Smo agonist or antagonist (Taipale et al, 2002). Several candidates for this small molecule have been proposed, such as oxysterols (Corcoran and Scott, 2006) and provitamin D3 (Bijlsma et al, 2006). It has been demonstrated that addition of oxysterols causes Smo protein to move into the primary cilia and activate Shh signaling there (Rohatgi et al, 2009). Nevertheless, Ptch1 is not a typical transmembrane transporter since it lacks an ATP-binding domain (Goodrich et al, 1996; Levanat et al, 1998).

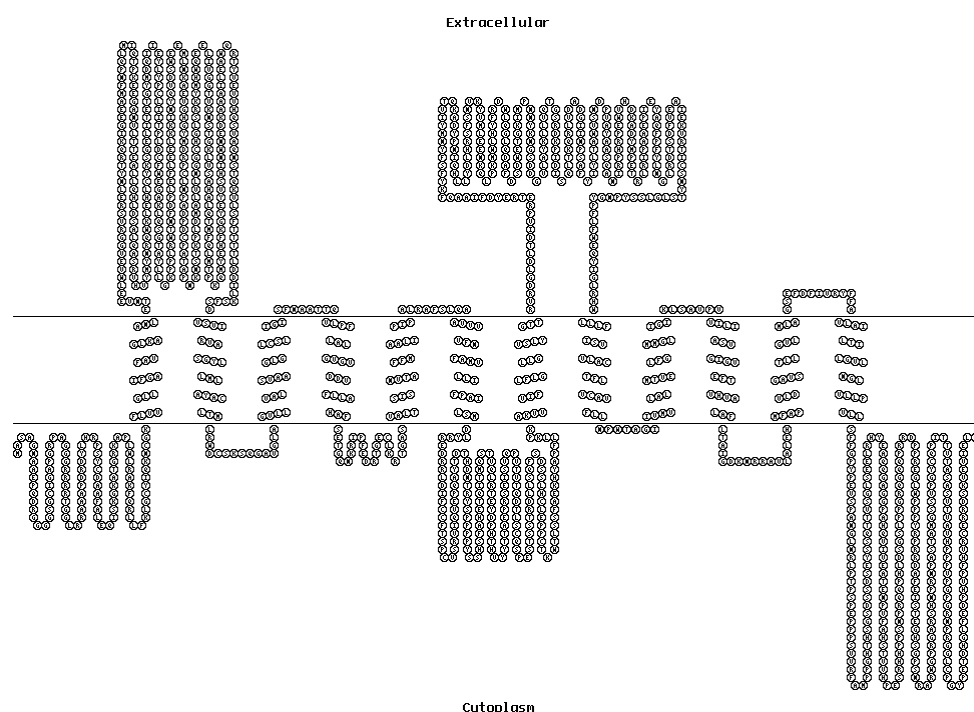


Figure 3. A snake-like diagram of human Ptch1 protein. According to the UniProt accession ID Q13635, the protein has 12 transmembrane domains and 2 big extracellular loops used for binding Hh ligand. The second to sixth transmembrane regions show high similarity to the sterol-sensing domain.

There are two Ptch homologues in vertebrates, Ptch1 and Ptch2 (Smyth et al, 1999; Zaphiropoulos et al, 1999), and they both bind Shh, Ihh and Dhh with similar affinity and form a complex with Smo (Carpenter et al, 1998). Ptch1 is primarily expressed in Shh-receiving mesenchymal cells, whereas Ptch2 is expressed in Shh-producing epithelial cells (Motoyama et al, 1998). Ptch1 is expressed in all major Shh target tissues, while Ptch2 distribution is detected almost exclusively in the skin and testis (Hahn et al, 1996; Motoyama et al, 1998). Knockout models of *PTCH1* and *PTCH2* have revealed that even though the proteins are similar (Ptch2 has 57% identity to Ptch1 and 90% identity to mouse Ptch2 (Carpenter et al, 1998; Kawamura et al, 2008), loss of *PTCH1* leads to embryonic lethality while loss of *PTCH2* only causes skin lesions and alopecia in male mice (Goodrich et al, 1997; Nieuwenhuis et al, 2006).

1.1.3. The Role of Ptch1 and Mechanisms of *PTCH1* Inactivation

Besides being a negative regulator of Hh-Gli signaling pathway, Ptch1 in interaction with Hh participate in the regulation of cell cycle in two ways (Fan and Khavari, 1999). In one way, Ptch1 without bound Hh can bind M-phase promoting factor (MPF), a complex consisted of cyclin B1 and cyclin-dependent kinase 1 (CDK1), and sequesters it to the cytoplasm, thus preventing progression into the M-phase of cell cycle. When Hh binds to Ptch1, it releases MPF and progression through cell cycle occurs (Barnes et al, 2001; Cross and Bury, 2004). Additionally, an active Hh-Gli pathway leads to the transcription of cyclin D and cyclin E, as well as promoting the progression through cell cycle (Duman-Scheel et al, 2002).

Gene *PTCH1* is suggested to be a tumor suppressor (Levanat et al, 1996), and inactivating germline mutations of *PTCH1* cause the Basal Cell Nevus Syndrome (BCNS) (MIM 109400) (Gorlin and Goltz, 1960; Farndon et al, 1992; Hahn et al, 1996). Other names for this syndrome are Nevoid Basal Cell Carcinoma Syndrome (NBCCS), multiple basal cell carcinoma syndrome, Gorlin syndrome, and Gorlin-Goltz syndrome. Gorlin syndrome, thanks to which the Hh-Gli pathway was discovered in mammals (Johnson et al, 1997), is an uncommon autosomal dominant inherited disorder, which is characterized by multiple skeletal, dental, ophthalmic, and neurological abnormalities, and predisposition for developing multiple basal cell carcinomas (BCC) (Kimonis et al, 1997). Mutations in *PTCH1* are also found in sporadic BCC, medulloblastoma (MB), rhabdomyosarcoma, rhabdomyoma, meningioma, esophageal carcinoma, squamous cell carcinoma (SCC), trichoepithelioma and breast carcinoma (Scales and de Sauvage, 2009; Yang et al, 2010; Kar et al, 2012).

Polymorphisms in *PTCH1* can modulate the risk for developing certain tumor types, such as BCC (Strange et al, 2004), ovarian cancer (Musani et al, 2013), or breast cancer in combination with oral contraceptives usage (Chang-Claude et al, 2003). In addition to the genetic mechanisms of *PTCH1* inactivation, the epigenetic mechanisms of *PTCH1* silencing, primarily by promoter hypermethylation, are also known (reviewed in Car et al, 2010). Recent studies have determined the *PTCH1* promoter hypermethylation in dermoid and ovarian fibroma (Cretnik et al, 2007), as well as breast cancer (Wolf et al, 2007).

1.1.4. A CGG-repeat Polymorphism in Five Prime Untranslated Region of *PTCH1* Transcript Variant 1b

The five prime untranslated region of transcript variant 1b (*PTCH1b* 5' UTR), the main transcript of *PTCH1* gene, is in two major nucleotide databases annotated with two different lengths. In the NCBI GenBank database (Benson, 2008) it is annotated as 188-nucleotide long (RefSeq ID NM_000264.3), while in the Ensembl (Flicek et al, 2011) it includes additional upstream 112 nucleotides (nts), giving the total length of 300 nucleotides (Transcript ID ENST00000331920.6). Agren and colleagues considered that *PTCH1b* 5' UTR is even longer and includes 372 nucleotides (Figure 10) (Agren et al, 2004).

In 2004, Nagao and colleagues have discovered a novel polymorphism involving a CGG repeat in the *PTCH1b* 5' UTR (Nagao et al, 2004). It was located 4 nucleotides upstream of the translation initiation site, i.e., main AUG codon. The major allele contained 7 repeats, while the minor contained 8 (refSNP ID rs71366293), and no difference in the distribution of either alleles or genotypes between patients with basal cell nevus syndrome and healthy controls was initially observed. Pastorino and colleagues revealed that a frequency of minor (CGG)₈ allele in Italian basal cell nevus syndrome patients was 18% (Pastorino et al, 2005). First association of certain repeat-number with a disease have been shown by Kawabata and colleagues, when they found a higher risk for developing ameloblastoma (rare, benign tumor of odontogenic epithelium) among the (CGG)₈ allele carriers (Kawabata et al, 2005). In 2010, in addition to the (CGG)₇ and (CGG)₈, alleles with 5 and 6 CGG repeats have been found among the patients who developed BCC after organ transplantation and healthy control population, but again with no difference in their distribution (Begnini et al, 2010). The latest allele found includes 3 CGG repeats and in addition to (CGG)₅, (CGG)₇ and (CGG)₈, it was found in both healthy controls and patients with head and neck squamous cell carcinoma (HNSCC). Surprisingly, in this research it was found that carriers of major (CGG)₇ allele,

within either heterozygous or homozygous genotype, bear a higher risk for HNSCC (Ghosh et al, 2011). In our laboratory, a genomic screening of *PTCH1b* gene in the patients with fibroma, dermoid, ovarian carcinoma and healthy control population has established that (CGG)₇ and (CGG)₈ alleles are shared among all 4 groups, while (CGG)₅ was found only in one control sample and (CGG)₆ in one ovarian cancer patient. Unfortunately, we couldn't establish any association between certain CGG-repeat number and ovarian neoplasms (Musani et al, 2013).

In spite of the absence of a direct association of *PTCH1b* 5' UTR CGG-repeat polymorphism with a disease, this polymorphism remains a very interesting topic for further research, especially in the potential context of triplet repeat disorders and mechanisms of their formation (Orr and Zoghbi, 2007).

1.2. The Five Prime Untranslated Regions of mRNA Molecules

The five prime untranslated region (5' UTR) is a part of mature messenger RNA molecule (mRNA) from the transcription start site (TSS) to the translation initiation site (TIS), i.e., main AUG codon (Mignone et al, 2002). It is transcribed from a DNA but it is not translated into a protein product and thus, it is considered as a non-coding RNA (ncRNA). One of the main role of 5' UTR is the post-transcriptional regulation of gene expression, starting from the initiation of protein translation to the tissue-specific, fine-tuned protein expression enabling developmental, physiological and pathological regulation (van der Velden and Thomas, 1999; Chamas and Sabban; 2002; Pickering and Willis; 2005). The 5' UTRs can differ in length, nucleotide content, secondary structures, and the presence of different functional elements, important for performing their role in gene expression regulation (Araujo et al, 2012; Barrett et al, 2012).

1.2.1. A 7-methylguanosine Cap and Cap-dependent Initiation of Translation

Protein synthesis is the final step in the flow of genetic information, the process in which the nucleotide sequence encoded in an mRNA molecule is translated into a protein product. It is divided into three consecutive stages – initiation, elongation, termination – and it is considered that the initiation is the rate-limiting, highly regulated step in eukaryotes (Sonenberg and Hinnebusch, 2009). The mechanism of eukaryotic protein synthesis initiation relies on a complex interplay involving recognition of an mRNA by specific subset of

eukaryotic initiation factors (eIFs) followed by recruitment of the ribosome subunits, recognition of the translation initiation codon and initiation of protein synthesis (Marintchev and Wagner, 2004).

The vast majority of eukaryotic mRNAs initiate translation by a mechanism that require a presence of the 7-methylguanosine structure (termed *m*⁷*G-cap* or merely *cap*), which is added to the 5'-end of most mRNAs shortly after the start of transcription (Figure 4A) (Banerjee, 1980; Mitchell et al, 2010). The 5' cap is recognized by cap-binding complex eIF4F that is composed of eIF4E (cap-binding protein), eIF4A (an RNA helicase) and eIF4G (a scaffolding protein). The eIF4G further interacts with eIF3 and the poly(A)-binding protein (PABP) that is bound to the poly(A)-tail of the mRNA, leading to the functional circularization and activation of the mRNA molecule. Binding of eIF4F leads to the recruitment of 43S pre-initiation complex that is composed of the 40S ribosomal subunit, eIF2, eIF3 and the initiator methionyl-transfer RNA (Met-tRNA_i). The 43S complex with assistance of eIF1 and eIF1A scans the mRNA in 5' to 3' direction until the first start codon (AUG) within an appropriate sequence context termed Kozak consensus sequence (GCC[A/G]CCAUGG; Kozak, 1987) is found, which leads to the formation of the 48S initiation complex. At this step eIF1 is released, eIF5 mediates the hydrolysis of eIF2-bound GTP and eIF5B mediates the joining of 60S ribosomal subunit with the 40S subunit into a mature, translationally capable 80S ribosome (Asano and Sachs, 2007).

This cap-dependent translation initiation mechanism is predominantly used by eukaryotic cellular mRNAs to recruit and position the ribosome, and is controlled by the availability and the phosphorylation status of different initiation factors (Jackson et al, 2010).

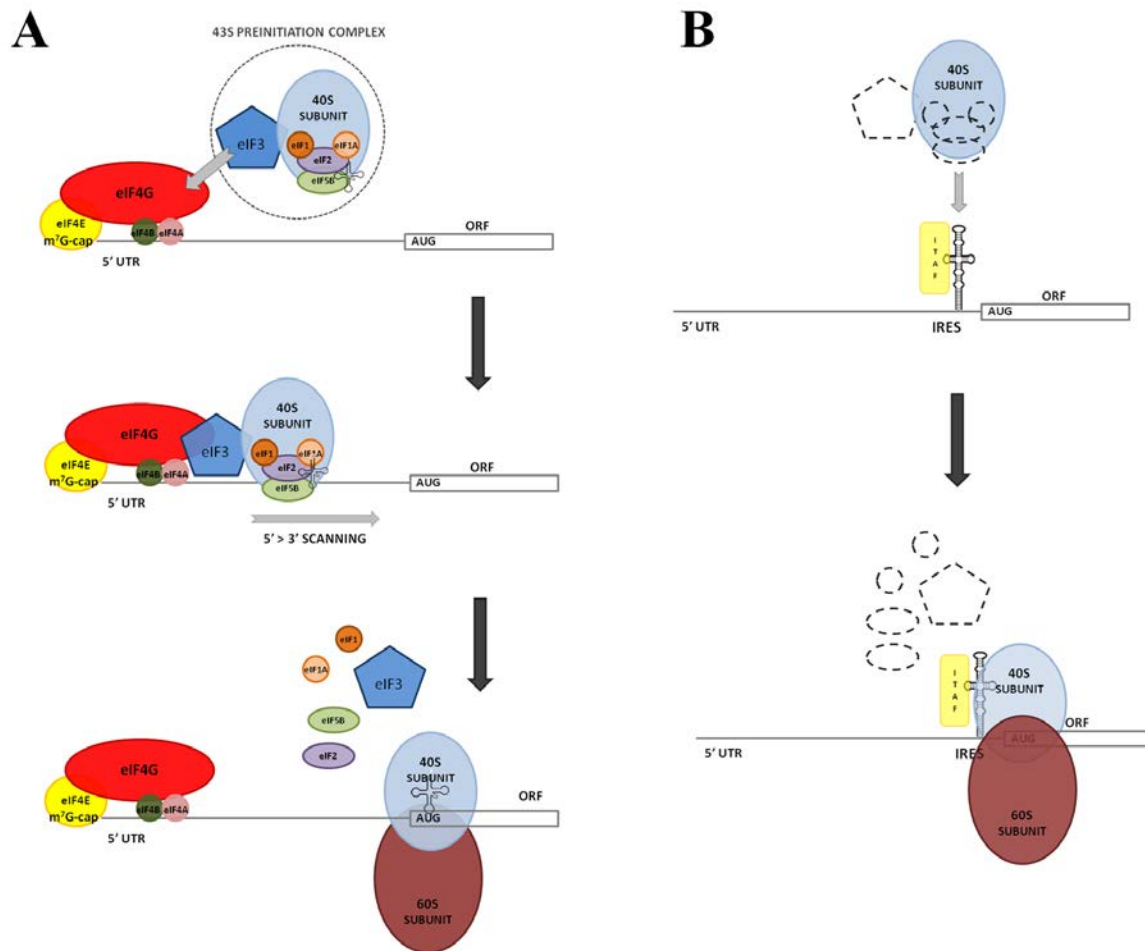


Figure 4. Similarities and differences between cap-dependent and cap-independent internal initiation of translation. **A)** Cap-dependent initiation mechanism requires an mRNA molecule with an m^7G -cap on its 5' end. A large number of proteins termed eukaryotic translation factors (eIFs) participate in the processes of recognition of the m^7G -cap operated by cap-binding complex eIF4F (composed of eIF4E, eIF4A and eIF4G), but also in the binding of mRNA to the ribosomes (eIF4B), recruitment of a 43S pre-initiation complex (composed of 40S ribosomal subunit, eIF1, eIF1A, eIF2, eIF3 and initiator methionyl-transfer RNA), 5' to 3' directional scanning of the 43S complex along mRNA 5' untranslated region, recognition of start codon (AUG) in appropriate context, and joining of the 60S ribosomal subunit with 40S subunit into the 80S ribosome ready to translate an open reading frame (ORF). **B)** In cap-independent initiation, the main difference is that an element within an mRNA molecule named *internal ribosome entry site* (IRES) recruits 40S ribosomal subunit directly or close to the translation start codon, independently of m^7G -cap and eIF4E. Molecular mechanisms behind cap-independent initiation depend on the presence of an IRES element and may or may not require canonical eIFs and/or auxiliary proteins named *IRES trans-acting factors* (ITAFs). (figure from: Ozretić et al, 2012)

1.2.2. Internal Ribosome Entry Sites and Cap-independent Initiation of Translation

Lack of oxygen (hypoxia), starvation and response to a DNA damage-inducing therapy represses cap-dependent translation and leads to reduced levels of overall protein synthesis (Sprigs et al, 2010). In parallel, inhibition of cap-dependent protein synthesis allows a subset of mRNAs to be translated in a cap-independent manner using mRNA elements termed *internal ribosomal entry sites* (IRESes), which are predominantly located in the 5' UTR (Hellen and Sarnow, 2001). As suggested by the name, a cap-independent initiation does not require an m⁷G-cap to recruit a ribosome to an mRNA (Figure 4B) (Merrick, 2004). According to this mechanism, an mRNA sequence itself has the ability to bind and activate the translational machinery. There are many different mechanisms by which IRESes can initiate translation – some of them require canonical eIFs while the others can engage auxiliary proteins not normally associated with translation (Martínez-Salas et al, 2012). These RNA-binding proteins named *IRES trans-acting factors* (ITAFs) are thought to help in proper folding of the IRES region facilitating the recruitment of the translation machinery onto the mRNA (King et al, 2010). The ability of an RNA molecule to function as IRES is entirely encoded in its primary sequence but it is also apparent that higher order secondary and three-dimensional structures are determinants of IRES activity (Plank and Kieft, 2012).

The cap-independent mechanism was first discovered in the 5' UTR of two picornaviruses – encephalomyocarditis virus (EMCV) and poliovirus (PV) (Jang et al, 1988; Pelletier and Sonenberg, 1988). Some picornaviruses can inhibit cap-dependent protein synthesis in infected host cells by virus-encoded proteases that are able to cleave eIF4G and PABP, the key components of cap-dependent translation initiation and its regulation (Willcocks et al, 2004; Kuyumcu-Martinez et al, 2004). In that way a virus can block host anti-viral response and successfully translate its own proteins (Thompson et al, 2012). The first IRES motif found within eukaryotic mRNA molecule (so-call cellular IRES) was found in the mRNA coding for the immunoglobulin heavy chain-binding protein (BiP). It was discovered owing to its persisting activity in poliovirus-infected cells although the translation of majority of host mRNAs was stopped (Sarnow, 1989). There are at least 68 viral and 115 cellular mRNAs reported to contain an IRES motif (Mokrejs et al, 2009), of which the most interesting for our research are the cellular IRESes found in cancer-related genes (Table 1) (reviewed in Ozretić et al, 2012).

Table 1. Some of the internal ribosome entry site (IRES) elements identified in viral and cellular RNAs, including their known *IRES trans-acting factors* (ITAFs). (table from Fitzgerald and Semler, 2009)

Virus family	Virus	Known ITAFs	Gene	Cellular conditions for translation	Known ITAFs			
DNA viruses								
Herpesvirus	Kaposi-sarcoma-associated herpesvirus (KSHV)		<i>Apaf-1</i>	Apoptosis	PTB, unr, DAP5			
			<i>XIAP</i>	Apoptosis	La, hnRNP C1/C2, DAP5			
Polyomavirus	Simian vacuolating virus 40 (SV40)		<i>c-myc</i>	Apoptosis, development, genotoxic stress, cell cycle	PCBP2, PCBP1, hnRNP C1/C2, hnRNP K			
			<i>DAP5</i>	Apoptosis	DAP5, IRP, unr, YB-1, GRSF-1, PSF, P54nrb			
Nimavirus	White spot syndrome virus (WSSV)		<i>Reaper</i>	Apoptosis, heat shock	DAP5			
			<i>Hsp70</i>	Apoptosis, heat shock				
RNA viruses								
Picornaviruses	Poliovirus (PV)	PTB, PCBP2, PCBP1, La, unr, SRp20	<i>Bcl-2</i>	Apoptosis				
			<i>HIAP2/c-IAP1</i>	Apoptosis, ER stress	DAP5			
			<i>Antennapedia</i>	Development				
			<i>Ultrabithorax</i>	Development				
			<i>ODC</i>	Cell cycle				
			<i>PITSLRE</i>	Cell cycle	unr			
			<i>hnRNP A1</i>	Cell cycle				
			<i>hnRNP A/B</i>	Cell cycle				
			<i>Hairless</i>	Cell cycle				
			<i>Notch2</i>	Cell cycle				
Potyviruses	Foot-and-mouth disease virus (FMDV)	PTB, ITAF45, La	<i>IGF-II</i>	Cell Cycle				
			<i>VEGF</i>	Hypoxia	PTB			
			<i>HIF-1α</i>	Hypoxia	PTB			
			<i>Cat-1</i>	ER stress, hypoxia				
			<i>BiP</i>	Heat shock	La, NSAP1			
			Flaviviruses	Hepatitis C virus (HCV)	PTB, PCBP2, La, hnRNP D, hnRNP L	<i>BAG-1</i>	Heat shock	
						<i>FGF-2</i>	Tissue/cell specific	hnRNP A1
				<i>FGF-1</i>	Tissue/cell specific			
				<i>Kv1.4</i>	Tissue/cell specific			
			Dicistroviruses	Cricket paralysis virus (CrPV)		<i>LEF-1</i>	Oncogenesis	
<i>Drosophila C virus (DCV)</i>								
<i>Plautia stali intestine virus (PSIV)</i>								
<i>Human T-cell lymphotropic virus 1 (HTLV-1)</i>								
Retroviruses	Moloney murine leukemia virus (MoMuLV)	PTB, La						
	Human immunodeficiency virus type 1 (HIV)	La						

1.2.3. The Elements of 5' UTRs Involved in the Regulation of Gene Expression

As previously mentioned, 5' UTRs contain many different *cis*-regulatory elements that can be used for changing the stability or translational efficiency of mRNAs, resulting in rapid alteration of protein expression in response to internal and external stimuli, without the need for new mRNA transcription (Maier et al, 2009; de Sousa Abreu et al, 2009). The main regulatory elements in 5' UTRs are secondary structures (including IRESes), upstream open reading frames and upstream AUG codons, as well as binding sites for RNA-binding proteins (Figure 5) (Huang et al, 2006; Grillo et al, 2010; Araujo et al, 2012; Barrett et al, 2012). The biological activity of 5' UTR regulatory elements relies on a combination of primary and secondary structure (Wan et al, 2011).

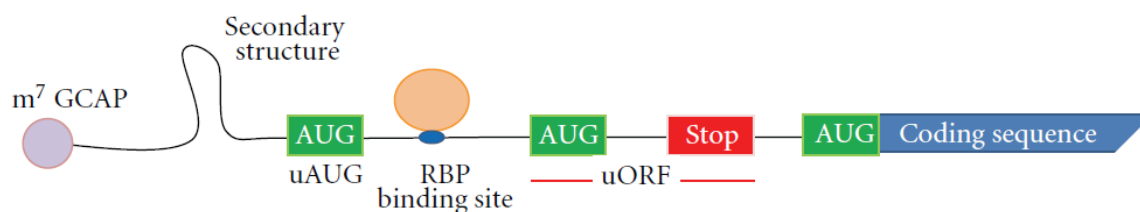


Figure 5. *Cis*-regulatory elements present in 5' UTR which participate in the initiation of protein translation and regulation of protein expression. m⁷GCAP, 7-methylguanosine cap; (u)AUG, (upstream) translation initiation site; RBP, ribosome binding protein; uORF, upstream open reading frame; Stop, translation termination site. (figure from: Araujo et al, 2012)

1.2.3.1. Secondary Structure

Secondary structure of an RNA molecule is defined by an intramolecular base-pairing between complementary and non-complementary base pairs (Holbrook, 2005). It is often computationally predicted by thermodynamic method, which assumes that a given RNA sequence will fold into the structure with the minimum free energy (MFE), and thus the most stable one (Mathews and Turner, 2006). Longer 5' UTRs, with higher GC-content are expected to be highly structured, and consequently repress cap-dependent translation by inhibiting binding or scanning of the translational machinery (Hall et al, 1982; Kozak, 1991). A hairpin structure (Figure 6) with a free energy of -30 kcal/mol situated close to the cap would be sufficient to block the access of the pre-initiation complex to the mRNA (Vega Laso et al, 1993). When located further away in the 5' UTR, hairpins require an MFE lower than -50 kcal/mol to be able to block translation (Gray and Hentze, 1994; Pickering and Willis, 2005). Stable secondary structures can resist the unwinding activity of the helicase eIF4A, which can be partially overcome by the overexpression of eIF4A, aided by eIF4B, and eIF4E (Rozen et al, 1994; Koromilas et al, 1992). It has been determined that secondary structures are particularly prevalent among the mRNAs coding for transcription factors, proto-oncogenes, growth factors and their receptors; or generally for proteins poorly translated under normal conditions (Kozak, 1991; Davuluri et al, 2000; Pesole et al; 2001).

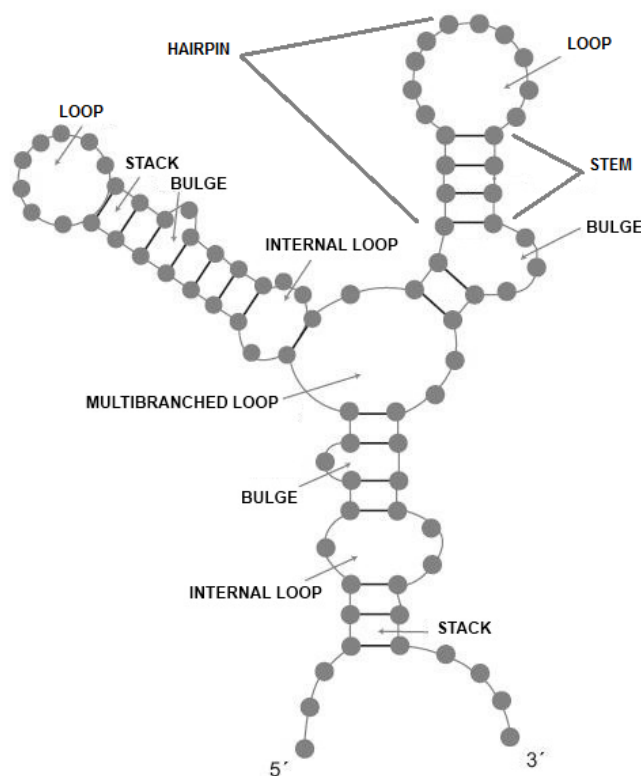


Figure 6. The elements of RNA secondary structure defined as intramolecular base pairing. Each loop has at least one base pair. A stem consists of two or more consecutive stacks. An mRNA molecule with more base pairs is considered to be more stable with lower minimum free energy (MFE). (figure from: Ozretić et al, 2010)

1.2.3.2. Upstream Open Reading Frames and Upstream AUG Codons

Upstream open reading frames (uORFs) and upstream AUG codons (uAUGs) are considered as major regulatory elements in the 5' UTRs (Araujo et al, 2012). As their names suggest, uORFs are sequences defined by a start and stop codons upstream of the main coding region, while uAUGs are start codons without an in-frame downstream stop codon located upstream of the main coding region (Figure 7). Both uORFs and uAUGs are extremely heterogeneous in their position in relation to the cap and main AUG, number per transcript and, in the case of uORFs, length (Morris and Geballe, 2000). Functional uORFs of lengths ranging from 3 (Zhang and Dietrich, 2005) to 86 residues (Oyama et al, 2006) have been described, whereas the average length in humans is 17 residues (Iacono et al, 2005). The uORFs are present in nearly 50% of human 5' UTRs and on average their presence reduces mRNA expression by 30% and reduces protein level by 30-80% (Calvo et al, 2009). Even short reading frames

within 5' UTR can inhibit translation by restricting the access of ribosomes to the correct start codon. Ribosomes bound to a uAUG may translate a uORF causing ribosome stalling and thus affecting the expression of the main ORF (Meijer and Thomas, 2002). Although some of proteins were identified, thousands of uORFs seem not to produce a detectable protein product. This indicates that either (a) proteins derived from uORFs are selectively proteolysed in the cells, (b) some of the uORFs are expressed but not in every cell type, or (c) many uORFs do not produce proteins (Oyama et al, 2007). Even though little is known about how exactly genes are regulated by uORFs in mammalian cells, uORFs and uAUGs are also overrepresented in genes such as transcription factors, proto-oncogenes, growth factors and their receptors (Kozak, 1991; Davuluri et al, 2000; Pesole et al; 2001).

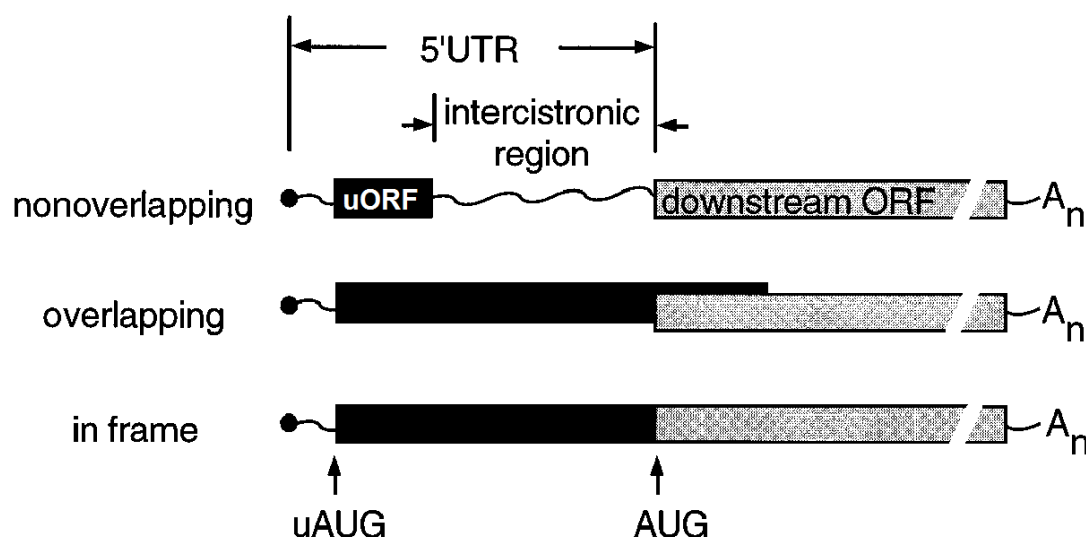


Figure 7. Three possible configurations of upstream open reading frames (uAUG) following an upstream AUG codon (uAUG). (figure from: Gebale and Sachs, 2000)

1.2.3.3. Length of 5' UTRs and Alternative 5' UTRs

The length of 5' UTR in human mRNAs spans from minimum of 18 to the maximal 2,858 nucleotides, with the average length of 210 nucleotides (Mignone et al, 2002). Even though the length of 5' UTR is not a regulatory determinant *per se*, a longer 5' UTR could be more structured and contain more different *cis*-regulatory elements (Pesole et al, 2001). Genes having alternative 5' UTRs within their transcript are relatively common, and their alternative

5' UTRs can arise from mechanisms such as utilization of multiple promoters, variation of transcription start site from the same promoter, or alternative splicing within the 5' UTR (Trinklein et al, 2003; Zhang et al, 2004). These variations in 5' UTRs can function as important switches to regulate gene expression, depending on the nature and the number of elements contained within each alternative 5' UTR (Hughes, 2006). Slight changes in the arrangement of control elements between each alternative 5' UTR can lead to major changes in target gene expression (Resch et al, 2009). As in the case of uORFs and secondary structures, transcription factors, proto-oncogenes, growth factors and their receptors are also more often regulated by expressing alternative 5' UTRs (Hughes 2006; Smith, 2008).

1.2.3.4. *Trans*-acting Factors

Trans-acting factors are usually considered as proteins that bind to the *cis*-regulatory elements within mRNA molecules, in order to control many processes related to mRNAs. It is predicted that human genome encodes for almost 1,000 RNA binding proteins (RBP), a large number of which is implicated in the translation (Hogan et al, 2008). They are categorized into two main groups: general RBPs that are part of basic translation machinery, e.g., eukaryotic initiation factors, and RBPs that are more specialized and function in a more selective way by recognizing specific UTR motifs and upon interacting with the translation machinery control either positively or negatively the translation level of specific target mRNAs, e.g., HuR, Musashi1 (Meng et al, 2005; MacNicol et al, 2008). One of the best characterized example of RBP-mediated regulation involving 5' UTR is the iron regulatory proteins (IRP1 and IRP2), which recognize a highly conserved stem-loop structure known as the iron response element (IRE). A large number of genes connected to the iron metabolism have their expression regulated by this system (Goss and Theil, 2011). When cellular iron levels are low, IRP1 and IRP2 bind the IRE and block translation of the downstream ORF, while during high intracellular iron levels, the RNA-binding activity of both IRPs is reduced (Recalcati et al, 2010).

1.2.4. The Role of 5' UTRs in Human Diseases

As explained in previous sections, post-transcriptional gene expression regulation is very complex and for proper functioning it requires fine-tuning by many different regulatory elements (Mathews MB, 2002). It is evident that improper regulation of protein synthesis can lead to many different diseases, one of which is cancer (Le Quesne et al, 2010; Scheper et al, 2007; Rugero et al, 2013). So far, many diseases are known to be caused by improper functioning of any of above mentioned *cis*-regulatory 5' UTR elements (Figure 8) (Mendell and Dietz, 2001; Pickering and Willis, 2005; Smith, 2008; Chatterjee and Pal, 2009; Wethmar et al, 2010).

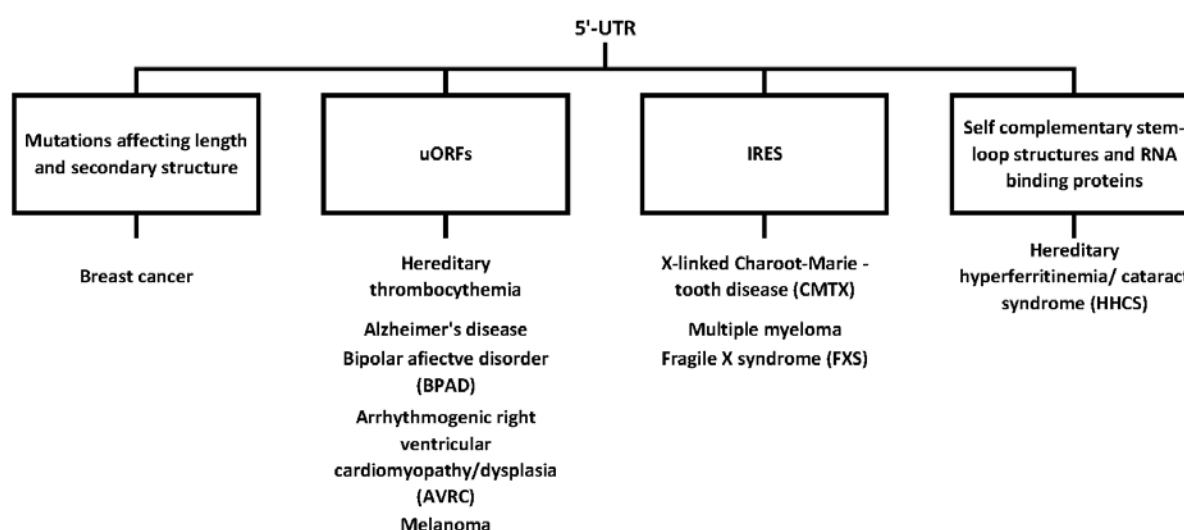


Figure 8. Involvement of different 5' UTR *cis*-regulatory elements in various human diseases. (figure adapted from: Chatterjee and Pal, 2009)

One good example to present how differential expression patterns of one gene can be caused by many different 5' UTR *cis*-regulatory elements is the tumor suppressor gene *BRCA1*. Besides being mutated in hereditary form of breast and ovarian cancer (HBOC) (Levanat et al, 2012), it is also involved in sporadic form of those two cancer types, mainly through a reduced expression on both mRNA and protein level (Birgisdottir et al, 2006). *BRCA1* can be transcribed from 2 different promoters, α and β , resulting in two transcript variants with alternative first exons, 1a and 1b. Since the main open reading frame starts in exon 2, alternative transcripts differ in 5' UTR. *BRCA1* transcript variant 1b was found to be

expressed in breast cancer tissues but not in normal mammary glands, where the transcript variant 1a is the predominant (Xu et al, 1995). Transcript 1b has longer, highly structured 5' UTR with a couple of uAUGs, which all together contribute to a 10-fold reduction in translational efficiency of *BRC1b* compared to *BRCA1a* (Sobczak and Krzyzosiak, 2002). Such down-regulated expression of Brca1 protein accelerates tumor growth (Thompson et al, 1995). Secondly, two point mutations have been found to affect optimal context for the initiation of translation (Kozak's sequence) from the main AUG codon. Mutation c.-3G>C decreases the translation efficiency by 30-50% (Signori et al, 2001), while c.-2A>T mutation causes 5-fold reduction of Brca1 protein expression (Wang et al, 2007).

Ever since it became evident that deregulated translation is behind many diseases, regulation of protein expression became an important therapeutic target and of great interest to the pharmaceutical industry (Dasgupta et al, 2004; Mavrakis and Wendel, 2008; Tain and Whitworth, 2009; Grzmil and Hemmings, 2012).

2. Aims

It is well known that 5' untranslated regions (5' UTRs) can contain many different *cis*-regulatory elements that have a role in regulating the expression of downstream coding region. Some of these *cis*-regulatory elements are: length and nucleotide content of 5' UTR, secondary structure, upstream open reading frames (uORF), internal ribosome entry site (IRES), regulatory polymorphisms. Prior to our study, the only known element found in the *PTCH1b* 5' UTR was the CGG-repeat polymorphism, which has been functionally analyzed but unfortunately not in the context of the complete *PTCH1b* 5' UTR (Nagao et al, 2004).

To thoroughly explore the regulatory role of different *cis*-regulatory elements present in the *PTCH1b* 5' UTR, by combining experimental work and computational analysis, the main goals of our study were directed to:

- a) Computational analysis of the *PTCH1b* 5' UTR sequence for the presence of known 5' UTR *cis*-regulatory elements.
- b) Re-evaluation of the effect of CGG-repeat polymorphism on the transcription and the translation of downstream mRNA, now in more physiological context of the complete *PTCH1b* 5' UTR sequence.
- c) Evaluation the effect of *PTCH1b* 5' UTR size on the transcription and/or the translation of downstream mRNA, and by *site-directed* mutagenesis verification of the significance of potential upstream open reading frames found in longer versions of *PTCH1b* 5' UTR.
- d) Revealing the expression patterns of two different-sized *PTCH1b* 5' UTR in cancer cell lines under basal and endogenously activated Hedgehog-Gli signaling pathway conditions.
- e) Assessing the impact of 5' UTR length and different number of CGG repeats on the computationally predicted *PTCH1b* 5' UTR secondary structure, and relation to the experimental results.
- f) Exploring the *PTCH1b* 5' UTR function as an internal ribosome entry site, precisely establishing its localization within the 5' UTR, and revealing the cellular conditions under which it shows the activity in the initiation of translation.

- g) Comparing the experimental results obtained from normal and malignant cell lines, for estimating the potential role of 5' UTR-regulated *PTCH1b* expression in cancer etiology.

3. Materials and Methods

3.1. Materials

We used a genomic DNA from healthy and cancer patients (DNA sample collection from the Laboratory for Hereditary Cancer, Division of Molecular Medicine, Ruđer Bošković Institute); for bacteria transformation we used DH5 α competent *E. coli* strain and the One Shot MAX Efficiency DH5 α -T1^R competent *E. coli* strain (Invitrogen, USA); in transfection experiments we used human colon cancer cell line HCT116, human breast cancer cell line MCF-7, and Human Embryonic Kidney HEK 293T cells; for constructing the luciferase reporter vectors, as a plasmid backbone we used the pGL3-Promoter Luciferase Reporter Vector (Promega, USA) and pRuF plasmid (Bisio et al, 2010); pRL-SV40 plasmid (Promega, USA) was used as a control vector and p4/TO-GLI1 expression vector (kind gift from Prof. Fritz Aberger, University of Salzburg, Austria) as endogenous activator of Hh-Gli signaling pathway.

As a DNA template for the amplification of 5' UTR of human *PTCH1b* gene we used a genomic DNA collected and genotyped in our previous studies (Cvok et al, 2008; Musani, 2008; Musani et al, 2013) For the alleles harboring 5, 7 and 8 CGG repeats we used a genomic DNA from the samples encoded as BR17, BR3 and BR19, respectively, which were collected from a healthy control population and have (CGG)₅/(CGG)₇, (CGG)₇/(CGG)₇ and (CGG)₈/(CGG)₈ genotypes, respectively. For the allele with 6 CGG repeats we used a genomic DNA from a sample encoded as 1542, which was collected from an ovarian cancer patient with the (CGG)₆/(CGG)₈ heterozygous genotype.

For the amplification, selection and extraction of cloned plasmids we used DH5 α competent *E. coli* strain. Its genome harbors several mutations that inactivate different genes and thus contribute to the increased DNA-insert stability and improved quality of extracted plasmid DNA.

In site-directed mutagenesis experiment, for the selection of only mutated plasmids we transformed the One Shot MAX Efficiency DH5 α -T1^R competent *E. coli* strain (Invitrogen, USA). This strain harbors a gene coding for the *McrBC* endonuclease which digests only methylated template DNA, thus leaving only unmethylated, mutated plasmids.

In transfection experiments we used three different adherent human cell lines: HCT116^{p53+/+}, human colon cancer cells expressing wild type p53; MCF-7, human breast adenocarcinoma

cells and HEK 293T, Human Embryonic Kidney 293 cells transduced with the SV40 (virus) large T antigen. This permits the amplification of plasmids containing the SV40 origin of replication. Although we chose these three cell lines primary because of their technical characteristics (e.g., high transfection efficiency), we wanted to include both a normal and a malignant human cell line. HEK 293T cells have been also chosen for repeating the experiment performed by Nagao K et al (2004), but now in the context of complete *PTCH1b* 5' UTR.

3.2. Methods

3.2.1. Construction of Monocistronic Luciferase Reporter Vectors

To quantitatively evaluate the effect of the CGG-repeat polymorphism and the different size of *PTCH1b* 5' UTR on the expression of downstream mRNA, a series of plasmids based on the pGL3-Promoter Luciferase Reporter Vector (Promega, USA) was constructed. As a reporter gene this plasmid bears a modified coding region for firefly (*Photinus pyralis*) luciferase (*luc*⁺) that has been optimized for monitoring transcriptional activity in transfected eukaryotic cells. The pGL3-Promoter vector (pGL3-P) contains an SV40 promoter upstream of the luciferase gene and also ampicillin-resistance gene (Amp^R) for easy selection. DNA fragments containing putative enhancer elements can be inserted using restriction sites either upstream or downstream of the promoter-*luc*⁺ transcriptional unit (Figure 9).

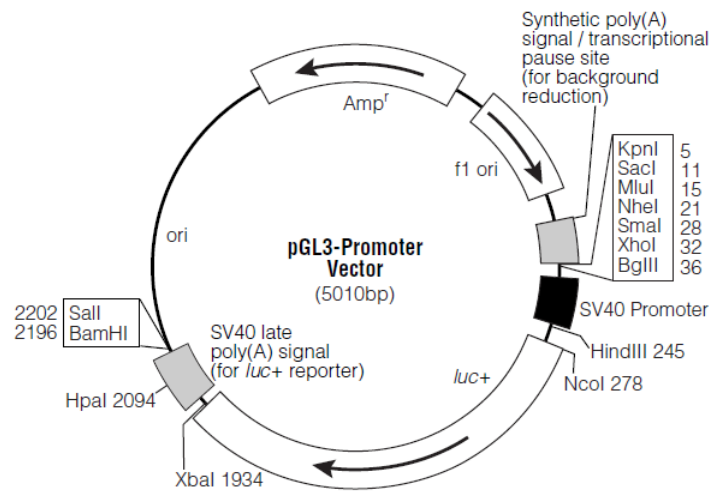


Figure 9. Circular map of pGL3-Promoter Luciferase Reporter Vector. It contains the following elements: *luc+*, cDNA for firefly luciferase; Amp^R, gene for ampicillin resistance in *E. coli*; f1 ori, origin of replication derived from filamentous phage; ori, origin of plasmid replication in *E. coli*. Arrows indicate direction of transcription. *PTCH1b* 5' UTR was cloned between *HindIII* and *NcoI* restriction sites. (figure from: pGL3 Luciferase Reporter Vectors technical manual, Promega)

3.2.1.1. Polymerase Chain Reaction (PCR)

To increase the specificity of *PTCH1b* 5' UTR amplification by polymerase chain reaction (PCR), a *nested* PCR approach was used. First a slightly bigger part of *PTCH1b* gene was amplified, which subsequently served as a template for amplifying only the *PTCH1b* 5' UTR (188-, 300- or 372-nucleotide long) and first 21 nucleotides of *PTCH1b* coding sequence (Figure 10). These additional nucleotides were included in the reverse primer because CGG-repeat polymorphism resides only 4 nucleotides before the 3' end of 5' UTR. Since they are in-frame with the *luc*⁺ coding sequence, if translated, they are not expected to have any impact on the luciferase activity. For cloning *PTCH1b* 5' UTR into the pGL3-P reporter vector, internal primers had non-complementary overhangs with one or more restriction sites at their 5' ends (Table 2). All three internal forward primers bear restriction sites for three different endonucleases: *HindIII*, *XbaI* and *EcoRI*. The common internal reverse primer has only the restriction site for *NcoI* endonuclease.

F1_EXT

ggttgccgag gagcacaagaaagcagagtc cgggaccgagcagcca ccgcaaccagcagccagagcccagca

gcccagcagcagctcctggagccgccaccgccagcagcagcca ccgcccggagcagcggcagctgcggctgcccg

ggccccgagcgcctgagaccgcccgggcaacctcgaccgccggcggggcgctctgccttgcctcccg

ccgctcggggcaccgggagggcggcagagagccagcggcggcggggagcaggggattcgctggctctttc

F_372

tgcagtgaaggggtcgcggcgcggggcgggggtaggggagttg gggaccgcaaggagtgccgccaagc

F_300

gcccgaaggacaggctcgcctcggcgcggcctctcgcctctccgc gaactggatgtgggcagcggcggccg cag

F2_EXT

agacctcggga cccccgcaatgtggcaatgga ggcagggctcgcactccccggcagcggccggccg cag

F_188

cggcagcag cgcgccgctgtgagcagcagcag cggctggtctgtcaaccggagcccagcccagcagcctgcg

gccagcagcgtcctcgcaagccgagcgcaccagcgcgccaggagcccgagcagcggcagcagcgcggccggccg

R_pGL3P / R_pRuF

ccccggaagcctcgcctccccg ggcggcggcggcggcggcggc caac ATGGCCTCGGCTGGTAACGCC GCCGAGCC

CCAGGACCGCGCGGCGGGCGGCAGCGGCTGTATCGGTGCCCGGGACGGCCGGCTGGAGGCGGGAGGCGCAGACG

GACGGGGGGCTGCGCCGTGCTGCCGCGCCGGACCGGGACTATCTGCACCGGCCAGCTACTGCGACGCCGCCTT

R_EXT

CG CTCTGGAGCAGATTTCCAAG gtgcatttca

Figure 10. Part of *PTCH1b* genomic region that served as a template for amplifying *PTCH1b* 5' UTR by two rounds of PCR. First PCR covered wider area of *PTCH1* gene and served as a template for *nested* PCR: forward primer F1_EXT was used for 372- and 300-nt-long 5' UTR, while F2_EXT primer was used for 188-nt-long 5' UTR; and in all three cases R_EXT was used as a reverse primer. For *nested* primers (F_372, F_300, F_188; R_pGL3P and R_pRuF) only complementary part of the sequence is designated, while non-complementary overhangs with one or more restriction sites are omitted. Highlighted is the sequence of *PTCH1b* 5' UTR annotated in 3 different lengths: blue, 188 bp (NCBI); green, 300 bp (Ensembl) and yellow, 382 bp (Agren et al, 2004).

Table 2. List of primers and their respective sequences used for PCR amplification of different sized 5' *PTCH1b* UTR. “F” sign denotes forward and “R” sign reverse primer.

Primer Name	Nucleotide Sequence of Primer	Reference
F1_EXT	5' GAGCACAAGAAAGCAGAGTC 3'	Musani, 2008
F2_EXT	5' CCCCCGCGCAATGTGGCAATGGAA 3'	Leovic et al, 2012
R_EXT	5' CTCTGGAGCAGATTTCCAAGG 3'	Musani, 2008
F_188	5' AAAAGCTTCTAGAATTCGCGCCCGCCGTGTGAGCAGCAGCAG 3'	newly designed
F_300	5' AAAAGCTTCTAGAATTCGAACTGGATGTGGGCAGCGGCGGCC 3'	newly designed
F_372	5' AAAAGCTTCTAGAATTCGGGACCGCAAGGAGTGCCGCGGAAG 3'	newly designed
R_pGL3P	5' TTCCATGGTGGCGTTACCAGCCGAGGCCATGTTG 3'	newly designed
R_pRuF	5' AACTCGAGTGGCGTTACCAGCCGAGGCCATGTTG 3'	newly designed
pRs-SV40_F	5' CAGAAGTTGGTCGTGAGGCA3'	unpublished

The PCR for bigger (“extensive”) amplicons was prepared in 20 µl reaction volume containing 1 µl (~300 ng) of genomic DNA, 12.5 µl of KAPA2G Robust HotStart ReadyMix (Kapa Biosystems, USA), 1 µl of each 10 mM primer and 9.5 µl of PCR water. The reaction was run in the Labcycler (SensoQuest, Germany) PCR machine according to the following protocol: first 7 min at 95°C followed by 35 cycles at 95°C for 30 s, 60°C for 30 s, 72°C for 40 s, and then final extension at 72°C for 7 min. Five µl of the PCR product were analyzed on 2% (w/v) agarose gel, and then this amplicon was used as a template in the second run of *nested* PCR. For cloning the plasmids with 372- and 300-nucleotide long *PTCH1b* 5' UTR, F1_EXT and R_EXT primers were used for making the template 913 base pairs (bp) in size. For cloning the shortest *PTCH1b* 5' UTR, F2_EXT and R_EXT primer pair was used for making the template which was 462 bp long.

Nested PCR was prepared in 50 µl reaction volume containing 2 µl of DNA template amplified in the first PCR run, 2 µl of each 10 mM primer, 25 µl of KAPA2G Robust HotStart ReadyMix and 19 µl of PCR water. *Nested* PCR was run under the same conditions as for the first run. Five µl of PCR products were inspected on a 2% (w/v) agarose gel, and if

proper sized, the remaining PCR products were purified using the QIAquick PCR Purification Kit (QIAGEN, USA), since enzymatic reactants can interfere with subsequent downstream application of PCR amplicons.

The remaining 45 μ l of PCR samples were complemented with 55 μ l of dH₂O in the centrifuge tubes and then 500 μ l of Buffer PB were added and tubes mixed well. The PCR sample mixtures were applied to the QIAquick columns placed into a 2 ml collection tubes and centrifuged for 60 s at 17,900 x g. After the flow-through was discarded, the QIAquick columns were washed with 0.75 ml of Buffer PE and centrifuged for 60 s at 17,900 x g. Again, the flow-through was discarded and the QIAquick columns were centrifuged for an additional 1 min for completely removing the residual ethanol from Buffer PE. Purified PCR products were eluted from the QIAquick columns into 1.5 ml collection tubes by adding 30 μ l of dH₂O, incubation at room temperature for 1 min and then centrifugation for 1 min at 17,900 x g.

3.2.1.2. Digestion by Restriction Endonucleases

For cloning a DNA fragment into a plasmid backbone, both plasmid and DNA fragment must be digested with the same restriction endonucleases. For cloning *PTCH1b* 5' UTR upstream of *luc+* gene into "empty" pGL3-P plasmid backbone we used double digestion with HindIII and NcoI.

Double digestion was performed in a reaction volume containing either 2 μ l of "empty" pGL3-P plasmid or 10 μ l of purified PCR amplicon, 2 μ l of HindIII (10 U/ μ l) (Thermo Fisher Scientific, USA) (10 U/ μ l), 1 μ L of NcoI (10 U/ μ l) (Thermo Fisher Scientific, USA), 2 μ l of 10X Buffer Tango (Thermo Fisher Scientific, USA) and dH₂O up to a volume of 20 μ l. The digestion reaction took place for 3 h at 37°C. After digestion, the plasmid and the PCR amplicons were inspected on a 1% (w/v) agarose gel, and then purified using the QIAquick PCR Purification Kit (QIAGEN, USA) as previously mentioned.

3.2.1.3. DNA Ligation

To join "sticky", cohesive ends of digested plasmid and PCR product DNA we used DNA ligase enzyme. First, 30 μ l of eluted plasmid DNA were concentrated to the volume of 14 μ l while 30 μ l of eluted PCR products were concentrated to the 10 μ l, using CentriVap DNA Vacuum Concentrator (Labconco, USA). Then 20 μ l of ligation reaction volume was prepared

with 10 µl of digested PCR product, 7 µl of digested “empty” plasmid, 1 µl of 400 U/µl T4 DNA Ligase (New England Biolabs, USA) and 2 µl of 10X T4 DNA Ligase Reaction Buffer (New England Biolabs, USA). The plasmid-PCR product ligation reaction was taking place overnight at 16°C, and then stored at -20°C for the afternoon bacteria transformation.

3.2.1.4. Transformation of DH5α Competent *E. coli* Strain

A tube of DH5α competent *E. coli* cells was taken from -80°C and thawed on ice for 10 min. Ten µl of plasmid-DNA insert ligate was mixed with 100 µl of cold 1X KCM buffer (100 mM KCl, 30 mM CaCl₂, 50 mM MgCl₂) in microcentrifuge tube and placed in ice for 5 min. A 100 µl of competent cells were added to DNA/KCM mixtures, stirred gently and placed in ice for 20 min. Bacteria were heat-shocked 1 min in a 42°C water bath and 1 min in ice. For recovery, 800 µl of LB (Luria-Bertani or lysogeny broth) media were added to the tubes with bacteria and rolled in a table-top incubator shaker for 1 h at 37°C. Tubes were centrifuged for 5 min at 1,700 *g* at room temperature and LB media were decanted. The pellets were resuspended in residual LB media and spread on LB agar plates with ampicillin (50 µg/ml). Plates were incubated at 37°C overnight, enabling forming colonies only to bacteria cells with plasmids harboring Amp^R gene.

3.2.1.5. Plasmid Preparations

For checking the efficacy of plasmid cloning or for the transfection of human cell lines, higher quantities of cloned plasmids were prepared using mini- and midi-preparation methods.

Mini-preparation method (*miniprep*) for the plasmid extraction from the bacteria cells was performed using QIAprep Spin Miniprep Kit (QIAGEN, USA) according to the manufacturer’s instructions. The QIAprep miniprep procedure is based on alkaline lysis of bacterial cells, lysate clearing followed by adsorption of plasmid DNA onto silica membrane in the presence of high salt, and elution in low-salt buffer or water. QIAprep miniprep procedure eliminates time consuming phenol–chloroform extraction and alcohol precipitation. Plasmid DNA prepared using the QIAprep system is suitable for a variety of routine applications including PCR, restriction enzyme digestion and sequencing.

A single, well-isolated colony was picked from each overnight LB agar plate and inoculated in Falcon tubes containing 3 ml of LB media and 3 µl of ampicillin (50 µg/ml). One tube

without inoculated bacteria colony was prepared as a negative control. Tubes were incubated in a table-top incubator shaker at 37°C overnight. Afterwards, 2 ml of overnight *E. coli* cultures were poured in microcentrifuge tubes and centrifuged at room temperature for 3 min at 11,000 x *g*. A complete supernatant was decanted and cell pellets were resuspended in 250 µl of Buffer P1, which contains RNase A to avoid RNA contamination and LyseBlue color indicator that provides visual identification of optimum buffer mixing. The 250 µl of Buffer P2 were added to the lysates and the tubes were mixed thoroughly by inverting 5 times until the solution became viscous and clear blue colored. Immediately 350 µl of Buffer N3 were added and tubes were mixed thoroughly by inverting 5 times, until the suspension became colorless. Then the tubes were centrifuged for 10 min at 17,900 x *g* at room temperature and the compact white pellets were formed. The supernatants were transferred to the QIAprep spin columns and centrifuged for 60 s at 11,000 x *g*. The flow-through solutions were discarded and the QIAprep spin columns were washed by adding 0.5 ml Buffer PB and centrifuging for 60 s at 11,000 x *g*. This step efficiently removes endonucleases to ensure that plasmid DNA is not degraded. After discarding the flow-through, QIAprep spin columns were washed by adding 0.75 ml of Buffer PE and centrifuging for 60 s at 11,000 x *g*. The flow-through solutions were discarded, and QIAprep spin columns were centrifuged at 17,900 x *g* for an additional 1 min to remove residual wash buffer because residual ethanol from Buffer PE may inhibit subsequent enzymatic reactions. At the end, the QIAprep columns were put in a clean 1.5 ml microcentrifuge tubes and plasmid DNA was eluted by adding 50 µl of ddH₂O, standing for 1 min, and centrifuging for 1 min at 17,900 x *g*. The QIAprep Spin Miniprep Kit enables purification of up to 20 µg molecular biology grade plasmid DNA. Since DNA may degrade in the absence of a buffering agent, when eluted with water, miniprep DNA is stored at -20°C. For future usage, 0.5 ml of remaining transformed *E. coli* cultures were mixed in plastic cryo-tubes with equal volume of autoclaved 40% (w/v) glycerol and stored at -80°C. To check if plasmids have inserted appropriate sized DNA fragment, miniprep plasmid DNA was digested with the same restriction endonucleases as used for cloning and the size of the bands was analyzed on an agarose gel. Plasmids that showed expected restriction patterns were sent for DNA sequencing.

For plasmids that were confirmed by DNA sequencing, larger quantity of high-quality ("transfection grade") plasmid DNA was obtained by midi-preparation method (*midiprep*) using PureYield Plasmid Midiprep System kit (Promega, USA) according to the manufacturer's instructions. In essence, this system is very similar to the QIAprep Spin Miniprep in using a silica-membrane column for DNA purification and avoiding phenol-

chloroform extraction and alcohol precipitation. The PureYield Midiprep System also incorporates a unique Endotoxin Removal Wash, designed for removing substantial amounts of contaminants such as endotoxins, proteins, RNAs and endonucleases from purified plasmid DNA, improving the robustness of sensitive downstream applications such as transfection of eukaryotic cells.

Frozen bacteria cultures transformed with the desired plasmids were streaked on the LB agar plates with ampicillin (50 µg/ml) and incubated at 37°C overnight. A single, well-isolated colony was picked from each overnight LB agar plate and inoculated in the Erlenmeyer flask containing 100 ml of LB media and 100 µl of ampicillin (50 µg/ml). As for the miniprep, one Falcon tube without inoculated bacteria colony was prepared as a negative control. The Erlenmeyer flasks were incubated in a table-top incubator shaker at 37°C overnight. Afterwards, per 50 ml of overnight *E. coli* cultures were centrifuged twice in Falcon tubes at 5,000 g for 18 min at 4°C. Supernatant was discarded and excess of media from tubes was removed with paper. Cell pellets were resuspended in 3 ml of Cell Resuspension Solution by micro-pipetting and vortexing. Three ml of Cell Lysis Solution were added to the suspensions; tubes were gently mixed by inverting 5 times, and incubated for 3 min at room temperature. Five ml of Neutralization Solution were added to the lysed cells, tubes were gently mixed by inverting 5 times and incubated for 3 min at room temperature in an upright position to allow a white flocculent precipitate to form. Neutralized lysates were poured in the PureYield Clearing Columns placed into a new 50 ml Falcon tubes and incubated for 2 min to allow the cellular debris to rise to the top. Uncapped tubes with the PureYield Clearing Columns were centrifuged at 1,500 x g for 5 min at room temperature. Uncapping of tubes ensures complete passage of solutions through columns. The centrifugation was repeated if not all the lysate has filtered through. The filtrated lysates were then poured in the PureYield Binding Columns placed into a new 50 ml Falcon tubes and centrifuged at 1,500 g for 3 min for binding of a plasmid DNA to a silica-membrane columns. Five ml of Endotoxin Removal Wash Solution containing isopropanol were added to the PureYield Binding Columns and uncapped tubes centrifuged at 1,500 x g for 3 min. The flow-through was removed; 20 ml of Column Wash Solution containing ethanol were added to the PureYield Binding Columns, and uncapped tubes centrifuged at 1,500 x g for 5 min. After removing flow-through, the tubes were centrifuged at 1,500 x g for an additional 10 min to ensure complete removal of ethanol. The PureYield Binding Columns were placed into a new 50 ml Falcon tubes and plasmid DNA was eluted by adding 600 µl of Nuclease-Free Water to the DNA binding membrane. The tubes were sealed with the parafilm and centrifuged at 2,000 x g for 5 min.

Subsequent pressing of a parafilm seal allows higher eluted volumes. The filtrates were then collected in the 1.5 ml microcentrifuge tubes, plasmid DNA concentration and purity was determined by measuring absorbance at 260 and 280 nm with ND-1000 Spectrophotometer (NanoDrop, USA) and midiprep plasmid DNA was stored at -20°C for further usage. The PureYield Plasmid Midiprep System enables purification of 100-200 µg of high-quality plasmid DNA. The size of midiprep plasmids was compared to corresponding minipreps and original “empty” plasmid used for cloning. The plasmids DNA was also linearized using one of the restriction endonuclease and uncut and cut plasmids were checked on agarose gel.

3.2.2. Agarose Gel Electrophoresis

The appropriate size of undigested and digested PCR amplicons, various plasmid constructs and mini- and midi-prep isolated plasmids was analyzed by electrophoresis in adequately dense agarose gel. For both agarose gel preparation and electrophoresis, 1X TAE buffer was used (50X TAE, 40mM Tris, 20mM acetic acid, 1mM EDTA, pH 8.0). For the sake of DNA visualization, ethidium bromide (1 µg/ml) (Sigma, USA) was added during gel preparation. For tracking and loading DNA samples into gel 6X DNA Loading Dye (10 mM Tris-HCl, 0.03% bromophenol blue, 0.03% xylene cyanol FF, 60% glycerol, 60 mM EDTA, pH 7.6) (Thermo Fisher Scientific, USA) was used. The size of DNA fragments bigger than 1,000 bp was estimated according to the GeneRuler 1 kb Plus DNA Ladder standard (0.5 µg/µl) (Thermo Fisher Scientific, USA) on 1% (w/v) agarose gels, while DNA fragments smaller than 1,000 bp were compared to the GeneRuler 100 bp DNA Ladder (0.5 µg/µl) (Thermo Fisher Scientific, USA) on 2% (w/v) agarose gels. Electrophoresis was run for approximately 40 minutes at 80-90 V and DNA bands were visualized at 254 nm using BioDoc-It Imaging System (UVP, Canada).

3.2.3. Site-directed Mutagenesis

Two out of three upstream translation initiation codons present in the 300-nt-long *PTCH1b* 5' UTR, uAUG² and uAUG³ (Figure 29), were mutated using GENEART Site-Directed Mutagenesis System (Invitrogen, USA) resulting in AUG>AUU and AUG>UUG changes, respectively. Site-directed mutagenesis protocol includes the following steps: methylation of template plasmid DNA, amplification of plasmid with high fidelity DNA polymerase (AccuPrime *Pfx*) using two complementary mutagenic oligonucleotide primers each harboring

two mutated nucleotides, circularization of newly synthesized mutated plasmid by *in vitro* recombination, transformation of DH5 α -T1R competent *E. coli* strain, digestion of methylated non-mutated parental plasmid DNA by bacterial McrBC endonuclease, selection of transformed bacteria cells with antibiotic, miniprep of mutated plasmid, confirmation of successful mutagenesis with Sanger sequencing and midiprep of appropriate mutated plasmid clone (Figure 11).

Methylation and amplification were performed together in the 50 μ l reaction volume containing 5 μ l of 10X AccuPrime *Pfx* Reaction mix, 5 μ l of 10X Enhancer, 1.5 μ l of each 10 μ M primer (F_SDM 5' ACCCCCCGCGCAATTTGGCATTGGAAGGCGCAGGGTCTGAC 3' and R_SDM 5' GTCAGACCCTGCGCCTTCCAATGCCAAATTGCGCGGGGGT 3', changed nucleotides are in bold), 10 ng of pGL3-P PTCH1 300/7 plasmid DNA, 1 μ l of DNA Methylase (4 U/ μ l), 2 μ l of 25X SAM (S-adenosine methionine), 0.4 μ l of AccuPrime *Pfx* (2.5 U/ μ l) and 32.6 μ l of PCR water. Reaction was performed using the Labcycler PCR machine (SensoQuest, Germany) under the following conditions: methylation at 37°C for 20 min, initial DNA denaturation at 94°C for 2 min followed by 18 cycles at 94°C for 20 s, 57°C for 30 s, 68°C for 2:30 min, and then final extension at 68°C for 5 min. Five μ l of the PCR product were analyzed on 1% (w/v) agarose gel. Immediately after, the recombination reaction was performed in the 20 μ l reaction volume containing 4 μ l of 5X Reaction Buffer, 2 μ l of 10X Enzyme mix, 10 μ l of PCR water and 4 μ l of PCR sample. The tube was mixed well and incubated at room temperature for 10 min. The recombination reaction was stopped by adding 1 μ l of 0.5 M EDTA; the tube was placed on ice and immediately carried on to the transformation.

One tube with 50 μ l of DH5 α -T1^R cells was thawed on ice for 10 min, and then 2 μ l of the recombination reaction mix were added to the bacteria and mixed gently by tapping. The tube was capped and incubated completely covered with ice for 12 min. Bacteria were heat-shocked in a 42°C water bath for exactly 30 s and then again covered with ice for 2 min. For recovery, 250 μ l of pre-warmed SOC medium (2% tryptone, 0.5% yeast extract, 10 mM NaCl, 2.5 mM KCl, 10 mM MgCl₂, 10 mM MgSO₄, 20 mM glucose) was added to the tube and then rolled in a table-top incubator shaker for 1 h at 37°C. At the end, 10 μ l of the transformation reaction was diluted with 90 μ l of SOC medium, spread on the LB agar plate with ampicillin (50 μ g/ml) and incubated at 37°C overnight. After the miniprep DNA of mutated pGL3-P PTCH1 300/7 plasmid was verified by sequencing, the midiprep DNA was prepared for the transfection experiments.

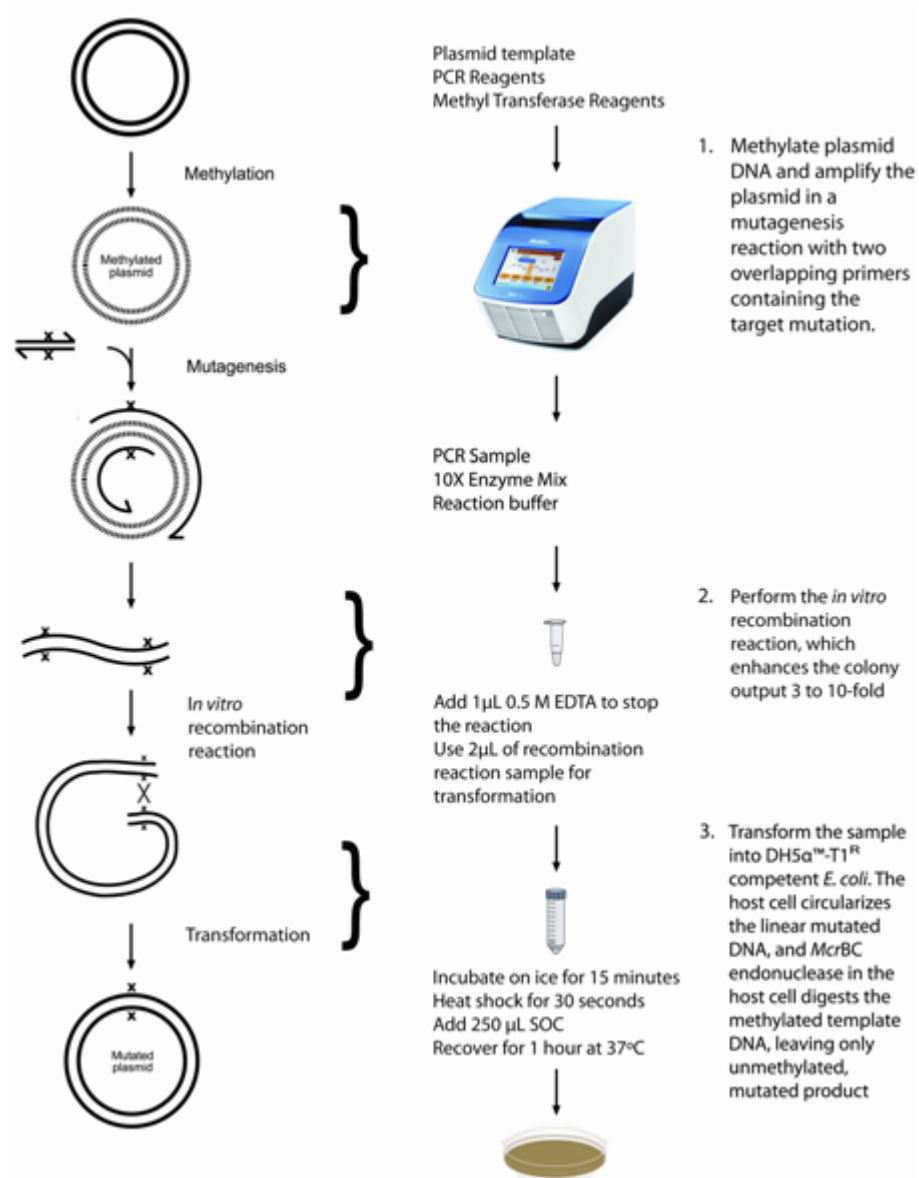


Figure 11. The workflow of site-directed mutagenesis protocol. (figure from: GENEART Site-Directed Mutagenesis System manual, Invitrogen)

3.2.4. DNA Sequencing by Sanger Method

For all newly constructed plasmids, miniprep or midiprep DNA was sent to BMR Genomics (Padua, Italy) for direct sequencing using Sanger's dideoxy method (Sanger et al, 1977). They require 250-350 ng of DNA, if the plasmid is from 5,000 to 10,000 bases in size, and 3.2 pmol of primer per one sequencing reaction. We used to send plasmid DNA lyophilized at 70°C for 30 min, sufficient for two reactions. For the pGL3-P-based plasmids the sequencing primer was 5' AAAC TAGCAA AATAGGCTGT 3', while for the pRuF-type ones was 5' GAATCGGACCCAGGATTCTT 3'. Electropherograms were visually inspected using BioEdit program version 7.1.11 (Hall, 1999) and the sequences were compared to the wild-type ones using built-in ClustalW multiple sequence alignment algorithm (Thompson et al, 1994).

3.2.5. Construction of Bicistronic Dual-luciferase Reporter Vectors

The generally accepted approach for experimentally testing if a certain mRNA molecule, more precisely a 5' UTR, has an ability to initiate translation in an IRES-dependent manner is to construct a bicistronic dual-luciferase reporter vector and clone sequence of interest into the inter-cistronic region, *i.e.* between the two different reporter genes (e.g., firefly/*Renilla* luciferase) (Van Eden et al, 2004, Baird et al, 2006, Bert et al, 2006, Thompson, 2012). The rationale behind this approach is that transcription driven from an upstream plasmid promoter should give one bicistronic mRNA transcript, from which the expression of the upstream reporter should occur through the cap-dependent mechanism, whereas the downstream reporter should be translated only if the inserted sequence exhibits IRES activity, thus allowing ribosomes to be recruited to the mRNA internally (~1kb downstream from m⁷G-cap) (Figure 12). The same dual reporter vector without inserted fragment ("empty" vector) is often used as a negative control while a proven IRES sequence (e.g., c-Myc 5' UTR) is used as a positive control. If activity of the downstream reporter is greater for the putative IRES element than non-IRES control, the candidate RNA is considered as a potential IRES-containing sequence (Ozretić et al, 2012).

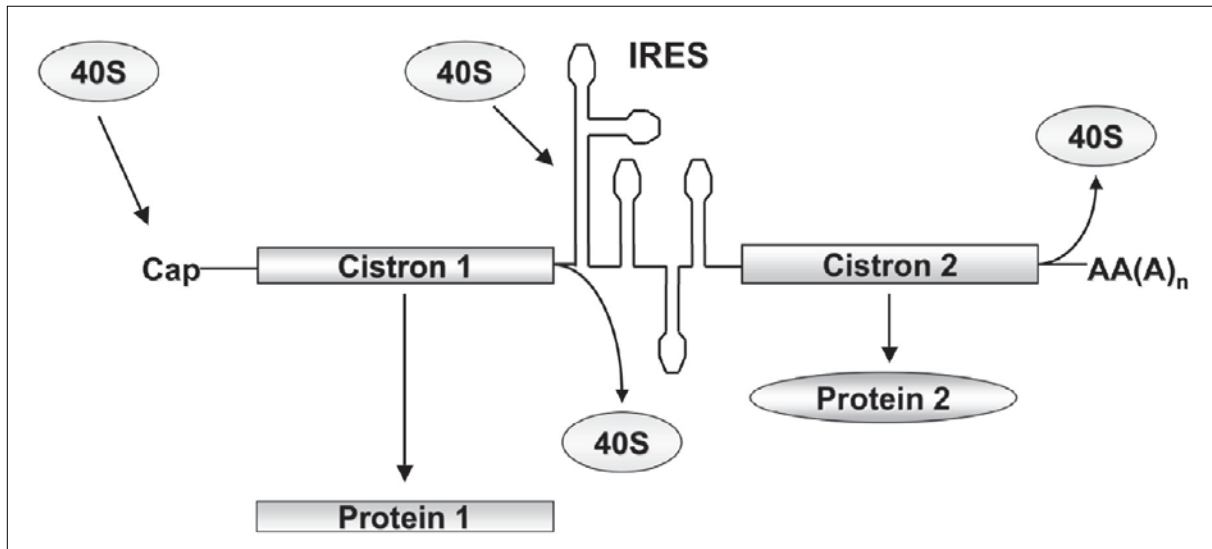


Figure 12. Schematic representation of bicistronic mRNA. In bicistronic vector constructs, the first cistron is translated in cap-dependent manner while the second cistron will be translated only if the inter-cistronic sequence can function as an internal ribosome entry site (IRES), which initiates translation independently from the 5' cap structure. (figure from: López-Lastra et al, 2005)

For constructing the bicistronic dual-luciferase reporter vectors we used an “empty” pRuF plasmid (R, *Renilla*; u, 5' UTR; f, firefly) as a backbone for cloning the *PTCH1b* 5' UTR into the inter-cistronic region between *Renilla* and firefly luciferase gene. The “empty” pRuF plasmid was constructed by cutting out the firefly luciferase cDNA (*luc*⁺) from pGL3-P plasmid harboring 5' UTR of *p16* gene (Figure 9) (Bisio et al, 2010), its subsequent cloning into the pRL-SV40 plasmid (Promega, USA) (Figure 13), downstream of the *Renilla* luciferase cDNA (*Rluc*) (cloned from the marine organism *Renilla reniformis*, sea pansy). Multiple cloning site in the inter-cistronic region allows further cloning of DNA inserts of interest.

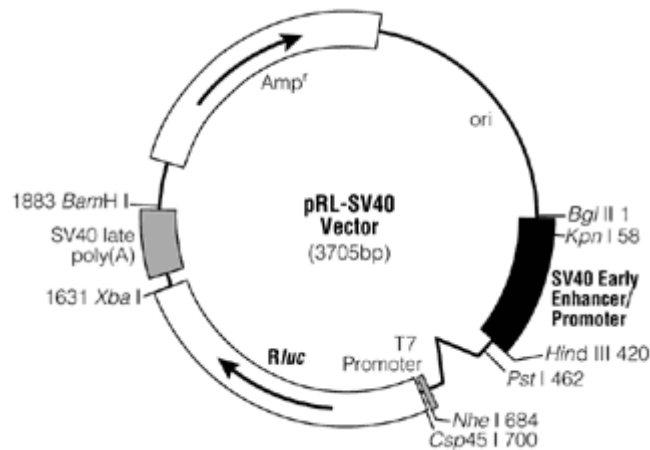


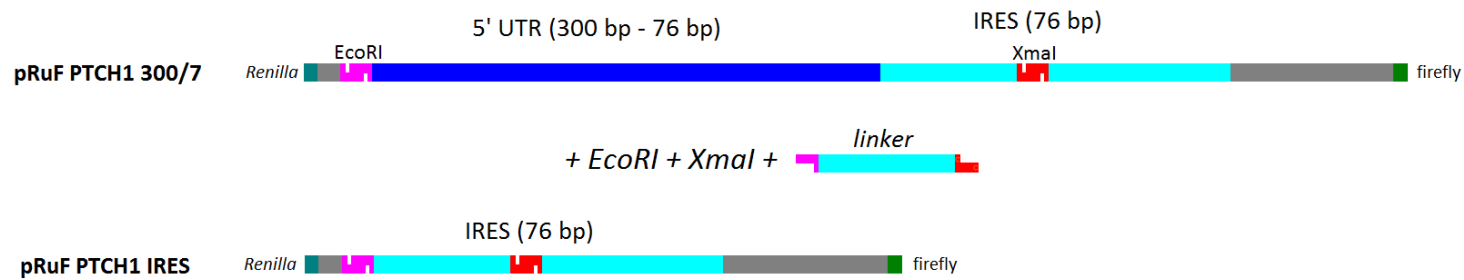
Figure 13. Circular map of the pRL-SV40 Luciferase Reporter Vector. It contains the following elements: Rluc, cDNA for Renilla luciferase; Amp^R, gene for ampicillin resistance in *E. coli*; ori, origin of plasmid replication in *E. coli*; Δ , cryptic intron. Arrows indicate direction of transcription. It was used as an internal control reporter vector in combination with any experimental reporter vector for co-transfecting mammalian cells. (figure from: <http://www.promega.com/~media/images/resources/figures/1300-1399/1353vaw4.gif>)

For the construction of pRuF-based reporter vectors, as a DNA template for PCR amplification of the *PTCH1b* 5' UTR, we used 10 ng of pGL3-P plasmids with cloned *PTCH1b* 5' UTR harboring corresponding number of CGG repeats. For forward primers we used the same ones as for the pGL3-P construction (Figure 10, Table 2), although this time as a reverse primer we used R_pRuF. It also amplifies the first 21 nucleotides of *PTCH1b* coding sequence in-frame with the *luc*⁺ cDNA, except its overhang contains a restriction site for XhoI endonuclease. The PCR conditions were the same as for the pGL3-P construction. In essence, all further steps in constructing the pRuF-type plasmids were exactly the same as for the pGL3-P construction, except both the “empty” pRuF plasmid and the PCR amplicon were double digested using EcoRI and XhoI endonuclease. Double digestion was performed in a reaction volume containing either 2 μ l of “empty” pRuF plasmid or 10 μ l of purified PCR amplicon, 1 μ l of 10 U/ μ l EcoRI (Thermo Fisher Scientific, USA), 1 μ l of 10 U/ μ l XhoI (Thermo Fisher Scientific, USA), 4 μ l of 10X Buffer Tango (Thermo Fisher Scientific, USA) and dH₂O up to a volume of 20 μ l, and it took place for 3 h at 37°C.

3.2.5.1. Precise Localization of Putative IRES Motif within the *PTCH1b* 5' UTR

For more accurate localization of the putative IRES motif within the 5' UTR of *PTCH1b* gene we have constructed three additional pRuF-based plasmids. *UTRscan* tool (Grillo et al, 2010) has predicted, based on a rule proposed by Le and Maizel Jr (1997), that first 76 nucleotides from a 3' end of *PTCH1b* 5' UTR (c.-1_-76) harbors potential internal ribosome entry site. For that reason we decided to remove those 76 nucleotides from pRuF plasmids harboring 300- or 188-nucleotide long *PTCH1b* 5' UTR. In addition, we built a pRuF plasmid which has only those 76 nucleotides cloned within the intercistronic region. To precisely remove or preserve those 76 nucleotides we used double stranded linkers with the cohesive ends that are complementary with the ends which remain after the original plasmids were treated with two endonucleases, as depicted in Figure 14.

A) PRESERVING IRES MOTIVE



B) REMOVING IRES MOTIVE

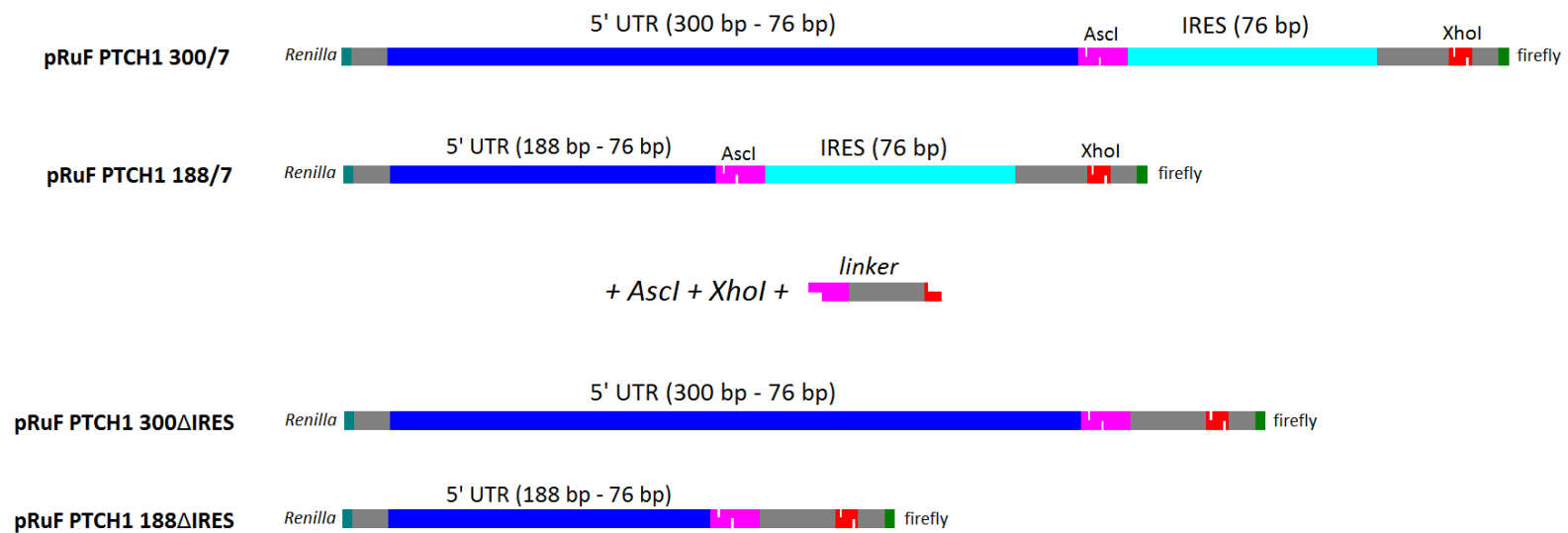


Figure 14. Precise localization of putative IRES motif within the *PTCH1b* 5' UTR. Three additional pRuF-based plasmids were constructed by **A)** preserving or **B)** removing 76 nucleotides from 3' end of *PTCH1b* 5' UTR, which were predicted by UTRscan software to have an internal ribosome entry site motif.

For constructing a pRuF plasmid which would contain only the first 76 nucleotides from 3' end of *PTCH1b* 5' UTR cloned into its intergenic region, we first double digested 3 µl of pRuF PTCH1 300/7 plasmid with 1.5 µl of 10 U/µl Cfr9I (XmaI) (Thermo Fisher Scientific, USA) and 3 µl of 20 U/ml of EcoRI (New England Biolabs, USA) in 20 µl reaction mixture which also contained 1X of Buffer Cfr9I (Thermo Fisher Scientific, USA) and dH₂O. During digestion reaction, which took place for 3 h at 37°C, we prepared linker molecules which will serve for re-circularization of digested plasmid (Figure 14A).

Linker molecule was prepared by annealing two almost complementary oligonucleotides which at their 5' and 3' end have the same cohesive ends like digested plasmid. First the oligonucleotides were phosphorylated in a reaction mixture containing 500 ng of each oligonucleotide (forward 5' AATTCCCGCAGCAGCGGCAGCAGCGCGCCGGGCCGC 3' and reverse 5' CCGGGCGGCCCGGCGCGCTGCTGCCGCTGCTGCGGG 3'), 1 µl of 10 U/µl T4 polynucleotide kinase (PNK) (New England Biolabs, USA), 2 µl of 10X T4 DNA Ligase Reaction Buffer (New England Biolabs, USA) and dH₂O to a total volume of 20 µl. Phosphorylation reaction took place at 37°C for 30 min, after which the phosphorylated oligos were annealed using the Labcycler PCR machine (SensoQuest, Germany) under the following conditions: first 2 min at 95°C, then the temperature was lowered to 50°C at a rate of 0.1°C/s, and at the end 4 min incubation at room temperature.

After digestion, plasmid DNA has to be dephosphorylated to prevent a plasmid self-circularization. Dephosphorylation was performed in a reaction volume of 11.5 µl containing 10 µl of digested plasmid, 1.15 µl of 10X Antarctic Phosphatase Reaction Buffer (New England Biolabs, USA) and 0.35 µl of 5 U/µl Antarctic Phosphatase (New England Biolabs, USA). Reaction took place at 37°C for 1 h, and was stopped by incubation in a 65°C water bath for 5 min. Dephosphorylated DNA was purified using the QIAquick PCR Purification Kit (QIAGEN, USA) and then the linker molecule was ligated into a plasmid. Ligation mixture was consisted of 10 µl of purified dephosphorylated plasmid DNA, 5 µl of linker molecule, 1.5 µl of 10X T4 DNA Ligase Reaction Buffer (New England Biolabs, USA), 1 µl of 400 U/µl T4 DNA Ligase (New England Biolabs, USA) and dH₂O to a total volume of 20 µl. Ligation was taking place overnight at 16°C, after which all usual steps were taken for obtaining a midprep plasmid DNA, required for the transfection experiments.

For constructing the pRuF-based plasmids without the 76 IRES nucleotides, the same protocol was followed. Except this time both pRuF PTCH1 188/7 and pRuF PTCH1 300/7 plasmids were remodeled, for double digestion AscI (SgsI) (Thermo Fisher Scientific, USA) and XhoI (Thermo Fisher Scientific, USA) enzymes were used, and linker molecule was built

with 5' CGCGCCAGGAGCTAAC 3' forward and 5' AGCTCAATCGAGGACC 3' reverse oligonucleotide (Figure 14B)

3.2.5.2. Alternative Splicing of pRuF-based Plasmid mRNA

One possible explanation for an increased firefly luciferase activity observed in pRuF-based luciferase assays could be due to an alternative splicing event occurring between the cryptic intron downstream of SV40 promoter and intercistronic DNA insert (Figure 13). This could result in capped firefly luciferase mRNA which is not translated by IRES-dependent mechanism. To rule this out, we performed two separate PCR reactions using pRuF-type plasmid cDNA as a template. Using a forward primer sitting upstream of the viral intron near the promoter and the specific reverse primers annealing at the two reporter ORFs, if there are no alternative splicing events there should be only two specific PCR amplicons: one sized 877 bp and another one which should be 2,204 bp plus our cloned DNA in size (Figure 15).

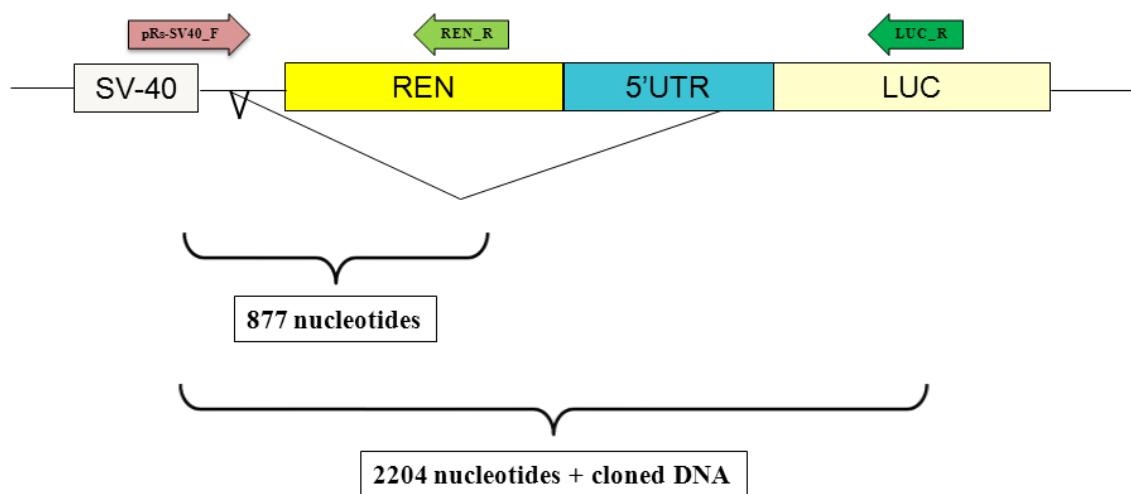


Figure 15. Activity of firefly luciferase can originate from an alternative splicing of bicistronic pRuF-type plasmid mRNA, resulting in monocistronic, capped luciferase mRNA which will not be translated in IRES-dependent manner.

PCR amplification of *Renilla* luciferase cistron was performed in 20 µl reaction volume containing 25 ng of pRuF-type plasmid DNA, 1 µl of 10 mM pRs-SV40_F primer, 1 µl of 10 mM REN_R primer, 10 µl of KAPA2G Robust HotStart ReadyMix and 6 µl PCR water. Conditions for PCR were: first 2 min at 95°C followed by 35 cycles at 95°C for 20 s, at 50°C for 30 s, at 72°C for 1 min, and final extension at 72°C for 7 min. The PCR reaction for firefly luciferase cistron was performed in 20 µl reaction volume containing 25 ng of pRuF-type plasmid DNA, 1 µl of same 10 mM pRs-SV40_F primer, 1 µl of 10 mM LUC_R primer, 10 µl of KAPA2G Robust HotStart ReadyMix and 6 µl PCR water. Conditions for this PCR were: first 2 min at 95°C followed by 35 cycles at 95°C for 20 s, at 55°C for 40 s, at 72°C for 2:30 min, and final extension at 72°C for 7 min. Both PCR reactions were performed in the Labcycler PCR machine (SensoQuest, Germany). At the end, amplicons were inspected on a 1% (w/v) agarose gel.

3.2.6. Transient Transfection of Human Cells

HCT116 cells were cultured in RPMI (Roswell Park Memorial Institute) 1640 media supplemented with 10% (v/v) fetal bovine serum (FBS), 2 mM of L-glutamine and two antibiotics, penicillin (100 U/ml) and streptomycin (100 µg/ml). MCF-7 and HEK 293T cells were cultured in DMEM (Dulbecco's Modified Eagle's Medium) supplemented with the same additives. The cells were incubated at 37°C in humidified atmosphere with 5% CO₂. Twenty-four hours before the transfection experiment, cells were seeded in a 24- or 6-well plastic plate in an appropriate density (Table 3).

Once reached 60-70% confluence, the cells were transiently transfected with plasmid DNA using *TransIT-LT1* Transfection Reagent (Mirus Bio LLC, USA). It is a cationic lipopolyplex polymer able to form insoluble complexes with DNA that precipitate on the cell membrane allowing both high efficient and low toxic entrance of the DNA by endocytosis. The ratio between the *TransIT-LT1* Reagent and the DNA used for the transfection is 3:1 (µl of reagent/µg of DNA).

Table 3. Number of the cells needed to be seed per well depends on both the cell type and the size of the plate and differed in two types of transfection experiments.

EXPERIMENT	TYPE OF PLATE	HCT116 ^{p53+/+}	MCF-7	HEK 293T	MEDIA VOLUME / WELL
luciferase assay	24-well	1.5 x 10 ⁵	8 x 10 ⁴	2 x 10 ⁵	0.5 ml
RNA/DNA extraction	6-well	6 x 10 ⁵	3 x 10 ⁵	6 x 10 ⁵	2 ml

3.2.6.1. Transfection for Luciferase Assay

When the cells were transfected with the pGL3-Promoter-type plasmids, co-transfection with the pRL-SV40 plasmid (Promega, USA) (Figure 13) was used as an internal control. Activity of the “experimental” reporter is correlated with the effect of specific experimental conditions, while the activity of the co-transfected “control” reporter serves as the baseline response. Normalizing the activity of the experimental reporter to the activity of the control minimizes experimental variability caused by differences in cell viability or transfection efficiency (Sherf et al, 1996).

For the luciferase assays, the cells were transfected in a 24-well plate and per one transfection reaction (one well) it is required 1.2 µl of room-temperature *TransIT-LT1* Transfection Reagent, 400 ng of plasmid DNA and 50 µl of DMEM without serum. First, 1.2 µl of the transfection reagent were mixed with 18.8 µl of DMEM in the microcentrifuge tube, and incubated for 5 min at room temperature. Meanwhile, in another tube 350 ng of pGL3-P-type plasmid DNA and 50 ng of pRL-SV40 DNA were dissolved in 30 µl of DMEM. After mixing 20 µl of transfection reagent solution together with 30 µl of plasmid DNA solution, the tube was incubated at room temperature for 30 min. This incubation period allows *TransIT-LT1* Reagent-DNA complex formation, after which the cells were transfected with 50 µl of this complex per well, and the transfection with each type of plasmid was performed in triplicate. Since dual-luciferase pRuF-type plasmids already code for two different reporters, there is no need for pRL-SV40 control co-transfection, and all 400 ng of required DNA come from pRuF-type plasmid. When pRuF-type plasmids were used for transfection, a pRuF plasmid with cloned 5' UTR of *MYC* (c-Myc) gene was used as positive control (Carter et al, 1999). After the transfection, the plate with cells was gently shaken to evenly distribute the transfection reagent-DNA complex and put in the incubator at 37°C with 5% CO₂.

3.2.6.2. Transfection for RNA/DNA Extraction

The transfection for the purpose of total RNA and/or genomic DNA extraction requires both the higher number of cells (Table 3) and the DNA quantity per well (1.2 µg/well). This type of transfection is performed in a 6-well plate and each type of plasmid is used for the transfection only once. Also, there is no need for pRL-SV40 control co-transfection.

At first, 3.6 µl of room-temperature *TransIT-LT1* Transfection Reagent were mixed with 96.4 µl of DMEM in the microcentrifuge tube, and incubated for 5 min at room temperature. Meanwhile, in another tube 1.2 µg of any type of plasmid DNA used were dissolved in 100 µl of DMEM. After mixing 100 µl of transfection reagent solution together with 100 µl of plasmid DNA solution, the tube was incubated at room temperature for 30 min. This incubation period allows transfection reagent-DNA complex to form, after which the cells were transfected with 200 µl of that complex per well, gently shaken and incubated at 37°C in humidified atmosphere with 5% CO₂.

3.2.6.3. Transfection for Hedgehog-Gli Signaling Pathway Activation

Since 5' UTR of *PTCH1* gene, transcript variant 1b is annotated in two different sizes, we wanted to inspect if either sized 5' UTRs even exist, individually or both in a particular cell line. We also wanted to inspect if an activated Hh-Gli signaling pathway preferentially increases the expression of one or both sized *PTCH1b* 5' UTR. For that purpose we have endogenously activated the Hh-Gli pathway by transfecting two cancer cell lines with p4/TO-GLI1 plasmid (Figure 16) and measured the expression of both sized *PTCH1b* 5' UTR. The p4/TO-GLI1 is an expression vector for GLI1 transcription factor, the main transcriptional activator of Hh-Gli target genes (Kasper et al, 2006).

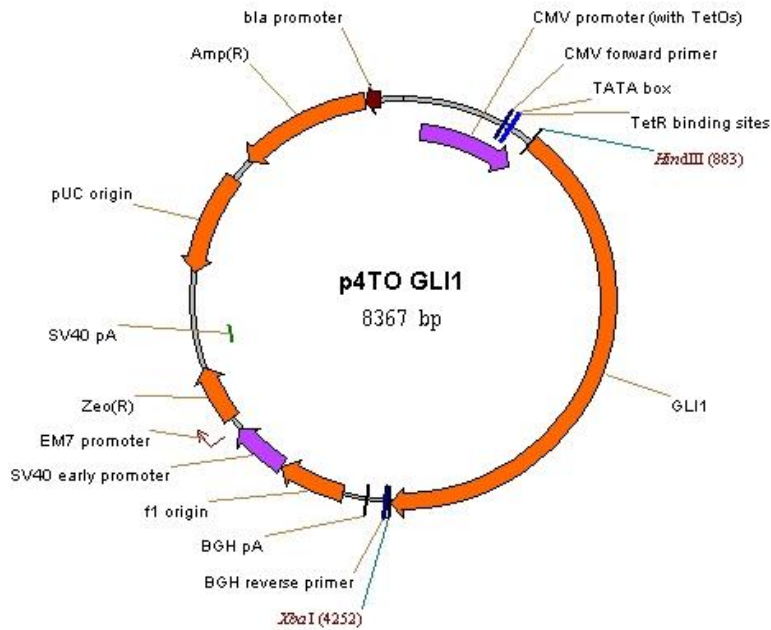


Figure 16. The p4/TO-GLI1 expression vector containing the coding sequence for Gli1 transcription factor (kind gift from Prof. Fritz Aberger, University of Salzburg, Austria).

Transfection for the subsequent RNA extraction was performed as previously mentioned, except this time HCT116 ^{p53+/+} and MCF-7 cells were transfected with 2 µg/well of either p4/TO-GLI1 or pCMV-NEO-BAM plasmid as a control, and the transfected cells were incubated for 48 hours at 37°C in humidified atmosphere with 5% CO₂.

3.2.6.4. Treatment of Transfected Cells with Hypoxia and Rapamycin

To find out which cellular stress condition can activate the initiation of protein translation governed by the putative *PTCH1b* 5' UTR IRES motif (Spriggs et al, 2008), we treated the transfected cells with rapamycin and hypoxia.

Rapamycin (Figure 17) is a specific inhibitor of mTOR (mechanistic target of rapamycin), a serine/threonine protein kinase that phosphorylates the translation repressor 4E-BP1 (eIF4E-binding protein-1), resulting in its inactivation and thus initiating the cap-dependent protein translation (Gingras et al, 2001, Ballou and Liz, 2008). When the global cap-dependent protein synthesis is blocked, it is presumed that mRNAs having IRES elements can be continuously translated by cap-independent mechanism.

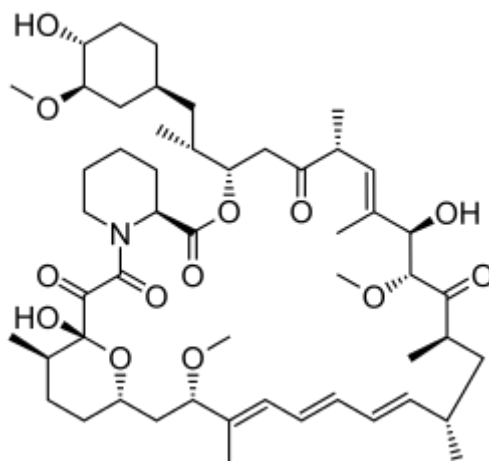


Figure 17. Structure of rapamycin, a macrolide compound that forms a complex with the immunophilin FKBP12 which then inhibits the activity of mTOR protein kinase and thus blocking the cap-dependent initiation of protein translation. (figure from: <http://upload.wikimedia.org/wikipedia/commons/0/0f/Sirolimus.svg>)

It was suggested that hypoxic conditions activate the Hh-Gli signaling pathway, resulting in an increased expression of *PTCH1* gene, among others (Bijlsma et al, 2009). Since it is known that several genes are being translated under the hypoxia by IRES-dependent mechanism (Thomas and Johannes, 2007), we wanted to explore if putative *PTCH1b* 5' UTR IRES can be activated by oxygen deprivation condition.

When the cell treatments were going to be applied, the transfection experiment using pRuF-type plasmids was performed in triplicate. One 24-well plate was used as a control and handled as usual, another one was used for treating the cells with 50 nM/well of rapamycin 6 hours after the transfection, and the third plate was put under strong hypoxic condition also 6 hours post-transfection. For achieving a hypoxic condition the transfected cells were put in a GENbox jar (bioMérieux, France) together with a GENbag anaer (bioMérieux, France), a combination of oxygen-absorbing and carbon dioxide-releasing compounds which in very short time establishes a low-oxygen condition. The jar was hermetically closed and incubated at 37°C as usual (Figure 18). Twenty-four hours after the transfection, a dual-luciferase assay was performed according to the protocol described in the following section.



Figure 18. Device for incubation of transfected cells under the hypoxic condition. Low oxygen atmosphere in a hermetically closed plastic box is achieved by a combination of oxygen-absorbing and carbon dioxide-releasing organic and inorganic compounds. (figure from: <https://static.thermoscientific.com/images/F103563~wl.jpg>)

3.2.7. Dual-Luciferase Reporter Assays

To investigate the influence of various types of DNA inserts (e.g., different sized *PTCH1b* 5' UTR, number of CGG repeats, mutated uORFs, potential *PTCH1b* 5' UTR IRES motif) on translation efficiency of the firefly luciferase reporter gene (Figure 9), the dual-luciferase reporter assays were performed to measure the firefly luciferase activity. Since *Renilla* luciferase activity was used as an internal control, the Dual-Luciferase Reporter (DLR) Assay System (Promega, USA) provides an efficient way for measuring the activity of both luciferase reporters, sequentially from a single sample. The firefly and *Renilla* luciferases, because of their distinct evolutionary origins, have dissimilar enzyme structures and substrate requirements (Figure 19). These differences make it possible to selectively discriminate between their respective bioluminescent reactions. Thus, using the DLR Assay System, the luminescence from the firefly luciferase reaction may be quenched while simultaneously activating the luminescent reaction of *Renilla* luciferase. Both enzymes do not require post-translational modification for their activity, so the enzymes may function as a genetic reporter immediately following translation. The luminescent reaction catalyzed by both luciferases provides extreme sensitivity and shows very high linear correlation with enzyme concentration.

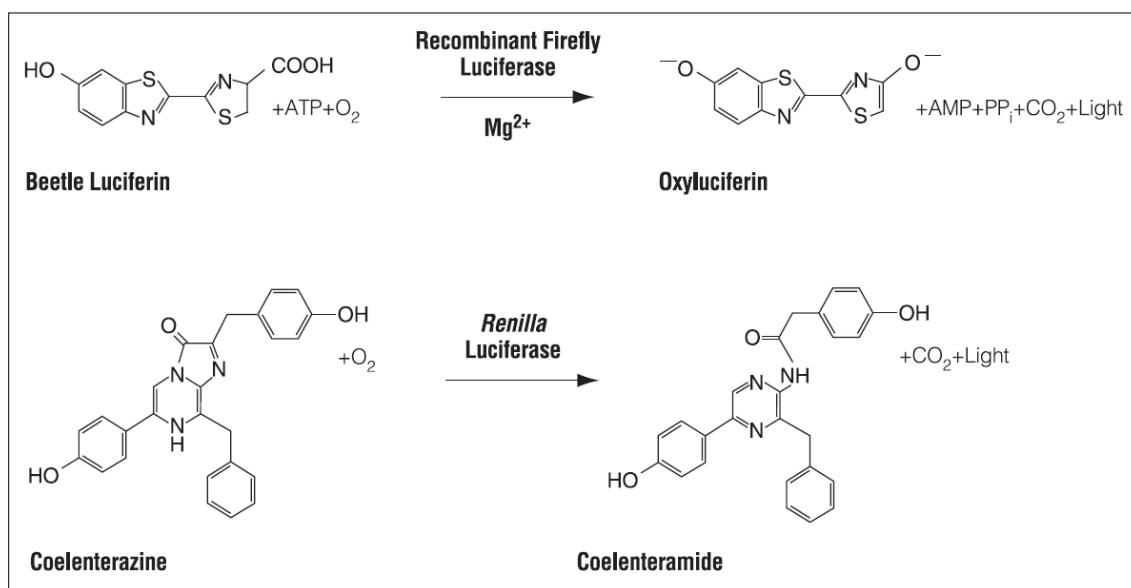


Figure 19. Bioluminescent reactions catalyzed by firefly and *Renilla* luciferases. (figure from: Dual-Luciferase Reporter Assay System technical manual, Promega)

3.2.7.1. Dual-Luciferase Reporter Assay Protocol

Twenty-four or forty-eight hours post-transfection the 24-well plates were taken from the incubator and the medium was aspirated with the vacuum pump. The cells were rinsed with 0.5 ml of 1X PBS (Phosphate Buffered Saline) buffer. After removing PBS, the cells were lysed directly in the plate by adding 75 μ l/well of 1X PLB (Passive Lysis Buffer), provided with the DLR Assay System kit, and the plates were shaken for 15 min at room temperature. The cell lysates were then thoroughly mixed by pipetting and 20 μ l of the lysate were transferred into a white opaque 384-well plate in order to measure the activity of both luciferases. Pursuant to the transfection, each type of plasmid was represented in triplicate. Two additional wells containing only 20 μ l of 1X PLB were used as a negative control for measuring the background luminescence. The firefly luciferase reporter activity was measured first by adding 15 μ l/well of Luciferase Assay Reagent II (previously prepared by resuspending provided lyophilized Luciferase Assay Substrate in 10 ml of the supplied Luciferase Assay Buffer II) to generate a stabilized luminescent signal. The luminescence of firefly luciferase was measured 3-4 times for each sample in order to obtain a statistically significant mean value of luciferase activity (technical variation). After quantifying the firefly luminescence, this reaction was quenched and the *Renilla* luciferase reaction was

simultaneously initiated by adding 15 μ l of 1X Stop & Glo Reagent to the same well. The 1X Stop & Glo Reagent was prepared immediately before usage by dissolving the 50X Stop & Glo Substrate in the Stop & Glo Buffer. Since the Stop & Glo Substrate produces a stabilized signal from *Renilla* luciferase, which decays slowly over the course of the measurement, for calculating the mean value of *Renilla* luminescence, only 2-3 measurements for each sample were needed. Infinite 200 microplate reader (Tecan, Switzerland) was used for measuring the luciferase luminescence.

3.2.7.2. Luciferase Assays Data Analysis

First, the *Renilla* normalizing factor for each transfection experiment was calculated by subtracting the mean *Renilla* activity of the negative controls from each sample's mean *Renilla* luminescence, and then dividing each difference by the minimum value of all differences. To calculate Relative Luciferase Unit (RLU), the mean firefly activity of the negative controls was first subtracted from each sample's mean firefly luminescence, and then each of these differences were divided ("normalized") by the corresponding *Renilla* normalizing factor. Since each type of plasmid was present in triplicate, mean value and standard deviation (SD) of three RLU values were calculated, and then *relative fold of induction* was calculated by dividing each mean and its SD by the mean RLU value of either pGL3-Promoter- or pRuF-empty vector (Jacobs and Dinman, 2004). In that way we were able to observe how much has the inserted *PTCH1b* 5' UTR induced or reduced the activity of the downstream luciferase reporter. With the pRuF-based plasmids, we were able to observe if and to what extent the cloned DNA insert affects the translation of the downstream reporter cistron, presumably in the cap-independent manner.

3.2.8. Total RNA and Genomic DNA Extraction

Twenty-four or forty-eight hours post-transfection the plates were taken from the incubator and the medium was aspirated with the vacuum pump. The cells were rinsed with 1 ml of 1X PBS (Phosphate Buffered Saline) buffer and after removing PBS, trypsin was added to the cells (350 μ l/well for both HCT116 and MCF-7 cells, and 200 μ l/well for HEK 293T cells). Plates with trypsin were incubated for 5 min at 37°C and after addition of 1 ml of McCoy's 5A media the cell suspensions were collected with pipette into 1.5 ml microcentrifuge tubes.

The tubes were centrifuged for 6 min at 200 g, liquid supernatant was completely aspirated, and the cell pellets were stored at -80°C for further RNA/DNA extraction.

Total RNA and genomic DNA were simultaneously isolated from cell pellets using AllPrep DNA/RNA Mini Kit (QIAGEN, USA). The procedure is based on the lysis of plasma membranes and organelles by guanidine- isothiocyanate-containing buffer, in order to release all the nucleic acids. The 350 µl of Buffer RLT Plus were used for 5×10^6 pelleted cells. Before usage, 14.3 M β-mercaptoethanol was added to the RLT buffer (10 µl per 1 ml of buffer) to inactivate RNases released during cell lysis. Cell lysates were then homogenized by passing them five times through a 20-gauge needle (0.9 mm in diameter) and vortexing in order to reduce the viscosity of the lysate and to allow more efficient binding of nucleic acids to the purification columns. Homogenized lysates are then transferred to AllPrep DNA spin columns and centrifuged for 30 s at 9,700 x g at room temperature. The flow-through is immediately used for RNA purification while AllPrep DNA spin columns, in combination with high-salt buffer, allows selective and efficient binding of only genomic DNA, which contains also a plasmid DNA. At this point AllPrep DNA spin columns were stored at 4°C for later genomic DNA extraction.

One volume of 70% ethanol (350 µl) were added to the flow-through from the AllPrep DNA spin columns and mixed well by pipetting to provide appropriate binding conditions for RNA. Mixtures were then applied to the RNeasy spin columns and centrifuged for 30 s at 9,700 x g at room temperature. Total RNA stays bounded to the membrane and contaminants are efficiently washed away. RNeasy spin column membranes were then washed with 350 µl of Buffer RW1 and centrifuged for 30 s at 9,700 x g, and the flow-through was discarded. To avoid any potential contamination with DNA, 10 µl of DNase I stock solution was dissolved in 70 µl of Buffer RDD (both provided in RNase-Free DNase Set, QIAGENE, USA) and these 80 µl of DNase I incubation mix were added directly to the RNeasy spin column membrane. After incubation for 15 min at room temperature, 350 µl of Buffer RW1 were added to the RNeasy spin columns and centrifuged for 30 s at 13,000 x g. The flow-through was discarded and the columns were washed twice with 500 µl ethanol-contained Buffer RPE and centrifuged at 13,000 x g for 30 s and 2 min, respectively. A second, longer centrifugation dries the spin column membranes, ensuring that no ethanol traces are present because residual ethanol may interfere with downstream reactions. High-quality total RNA was then eluted from RNeasy spin columns in 1.5 ml collection tubes by adding 40 µl of RNase-free water and centrifugation for 1 min at 13,000 x g, and stored at -80°C.

Subsequently AllPrep DNA spin columns were washed twice with 500 μ l of ethanol-containing Buffer AW1 and centrifuged at 9,700 x *g* for 30 s and 2 min, respectively. A second, longer centrifugation dries the spin column membranes, again ensuring that no ethanol traces are present. Genomic DNA was then eluted from AllPrep DNA spin columns by adding 90 μ l of elution Buffer EB, incubation at room temperature for 1 min and then centrifugation for 1 min at 13,000 x *g*. Eluted genomic DNA was stored at -20°C for future usage. From the cells that were transfected with pRuF-type plasmids, only total RNA was extracted using the RNeasy Mini Kit (QIAGEN, USA), following the same procedure as previously mentioned. Quantity and purity of RNA and DNA were determined by measuring absorbance at 260 and 280 nm with ND-1000 Spectrophotometer (NanoDrop, USA).

3.2.9. Quantification of Luciferase mRNA and *PTCH1b* 5' UTR Expression by Quantitative Real-Time PCR

To reveal whether the results of the luciferase assays performed after the transfection with the monocistronic pGL3-Promoter-based plasmids are related to transcriptional or post-transcriptional effect of *PTCH1b* 5' UTR insertion, we quantified the firefly luciferase (LUC) mRNA extracted from the transfected cells and compared it to the firefly luciferase mRNA expression of the cells transfected with the “empty” pGL3-Promoter plasmid. To take into account differences in transfection efficiencies, we also quantified a specific fragment of the firefly luciferase sequence on the plasmid DNA-containing gDNA extracts, thus obtaining the average plasmid copy number.

From the cells transfected with the bicistronic dual-luciferase pRuF-based plasmids we quantified the mRNA of both *Renilla* (REN) and firefly luciferase (LUC). The relative ratio of firefly to *Renilla* luciferase mRNA equal to one would prove us that there is no cryptic promoter activity of *PTCH1b* 5' UTR, when inserted into the intercistronic region of the pRuF vector. If there is a cryptic promoter activity, besides one bicistronic mRNA, there would exist another, monocistronic mRNA coding only for the firefly luciferase. In that case, the higher activity of *PTCH1b* 5' UTR pRuF-based plasmids would be correlated not only to the firefly luciferase translated from the cap-independent manner, but also to the firefly luciferase translated in the cap-dependent manner from that monocistronic, capped mRNA.

Since 5' UTR of *PTCH1* gene transcript 1b is annotated in two different sizes, we wanted to inspect if transcripts 1b containing one or both sized 5' UTRs are evenly expressed in two

different cancer cell lines. Also, we wanted to see if endogenously activated Hh-Gli pathway, there will be a preferential changes of one or both sized 5' UTR-containing transcripts.

In two types of cancer cells, with their basal level of Hh-Gli activity and with endogenously activated signaling pathway, we quantified the expression of both 188- and 300-nucleotide long 5' UTR. The forward primers (Table 4) are positioned at the very beginning of each size 5' UTR while the reverse primer spans exon 1/exon 2 boundary.

Since RNA molecules are very easily degraded by omnipresent RNases, complementary DNA (cDNA) is a more convenient way to work with the coding sequence than mRNA. For this purpose, before quantification, total RNA (rRNA and mRNA) is usually converted to a cDNA using the reverse-transcriptase enzyme and random hexamer primer.

3.2.9.1. First Strand cDNA Synthesis

First strand cDNA from RNA templates was synthesized using RevertAid First Strand cDNA Synthesis Kit (Fermentas, USA). RNA extracted from the transfected cells was taken from -80°C and thawed in ice. Into a sterile tube on ice 1 µg of total RNA, 1 µl of 100 µM random hexamer primer and nuclease-free water to a total volume of 12 µl were added. The tubes were gently mixed, briefly centrifuged and incubated at 65°C for 5 min in order to denature GC-rich or secondary structures containing RNA templates. The tubes were then chilled on ice, spun down and placed back on ice. After this, the following components were added in the indicated order: 4 µl of 5X Reaction Buffer, 1 µl of RiboLock RNase Inhibitor (20 U/µl), 2 µl of 10 mM dNTP Mix and 1 µl of RevertAid M-MuLV Reverse Transcriptase (200 U/µl) to a final volume of 20 µl. The tubes were gently mixed and then incubated for 5 min at 25°C to achieve primer binding, followed by 60 min at 42°C for the cDNA synthesis. The reaction was terminated by heating at 70°C for 5 min. All these steps were performed in the Labcycler PCR machine (SensoQuest, Germany). Assuming that conversion was complete, the cDNA synthesized from 1 µg of total RNA will have a final concentration of 50 ng/µl. The working cDNA 1:4 solution (12.5 ng/µl) was prepared by adding 60 µl of nuclease-free water and directly used as a template in real-time PCR or stored at -20°C.

3.2.9.2. Quantitative Real-Time Polymerase Chain Reaction (qPCR)

Quantitative real-time polymerase chain reaction (qPCR) is a method used to amplify and simultaneously quantify a targeted mRNA/cDNA molecule due to the fact that during the

exponential amplification phase of PCR the amount of cDNA doubles with each cycle (Nolan et al, 2006).

The exponential increase of cDNA product in a sample is monitored by the increase in a fluorescence intensity of a dye, such as SYBR Green, that fluoresces only when bound to the double-stranded (ds) DNA. The fluorescence increases with each cycle, and by this method it is measured the cycle at which there is enough cDNA whose fluorescence is above the detection threshold (Ct value). So if the starting amount of mRNA/cDNA in the sample is higher, it will sooner increase enough to cross the detection threshold and its corresponding Ct value will be lower, while the samples with less cDNA reach the detection threshold later and therefore have higher Ct values (Figure 20). In order to normalize for variations in the amount and quality of mRNA/cDNA between different samples, the method also includes one or more referent (“housekeeping”) genes as an internal control. All Ct values are normalized by the value(s) of the reference gene(s) because their expression is very stable over time in all of the tissues and under any conditions (Dheda et al, 2004).

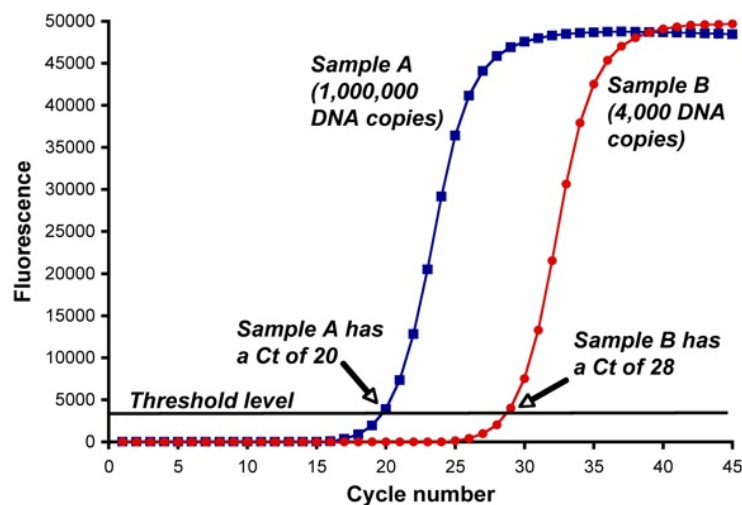


Figure 20. Fluorescence curves of two samples with different starting mRNA/cDNA amounts. The fluorescence grows exponentially with each cycle until it reaches a plateau where there is a saturation of amplification reaction. Ct values indicate the number of PCR cycles in which the fluorescence of the corresponding sample exceeds the detection threshold. Higher starting amount of mRNA/cDNA leads to a lower Ct value and vice versa. (figure from: http://www.langfordvets.co.uk/images/ct_values.jpg)

The qPCR was prepared in either 96- or 384-well plastic PCR plate (BIO-RAD, USA). In each well, 10 µl of the reaction mixture contained 2.2 µl of ddH₂O, 0.4 µl of 10 µM forward and reverse primers (Table), 5 µl of KAPA SYBR FAST Universal 2X qPCR Master Mix (Kapa Biosystems, USA) and either 25 ng of cDNA or 10 ng of gDNA. The KAPA SYBR FAST qPCR Master Mix contains the KAPA SYBR DNA Polymerase, the SYBR Green I fluorescent dye, MgCl₂, dNTPs and stabilizers. Each cDNA/gDNA sample was prepared in triplicate and for each pair of primers two additional samples without the template were prepared as a negative, no-template control (NTC). In each qPCR reaction two common human referent genes, glyceraldehyde 3-phosphate dehydrogenase (GAPDH) (Barber et al, 2005) and beta-2-microglobulin (B2M) (Lupberger et al, 2002), were used as an internal control.

Table 4. List of primers and their respective sequences used in qPCR experiments. “F” sign denotes forward and “R” sign reverse primer.

Primer Name	Nucleotide Sequence of Primer	Reference
B2M_F	5' AGGCTATCCAGCGTACTCCA 3'	Bisio et al, 2010
B2M_R	5' ATGGATGAAACCCAGACACA 3'	Bisio et al, 2010
GAPDH_F	5' TCCAAAATCAAGTGGGGCGA 3'	unpublished
GAPDH_R	5' AGTAGAGGCAGGGATGATGT 3'	unpublished
LUC_F	5' TCTGAGGAGCCTTCAGGATT 3'	Bisio et al, 2010
LUC_R	5' AGATGGAACCTCTTGGCAAC 3'	Bisio et al, 2010
REN_F	5' TTGAATCATGGGATGAATGG 3'	Bisio et al, 2010
REN_R	5' GGACGACGAACTTCACCTTT 3'	Bisio et al, 2010
qPTCH1_188_F	5' GCGCCCGCCGTGTGAGCAGCAGCAG 3'	newly designed
qPTCH1_300_F	5' GAACTGGATGTGGGCAGCGGCGGCC 3'	newly designed
qPTCH1_EX1_2_R	5' ATTTCCAAGGGGAAGGCTACTGGCC 3'	newly designed

The efficiency of new pairs of primers, i.e., primers for quantifying *PTCH1b* 5' UTR expression, was calculated from a standard curve which was generated by running qPCR on serial dilutions of MCF-7 cDNA.

The qPCR reaction was run in either CFX96 or CFX384 Touch Real-Time PCR Detection System (BIO-RAD, USA) according to the following cycling protocol: at first 3 min at 95°C for enzyme activation and complete denaturation of template DNA, followed by 39 cycles of 15 s at 95°C, 20 s at 60°C and 5 s at 72°C, and recording the fluorescence after each step. Finally, the melting curve was obtained by heating each amplified sample from 72 to 95°C. These melting curves help us to assess the specificity of qPCR quantification. For every PCR amplicon, i.e., each set of primers, melting curve shape must be known and specific. Only experiments with specific melting curve are taken into account when calculating the Ct values.

3.2.9.3. qPCR Data Analysis

Cycle threshold (Ct) values were obtained from the Bio-Rad CFX Manager software version 2.1 (BIO-RAD, USA). Relative mRNA quantity was expressed as a *fold change*, using $2^{-\Delta\Delta Ct}$ formula (Livak and Schmittgen, 2001). At first, for calculating ΔCt values, each Ct value of an “empty” plasmid replicate was subsequently subtracted from the triplicate Ct value of the plasmid with inserted DNA. Since two reference genes were used as an internal control, for each type of plasmid (each being presented with three Ct values) the geometric mean between B2M and GAPDH Ct values was calculated (Vandesompele et al, 2002). Then the geometric mean value of an “empty” plasmid was subtracted from each geometric mean value of plasmids with inserted DNA. To calculate $\Delta\Delta Ct$ values, the corresponding geometric mean difference of the referent genes was subtracted from each ΔCt value. So in that way ΔCt values were “normalized” with the reference genes expression. Finally, *fold change* was calculated using $2^{-\Delta\Delta Ct}$ formula, and for each type of plasmid used for the transfection, mean fold change and SD of three replicates were calculated. The “empty” plasmid has a fold change equal to 1 and its SD was calculated from its original Ct values.

When the luciferase mRNA was quantified from the cells transfected with the pGL3-P-based plasmids, the *average plasmid copy number* was calculated using $2^{-\Delta Ct}$ formula, where ΔCt was calculated by subsequently subtracting each gDNA Ct value of an “empty” plasmid from the triplicate gDNA Ct value of the plasmid with inserted DNA. Then each mRNA mean fold change and its SD were divided (“corrected”) by the average plasmid copy number. For the cells transfected with the pRuF-based plasmids, both the firefly (LUC) and the *Renilla* (REN) luciferase mRNA fold change was calculated, and the results were presented as the ratio of the firefly to the *Renilla* luciferase mRNA (LUC/REN). When quantifying different sized

PTCH1b 5' UTRs, Δ Ct values were calculated by subtracting Ct values of the non-activated cells from the corresponding Ct values of GLI1-transfected cells, so in that case the fold change is relative to the expression of *PTCH1b* 5' UTRs in the cells with their basal activity of Hh-Gli signaling pathway. Since part of longer *PTCH1b* 5' UTR was also amplified when qPTCH1_188_F primer was used, the actual expression of 188-nt-long *PTCH1b* 5' UTR must be calculated by subtracting the fold change of 300-nt-long 5' UTR from the fold change of the 188-nt-long 5' UTR.

3.2.10. *In Silico* Analysis of *PTCH1b* 5' UTR

SpliceMiner web-application (Kahn et al, 2007; <http://projects.insilico.us/SpliceMiner/>) was used for aligning and drawing *PTCH1* transcript variants. Web-servers *UTRscan* (Grillo et al, 2010; <http://itbtools.ba.itb.cnr.it/utrscan>) and *RegRNA 2.0* (Huang et al, 2006; <http://regrna2.mbc.nctu.edu.tw>) were used to analyze the sequence of *PTCH1b* 5' UTR for the presence of any known *cis*-regulatory element. The secondary structure of different sized *PTCH1b* 5' UTR and structural impact of different number of CGG repeats were predicted using the *mfold* web-server (Zucker, 2003; <http://mfold.rna.albany.edu/?q=mfold/RNA-Folding-Form>). Potential upstream open reading frames were predicted using *ATGpr* (Salamov et al, 1998; <http://atgpr.dbcls.jp/>) and *NetStart 1.0* (Pedersen and Nielsen, 1997; <http://www.cbs.dtu.dk/services/NetStart/>) web-based tools. *Blastx* algorithm from the NCBI BLAST web tool (McGinnis and Madden, 2004; <http://blast.ncbi.nlm.nih.gov/>) was used to find if any known protein exists with an amino acid sequence similar to the peptides potentially translated from the predicted *PTCH1b* uORFs. *IRESite* (Mokrejs et al, 2009; <http://iresite.org/>) and *IRSS2* IRES search system (<http://140.135.61.250/irss2/>) were used to find if there exist any experimentally proven viral or cellular IRES motif similar in sequence to the *PTCH1b* 5' UTR. Since very few species have accurately annotated 5' UTR of *PTCH1* gene, *nucleotide blast* from the NCBI BLAST web tool (McGinnis and Madden, 2004; <http://blast.ncbi.nlm.nih.gov/>) was used to collect genomic sequences homologous to the 372-nucleotide-long 5' UTR of human *PTCH1b* gene. *MUSCLE* web tool (Edgar, 2007; <http://www.ebi.ac.uk/Tools/msa/muscle/>) was used to perform multiple *PTCH1* sequence alignment for assessing evolutionary conservation of potential *PTCH1b* 5' UTR *cis*-regulatory elements.

3.2.11. Statistical Analysis

All calculations for analyzing the luciferase assays and qPCR results were performed in Microsoft Excel 2010 application (Microsoft, USA). Differences in luciferase activity and mRNA expression between various plasmids were analyzed by one-way analysis of variance (ANOVA), followed by Tukey's post-hoc test for multiple comparisons. Spearman's rank correlation coefficient (ρ) was used to assess the correlation between the number of CGG repeats and the luciferase activity for pGL3-P plasmids harboring 188-nt-long *PTCH1b* 5' UTR. Expression of different sized *PTCH1b* 5' UTR under basal level and endogenously activated Hh-Gli pathway was compared using unpaired t-test. Effects of hypoxia and rapamycin treatments on the activity of pRuF-type plasmids were analyzed by two-way ANOVA, followed by Tukey's post-hoc test. Two-tailed *P*-values less than 0.05 were considered statistically significant. Statistical analyses were performed using Prism 6 for Windows software, version 6.01 (GraphPad Software, USA).

4. Results

4.1. Monocistronic Luciferase Reporter Vectors with Cloned *PTCH1b* 5' UTR

In total, 9 different monocistronic plasmids were constructed using an “empty” pGL3-Promoter plasmid as a vector backbone (Figure 21). For the 188-nt-long 5' UTR we constructed 4 different plasmids harboring an allele with 5, 6, 7 or 8 CGG repeats that were named “pGL3-P *PTCH1* 188/5”, “pGL3-P *PTCH1* 188/6”, “pGL3-P *PTCH1* 188/7” and “pGL3-P *PTCH1* 188/8”, respectively. For the 300-nt-long 5' UTR we constructed 3 different plasmids harboring an allele with 5, 7 or 8 CGG repeats, named “pGL3-P *PTCH1* 300/5”, “pGL3-P *PTCH1* 300/7” and “pGL3-P *PTCH1* 300/8”, respectively. For the 372-nucleotide long 5' UTR we constructed one plasmid harboring the “wild type” allele with 7 CGG repeats, and named it “pGL3-P *PTCH1* 372/7”.

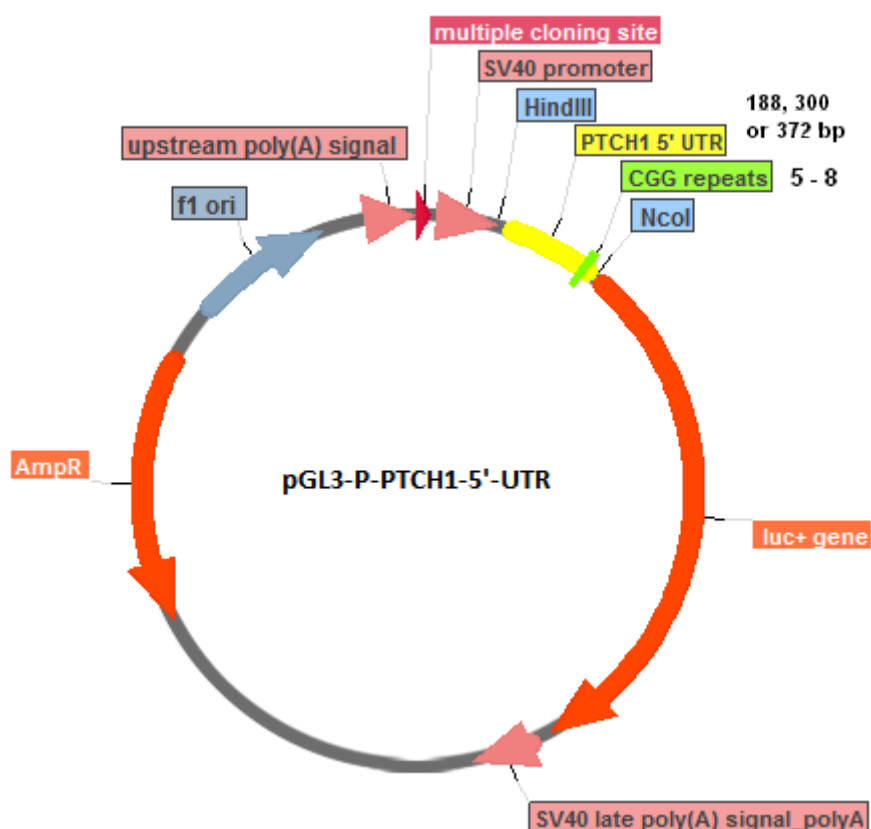


Figure 21. Circular map of monocistronic pGL3-P-based plasmids with different sized *PTCH1b* 5' UTR harboring different CGG-repeat allele, cloned upstream of the firefly luciferase gene. Potential impact of *PTCH1b* '5 UTR on the transcription and/or translation of downstream gene could be indirectly deduced from activity/mRNA quantity of the firefly luciferase.

Starting from the “pGL3-P PTCH1 300/7” plasmid, an additional one was constructed which harbors 2 point mutations within the 300-nt-long *PTCH1b* 5' UTR, c.-248G>T and c.-242A>T (Figure 22). These two mutations abolish 2 out of 3 upstream uAUGs found within the 112 nucleotides at the 5' end of the 300-nucleotide-long *PTCH1b* 5' UTR (Figure 28). This plasmid was named “pGL3-P PTCH1 300/7 SDM”.

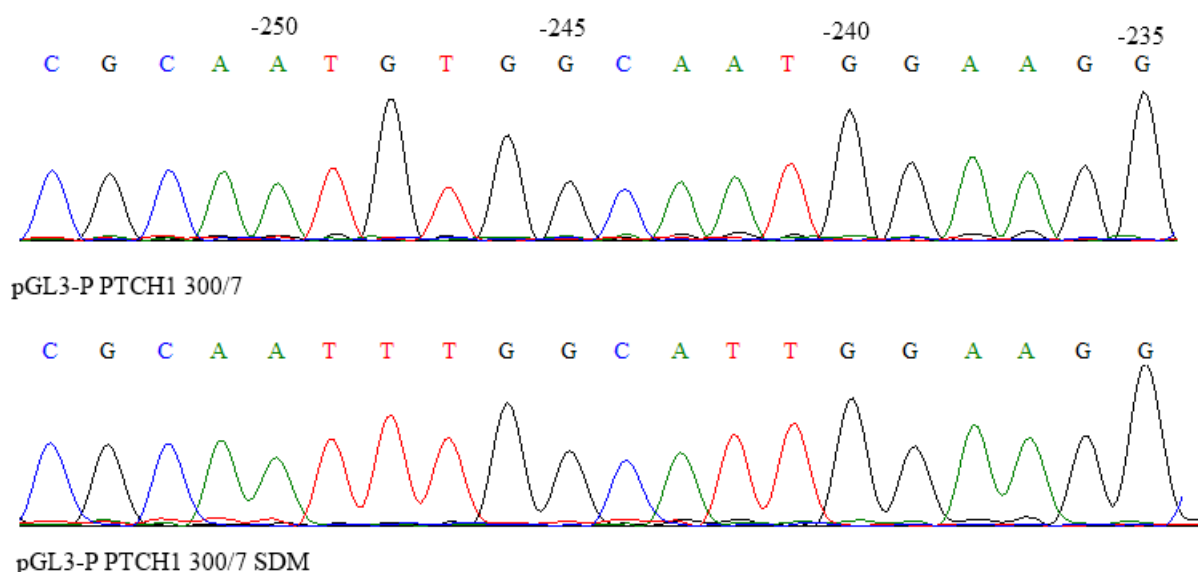


Figure 22. Electropherograms of “pGL3-P PTCH1 300/7” and “pGL3-P PTCH1 300/7 SDM” plasmids. In “pGL3-P PTCH1 300/7 SDM” two point mutations, c.-248G>T and c.-242A>T, were introduced into the 300-nt-long *PTCH1b* 5' UTR to diminish 2 out of 3 upstream AUG codons.

Since we obtained a DNA sample harboring (CGG)₆ allele in the late phase of our research, we constructed just the “pGL3-P PTCH1 188/6” plasmid, and the results with this plasmid proved that there was no need for additional plasmids harboring the 6 CGG repeats. Likewise, since computational analyses haven't found any additional regulatory elements within the 72 nucleotides at the 5' end of the 372-nucleotide-long 5' UTR, only “pGL3-P PTCH1 372/7” plasmid was constructed, and the results using that plasmid were consistent with the results obtained for the “pGL3-P PTCH1 300/7” plasmid.

4.2. Impact of Different *PTCH1b* 5' UTR Size and CGG-repeat Number on Translation or Transcription of Luciferase Reporter Gene

4.2.1. Results of Dual-Luciferase Reporter Assay in HCT116^{p53+/+} Cell Line

Results of luciferase assay performed in transfected HCT116^{p53+/+} cells showed that cloning of *PTCH1b* 5' UTR caused significant changes in luciferase activity compared to the “empty” pGL3-P plasmid [F (6, 14) = 173.0, $P < 0.0001$] (Figure 23). Cloning of 188-nt-long 5' UTRs caused on average more than 2-fold increase in activity, while cloning of 300-nt-long 5' UTRs decreased luciferase activity around 5-fold. A CGG-repeat number showed to have a significant impact only in the context of 188-nt-long 5' UTR, where (CGG)₅ allele led to slightly increased activity compared to both (CGG)₇ and (CGG)₈ alleles.

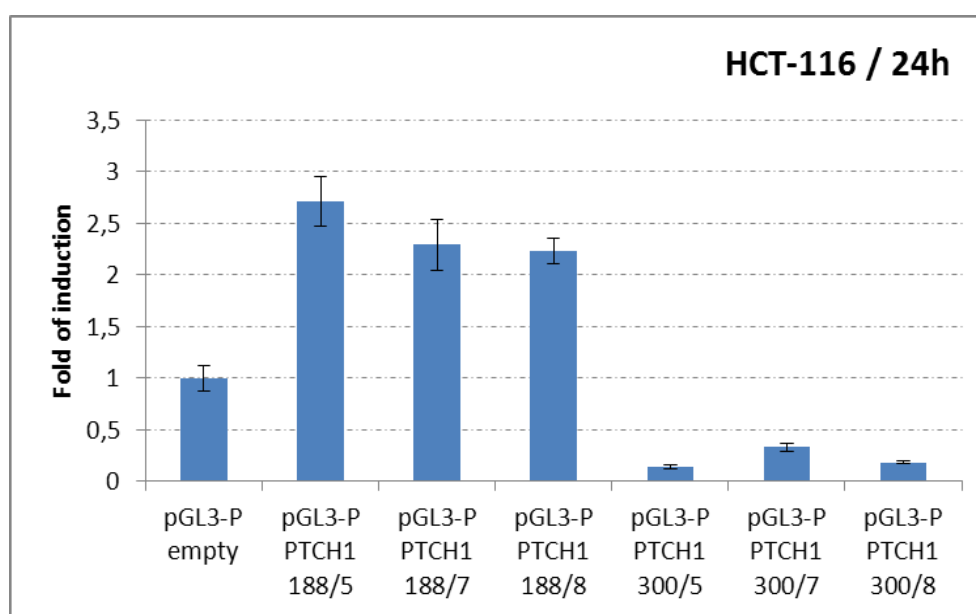


Figure 23. Impact of *PTCH1b* 5' UTR size and CGG-repeat number on firefly luciferase activity in HCT116^{p53+/+} cells. Cloning of 188-nt-long 5' UTR caused more than 2-fold increase in activity, while cloning of 300-nt-long 5' UTR decreased luciferase activity around 5-fold, both compared to the “empty” pGL3-P plasmid.

4.2.2. Results of Firefly Luciferase mRNA Quantification in HCT116^{p53+/+} Cell Line

Results of luciferase mRNA quantification performed in transfected HCT116^{p53+/+} cells showed that cloning of *PTCH1b* 5' UTR caused significant changes in firefly luciferase transcription compared to the “empty” pGL3-P plasmid [$F(5, 12) = 27.33, P < 0.0001$] (Figure 24). Cloning of 188-nt-long 5' UTR generally caused more than 4-fold increase in luciferase mRNA expression, while cloning of 300-nt-long 5' UTR increased luciferase transcription around 6-fold. A CGG-repeat number showed not to have a statistically significant impact on luciferase mRNA level.

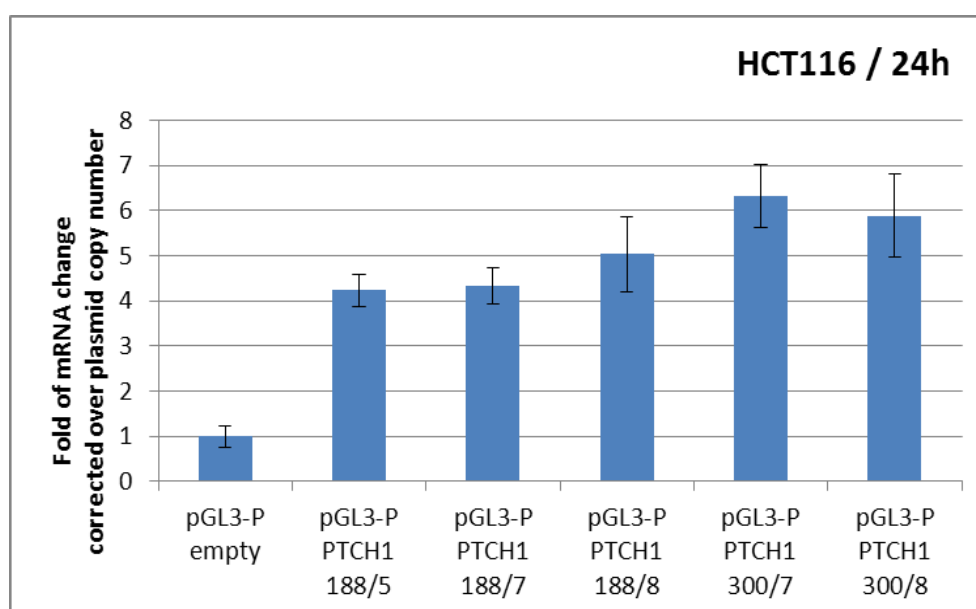


Figure 24. Impact of *PTCH1b* 5' UTR size and CGG-repeat number on firefly luciferase mRNA transcription in HCT116^{p53+/+} cells. Cloning of 188-nt-long 5' UTR caused more than 4-fold increase in luciferase mRNA expression, while cloning of 300-nt-long 5' UTR increased luciferase transcription around 6-fold, both compared to the “empty” pGL3-P plasmid.

4.2.3. Results of Dual-Luciferase Reporter Assay in MCF-7 Cell Line

Results of luciferase assay performed in transfected MCF-7 cells showed that cloning of *PTCH1b* 5' UTR caused significant changes in firefly luciferase activity compared to the “empty” pGL3-P plasmid [$F(6, 14) = 181.3, P < 0.0001$] (Figure 25). Cloning of 188-nt-long 5' UTR caused on average more than 7-fold increase in luciferase activity, while cloning of 300-nt-long 5' UTR decreased luciferase activity around 2-fold for (CGG)₅ and (CGG)₈ alleles. A CGG-repeat number showed only to have a statistically significant impact in the context of 188-nt-long 5' UTR, where (CGG)₅ allele led to slightly increased activity compared to both (CGG)₇ and (CGG)₈ alleles.

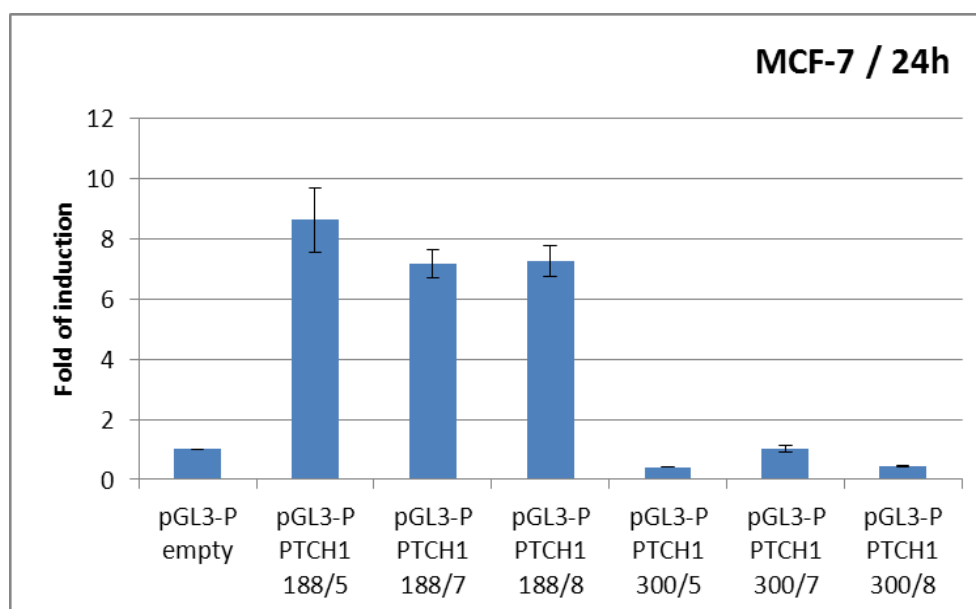


Figure 25. Impact of *PTCH1b* 5' UTR size and CGG-repeat number on firefly luciferase reporter activity in MCF-7 cells. Cloning of 188-nt-long 5' UTR caused on average more than 7-fold increase in activity, while cloning of 300-nt-long 5' UTR decreased luciferase activity around 2-fold for (CGG)₅ and (CGG)₈ alleles, when compared to the “empty” pGL3-P plasmid.

4.2.4. Results of Firefly Luciferase mRNA Quantification in MCF-7 Cell Line

Results of luciferase mRNA quantification performed in transfected MCF-7 cells showed that cloning of *PTCH1b* 5' UTR caused significant changes in firefly luciferase transcription compared to the “empty” pGL3-P plasmid [$F(5, 12) = 80.74, P < 0.0001$] (Figure 26). Cloning of 188-nt-long 5' UTR caused more than 5.5-fold increase in luciferase mRNA expression, while cloning of 300-nt-long 5' UTR increased luciferase transcription around 8-fold, compared to the “empty” pGL3-P plasmid. A CGG-repeat number showed only to have a statistically significant impact in the context of 188-nt-long 5' UTR, where (CGG)₅ allele led to increased luciferase mRNA transcription compared to both (CGG)₇ and (CGG)₈ alleles.

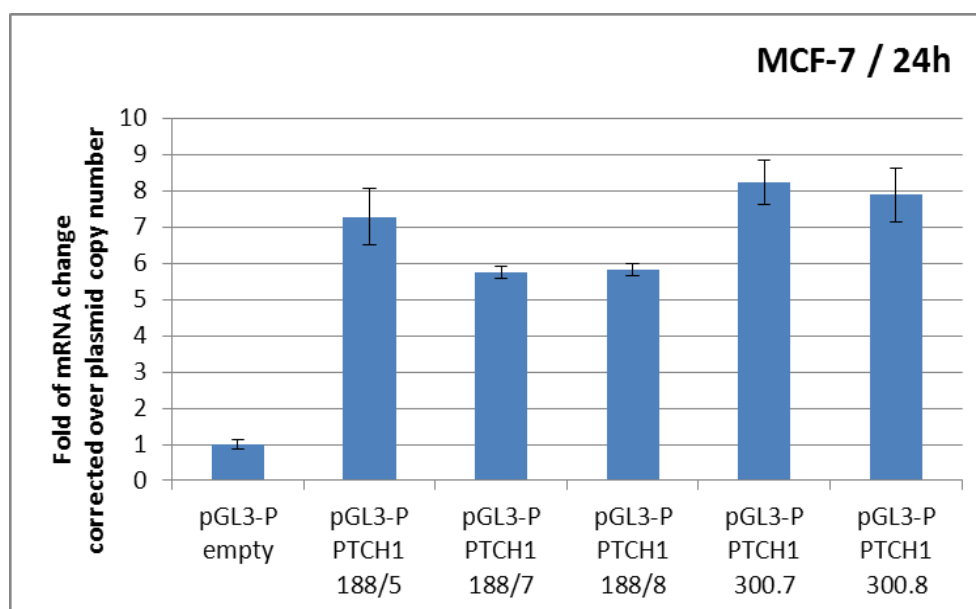


Figure 26. Impact of *PTCH1b* 5' UTR size and CGG-repeat number on firefly luciferase mRNA expression in MCF-7 cells. Cloning of 188-nt-long 5' UTR caused more than 5.5-fold increase in luciferase mRNA expression, while cloning of 300-nt-long 5' UTR increased luciferase transcription around 8-fold, compared to the “empty” pGL3-P plasmid.

4.2.5. Results of Dual-Luciferase Reporter Assay in HEK 293T Cell Line

Results of luciferase assay performed in transfected HEK 293T cells showed that cloning of *PTCH1b* 5' UTR caused significant changes in firefly luciferase activity compared to the “empty” pGL3-P plasmid [$F(6, 14) = 27.91$, $P < 0.0001$] (Figure 27). Cloning of 188-nt-long 5' UTRs caused on average only 1.5-fold increase in luciferase activity, of which an increase (around 2-fold) was statistically significant only for (CGG)₅ allele. Meanwhile, cloning of 300-nt-long 5' UTR on average caused 2-fold decrease in luciferase activity.

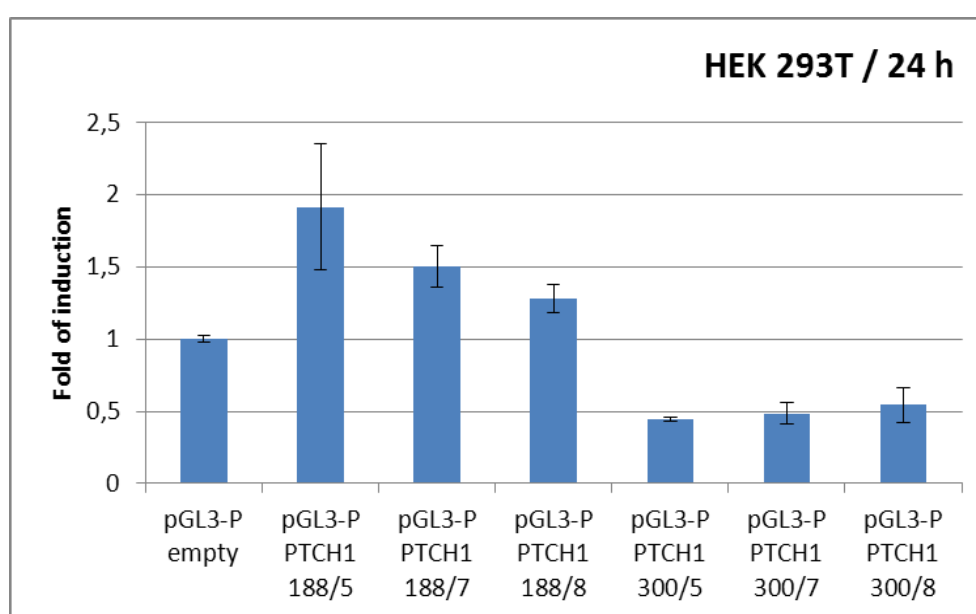


Figure 27. Impact of *PTCH1b* 5' UTR size and CGG-repeat number on firefly luciferase reporter activity in HEK 293T cells. For cloned 188-nt-long 5' UTR, only (CGG)₅ allele caused statistically significant increase in luciferase activity (around 2-fold), while cloning of 300-nt-long 5' UTR on average caused 2-fold decrease in luciferase activity.

4.2.6. Results of Firefly Luciferase mRNA Quantification in HEK 293T Cell Line

Results of luciferase mRNA quantification performed in transfected HEK 293T cells showed that cloning of *PTCH1b* 5' UTR caused significant changes in firefly luciferase transcription compared to the “empty” pGL3-P plasmid [$F(5, 12) = 21.23, P < 0.0001$] (Figure 28). Cloning of 188-nt-long 5' UTR harboring different number of CGG repeats caused from 3.7- to 5.6-fold increase in luciferase mRNA expression, while cloning of 300-nt-long 5' UTR caused 6.4- and 4.2-fold increase in luciferase transcription for (CGG)₇ and (CGG)₈ alleles, respectively. A CGG-repeat number showed a statistically significant impact only in the context of 300-nt-long 5' UTR, where (CGG)₇ allele lead to the higher luciferase mRNA expression compared to the (CGG)₈ allele.

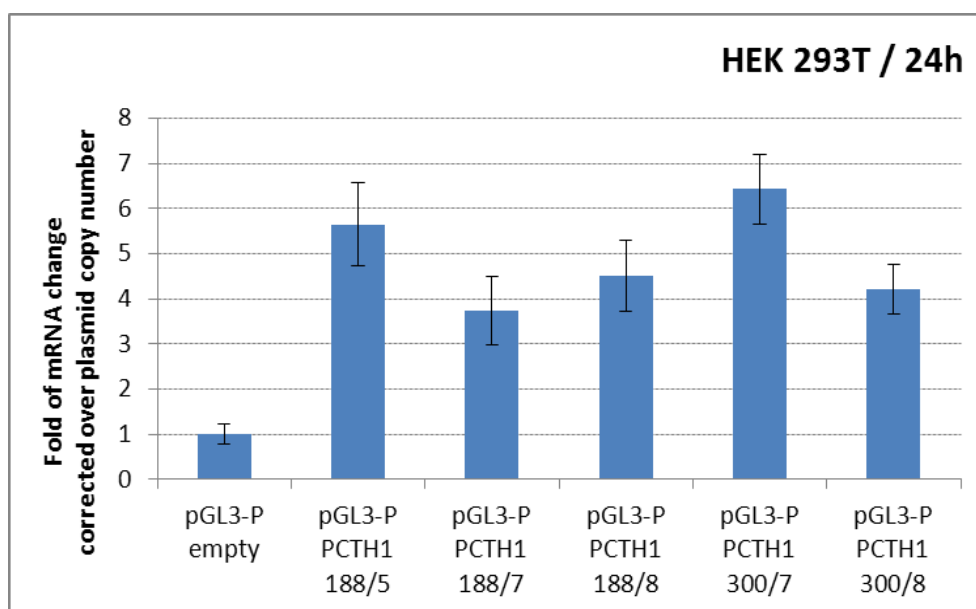


Figure 28. Impact of *PTCH1b* 5' UTR size and CGG-repeat number on firefly luciferase mRNA expression in HEK 293T cells. Cloning of 188-nt-long 5' UTR caused from 3.7- to 5.6-fold increase in luciferase mRNA expression, while cloning of 300-nt-long 5' UTR caused 6.4- and 4.2-fold increase in luciferase transcription for (CGG)₇ and (CGG)₈ alleles, respectively.

4.3. Upstream Open Reading Frames and Upstream AUG Codon in *PTCH1b* 5' UTR

Two web tools that were used predicted 2 upstream open reading frames (uORFs) and one upstream AUG codon within the first 112 nucleotides from the 5' part of the 300-nucleotide long *PTCH1b* 5' UTR (Figure 29). The uORF¹ and uORF² share the same TGA stop codon, while the open reading frame for uAUG² start codon overlaps with the main *PTCH1b* reading frame, meaning that its stop codon lies downstream from the main *PTCH1b* start codon. Among those three ORFs, this overlapping one codes for the longest peptide product (88 amino acids), but nevertheless there are no known proteins with amino acid sequences similar to any peptide potentially translated from the predicted *PTCH1b* uORFs.



Figure 29. Predicted upstream open reading frames and upstream AUG codon within the 372-nucleotide-long *PTCH1b* 5' UTR. First and third start codons (uAUG¹ and uAUG³) share the same STOP codon (“TGA”/“UGA” in brown color) while STOP codon for the second upstream AUG codon (uAUG²) lies within the main *PTCH1b* open reading frame (underlined nucleotides), thus creating an overlapping open reading frame. There is no known protein with an amino acid sequence similar to any peptide potentially translated from the predicted uORFs.

4.3.1 Site-directed Mutagenesis of Two Upstream AUG Codons in pGL3-P PTCH1 300/7 Plasmid

Two out of three upstream AUG codons, uAUG² and uAUG³, were mutated in the pGL3-P PTCH1 300/7 plasmid resulting in c.-248G>T and c.-242A>T point mutations within the 300-nt-long *PTCH1b* 5' UTR. Luciferase assay showed that removing those 2 uAUGs restored activity of the reporter gene to the level equal to the activity of pGL3-P PTCH1 188/7 plasmid which does not harbor either uAUG or uORF within cloned *PTCH1b* 5' UTR (Figure 30).

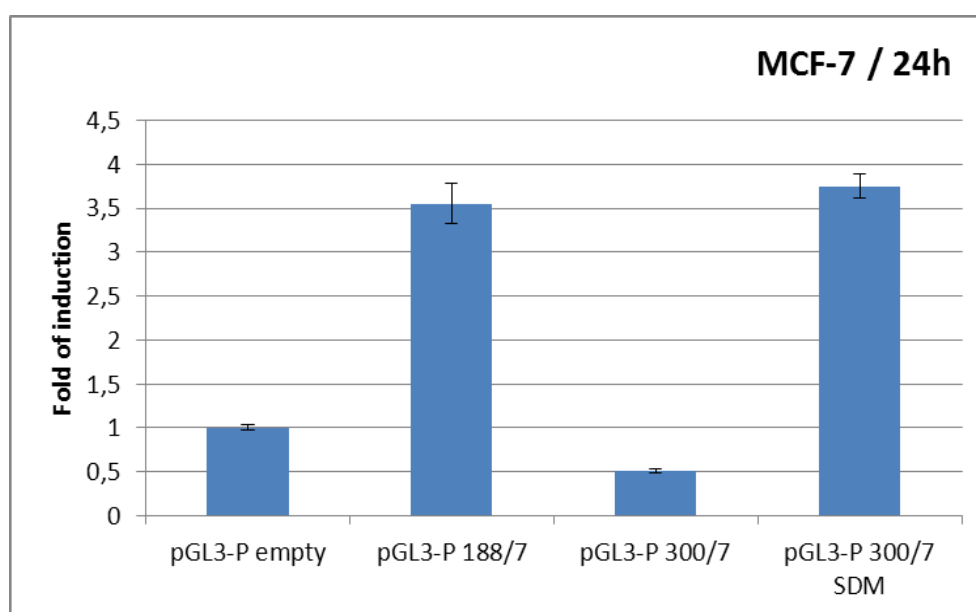


Figure 30. Effect of nullification of the two upstream AUG codons from pGL3-P PTCH1 300/7 plasmid on luciferase reporter activity in MCF-7 cell line. Two point mutations within 300-nucleotide long *PTCH1b* 5' UTR, c.-248G>T and c.-242A>T, restored luciferase activity to the level equal to the activity of pGL3-P PTCH1 188/7 plasmid.

4.4. Impact of Mutated pGL3-P PTCH1 300/7 Plasmid, 6 CGG Repeats and 372-nucleotide-long *PTCH1b* 5' UTR on Translation or Transcription of Luciferase Reporter Gene

4.4.1. Results of Dual-Luciferase Reporter Assay in MCF-7 Cell Line

Results of luciferase assay performed in transfected MCF-7 cells showed that the nullification of 2 uAUGs in pGL3-P PTCH1 300/7 plasmid, cloning of 372-nt-long *PTCH1b* 5' UTR and (CGG)₆ allele within the 188-nt-long 5' UTR caused significant changes in firefly luciferase activity compared to the “empty” pGL3-P plasmid [$F(7, 16) = 176.7, P < 0.0001$] (Figure 31). For completeness, (CGG)_{5,7,8} were included again in the experiment (see also Figure 25). When 188-nt-long 5' UTRs were cloned, on average 3-fold increase in luciferase activity was observed. Cloning of 300-nt-long 5' UTR caused 2-fold decrease in activity, while cloning the longest 5' UTR caused even higher, 4-fold reduction in reporter gene activity. Two mutations present in pGL3-P PTCH1 300/7 SDM plasmid restored luciferase activity to the level similar to the activity of pGL3-P PTCH1 188/7 plasmid. Regarding a number of CGG repeats in the context of 188-nt-long 5' UTR, only (CGG)₆ allele caused slight but statistically significant increase in activity compared to the “wild-type” (CGG)₇ allele, while in general the number of CGG repeats showed a negative correlation with the luciferase activity ($\rho = -0.76, P = 0.0034$).

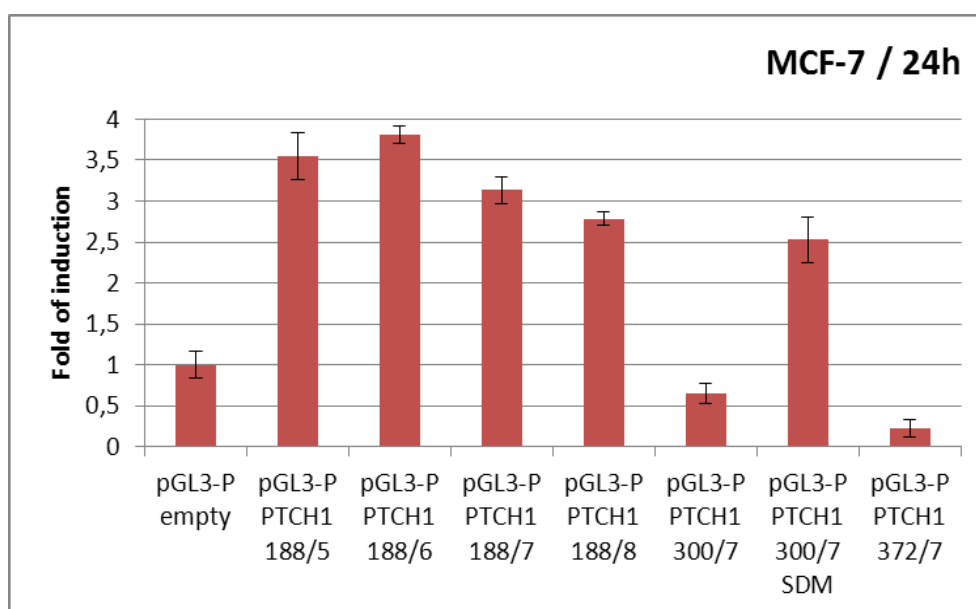


Figure 31. Impact of 372-nt-long *PTCH1b* 5' UTR, (CGG)₆ allele, and nullification of 2 upstream AUG codons on firefly luciferase reporter activity in MCF-7 cells. Cloning of the longest *PTCH1b* 5' UTR caused 4-fold reduction in luciferase activity while (CGG)₆ allele caused slight but statistically significant increase in luciferase activity compared to the “wild-type” (CGG)₇ allele.

4.4.2 Results of Firefly Luciferase mRNA Quantification in MCF-7 Cell Line

Results of luciferase mRNA quantification performed in transfected MCF-7 cells showed that nullification of 2 uAUGs in pGL3-P PTCH1 300/7 plasmid, cloning of 372-nt-long *PTCH1b* 5' UTR and (CGG)₆ allele within 188-nt-long 5' UTR caused significant changes in firefly luciferase transcription levels when compared to the “empty” pGL3-P plasmid [F (5, 12) = 194.4, $P < 0.0001$] (Figure 32). Cloning of 188-nt-long 5' UTR harboring either (CGG)₆ or (CGG)₇ allele caused around 4-fold increase in the luciferase mRNA expression, the same as cloning of 300-nt-long 5' UTR. Cloning of 372-nt-long 5' UTR or introduction of two mutations present in pGL3-P PTCH1 300/7 SDM plasmid caused even higher, more than 5-fold increase in firefly luciferase transcription.

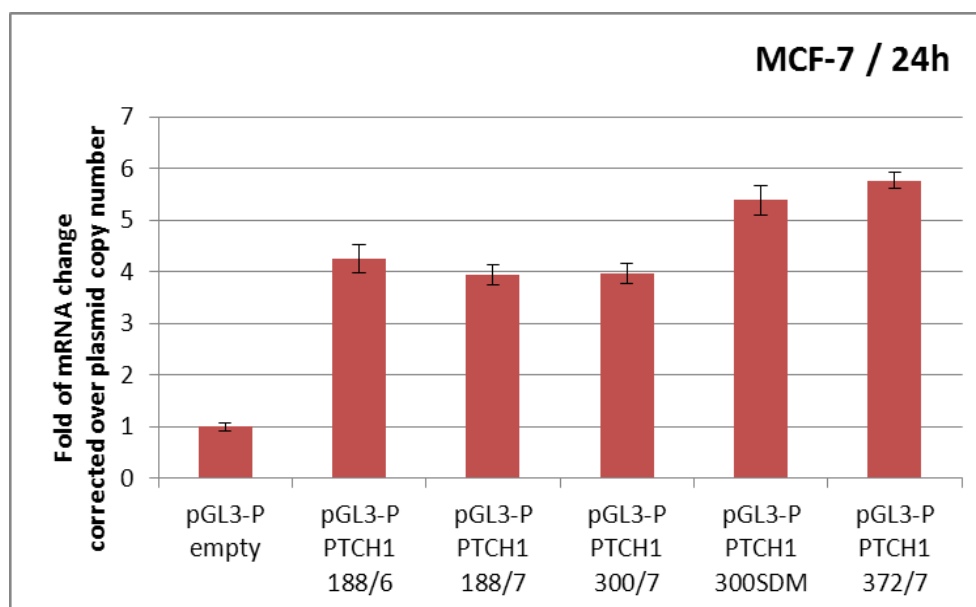


Figure 32. Impact of 372-nucleotide long *PTCH1b* 5' UTR size, (CGG)₆ allele, and removing 2 upstream AUG codons on firefly luciferase transcription in MCF-7 cells. Cloning of 188-nt-long 5' UTR harboring either (CGG)₆ or (CGG)₇ allele caused around 4-fold increase in luciferase mRNA expression, the same as cloning of 300-nt-long 5' UTR. Cloning of 372-nt-long 5' UTR or removing 2 upstream AUG codons from pGL3-P PTCH1 300/7 plasmid caused more than 5-fold increase in firefly luciferase transcription.

4.4.3. Results of Dual-Luciferase Reporter Assay in HEK 293T Cell Line

Results of luciferase assay performed in transfected HEK 293T cells showed that the nullification of 2 uAUGs in pGL3-P PTCH1 300/7 plasmid and cloning of (CGG)₆ allele within the 188-nt-long 5' UTR caused significant changes in firefly luciferase activity compared to the “empty” pGL3-P plasmid [$F(6, 14) = 19.82, P < 0.0001$] (Figure 33). For completeness, (CGG)_{5,7,8} alleles were included again in the experiment (see also Figure 27). Cloning of the 188-nt-long 5' UTRs on average caused 2.5-fold increase in the luciferase activity, with no statistically significant difference among a different CGG-repeat number. In general, the number of CGG repeats showed a strong negative correlation with the luciferase activity ($\rho = -0.67, P = 0.0134$). Cloning of 300-nt-long 5' UTR showed luciferase activity similar to the activity of “empty” pGL3-P plasmid, while two mutations present in pGL3-P PTCH1 300/7 SDM plasmid restored luciferase activity to the level similar to the activity of pGL3-P PTCH1 188/7 plasmid.

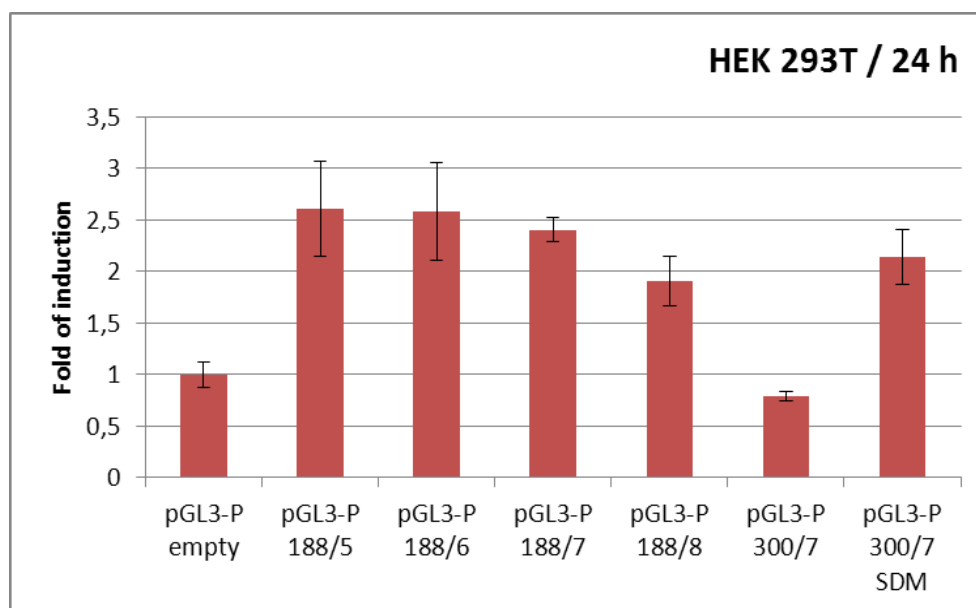


Figure 33. Impact of the *PTCH1b* 5' UTR (CGG)₆ allele and the nullification of 2 upstream AUG codons on the firefly luciferase reporter activity in HEK 293T cells. No statistically significant difference in firefly luciferase activity was observed regarding the number of CGG repeats within the 188-nucleotide-long 5' UTR. Two mutations present in pGL3-P PTCH1 300/7 SDM plasmid restored luciferase activity to the level similar to the activity of pGL3-P PTCH1 188/7 plasmid.

4.4.4. Results of Firefly Luciferase mRNA Quantification in HEK 293T Cell Line

Results of luciferase mRNA quantification performed in transfected HEK 293T cells showed that nullification of 2 uAUGs in pGL3-P PTCH1 300/7 plasmid and (CGG)₆ allele within 188-nt-long 5' UTR caused significant changes in firefly luciferase transcription when compared to the “empty” pGL3-P plasmid [$F(4, 10) = 44.06, P < 0.0001$] (Figure 34). Cloning of 188-nt-long 5' UTR harboring (CGG)₇ allele caused around 1.5-fold increase in luciferase mRNA expression, while (CGG)₆ allele caused more than 2-fold increase. Cloning of 300-nt-long 5' UTR showed the highest, 2.5-fold increase in reporter gene transcription, while introduction of two mutations which are present in pGL3-P PTCH1 300/7 SDM plasmid caused an increase in firefly luciferase transcription similar to the pGL3-P PTCH1 188/7 plasmid.

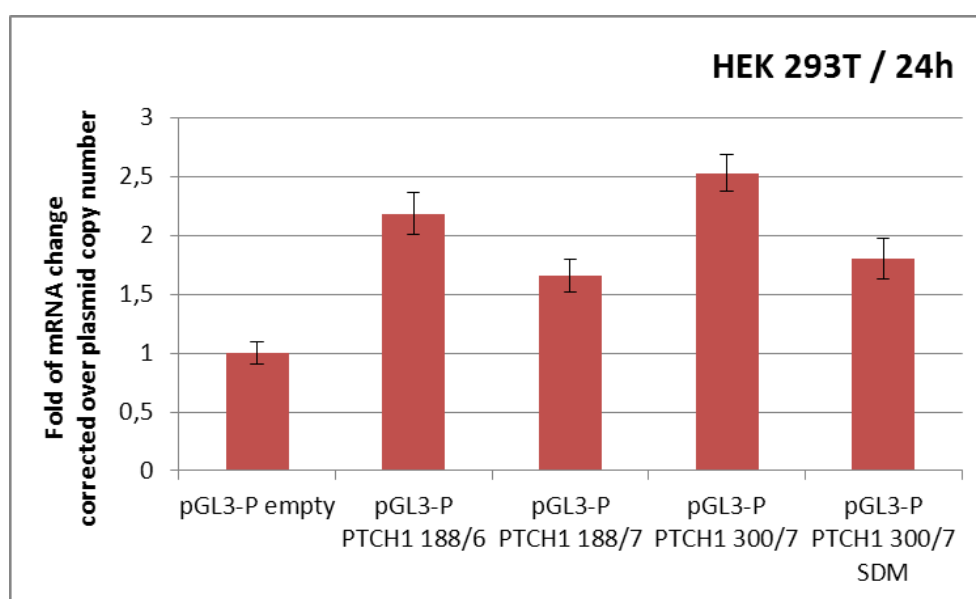


Figure 34. Impact of the *PTCH1b* 5' UTR (CGG)₆ allele and the nullification of 2 upstream AUG codons on the firefly luciferase mRNA expression in HEK 293T. Cloning of 188-nt-long 5' UTR harboring (CGG)₆ or (CGG)₇ allele caused more than 2-fold or 1.5-fold increase in luciferase mRNA expression, respectively. Cloning of 300-nt-long 5' UTR showed 2.5-fold increase in reporter gene transcription, while two mutations present in pGL3-P PTCH1 300/7 SDM plasmid caused an increase in firefly luciferase transcription similar to the pGL3-P PTCH1 188/7 plasmid.

4.5. Expression Patterns of 188- and 300-nucleotide-Long *PTCH1b* 5' UTRs in Cancer Cells under Basal and Endogenously Activated Hedgehog-Gli Signaling Pathway

Quantification of the expression of *PTCH1b* containing the 188- and 300-nucleotide-long 5' UTR under basal level and endogenously activated Hh-Gli signaling pathway showed that in both HCT116 and MCF-7 cells the longer transcript is preferentially expressed after pathway activation with Gli1 transcription factor, [$t(4) = 3.142$, $P=0.0348$] and [$t(4) = 15.47$, $P=0.0001$], respectively. It could be also seen that an activation of the Hh-Gli pathway caused much higher expression of *PTCH1b* 5' UTRs in MCF-7 breast cancer cells compared to the HCT116 cells (Figure 35).

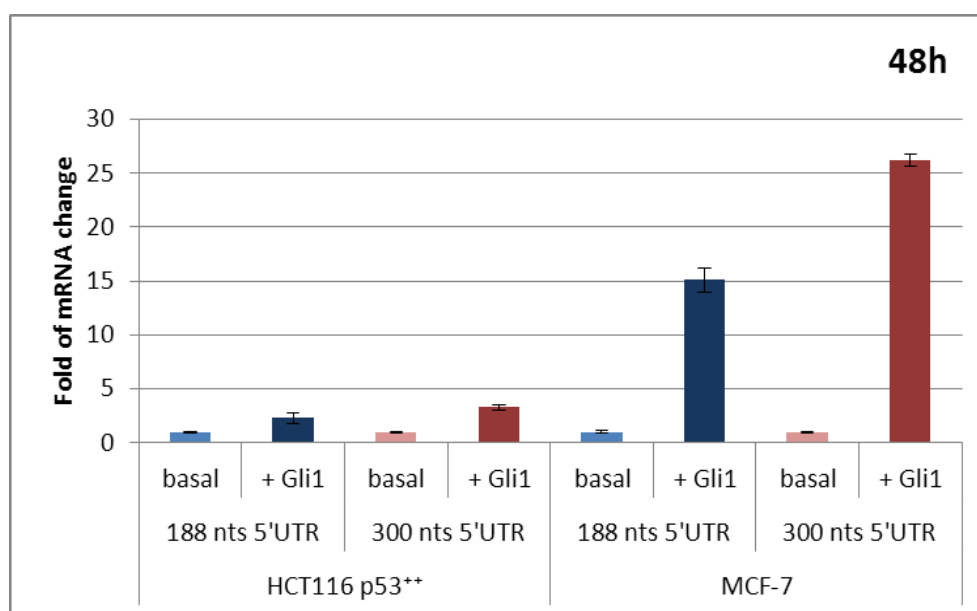


Figure 35. Quantification of 188- and 300-nucleotide-long *PTCH1b* 5' UTRs in 2 cancer cell lines under basal level and 48 hours after endogenously activated Hedgehog-Gli signaling pathway. In both cell lines activation of Hedgehog-Gli signaling resulted in preferential expression of longer 5' UTR. Under activated Hh-Gli pathway, expression of *PTCH1b* 5' UTRs is much higher in MCF-7 cells compared to HCT116 cells.

4.6. Prediction of Secondary Structure of *PTCH1b* 5' UTR

4.6.1. Prediction of Secondary Structure of 188-nucleotide-long *PTCH1b* 5' UTR

For 188-nucleotide-long *PTCH1b* 5' UTR harboring 5, 6, 7 or 8 CGG repeats the *mfold* server has predicted the secondary structures with the corresponding minimum free energy of -91.9 kcal/mol, -94.4 kcal/mol, -96.4 kcal/mol, and -100.3 kcal/mol, respectively (Figure 36). It can be seen that one additional CGG triplet on average gives more stable secondary structure by just -2.8 kcal/mol, which is insufficient for a significant impact on the translational efficiency.

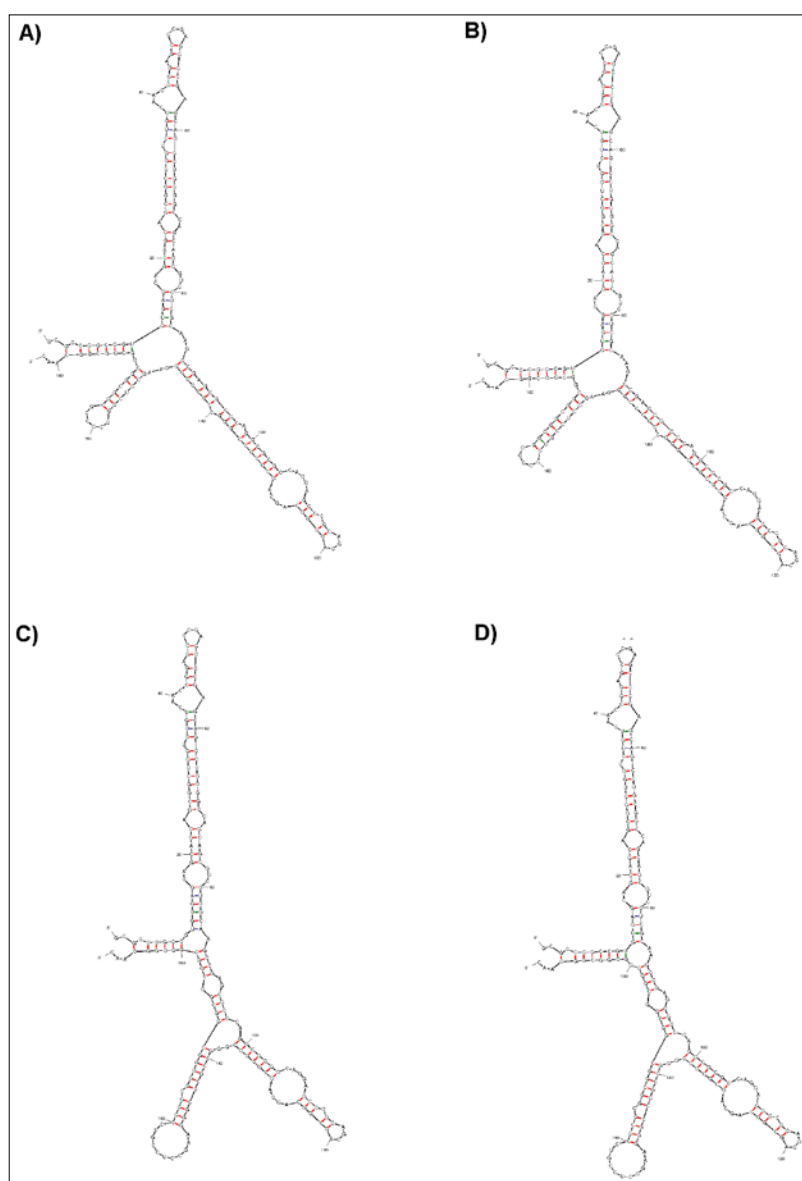


Figure 36. Predicted secondary structures of 188-nucleotide-long *PTCH1b* 5' UTR with **A)** 5, **B)** 6, **C)** 7 and **D)** 8 CGG repeats. One additional CGG triplet on average gives a more stable secondary structure by -2.8 kcal/mol.

4.6.2. Prediction of Secondary Structure of 300-nucleotide-long *PTCH1b* 5' UTR

For 300-nucleotide-long *PTCH1b* 5' UTR harboring 5, 6, 7 or 8 CGG repeats the *mfold* server has predicted the secondary structures with the corresponding minimum free energy of -148.9 kcal/mol, -152.9 kcal/mol, -153.9 kcal/mol, and -157.7 kcal/mol, respectively (Figure 37). It can be seen that one additional CGG triplet on average gives more stable secondary structure by just -2.93 kcal/mol, which is insufficient for a significant impact on the translational efficiency.

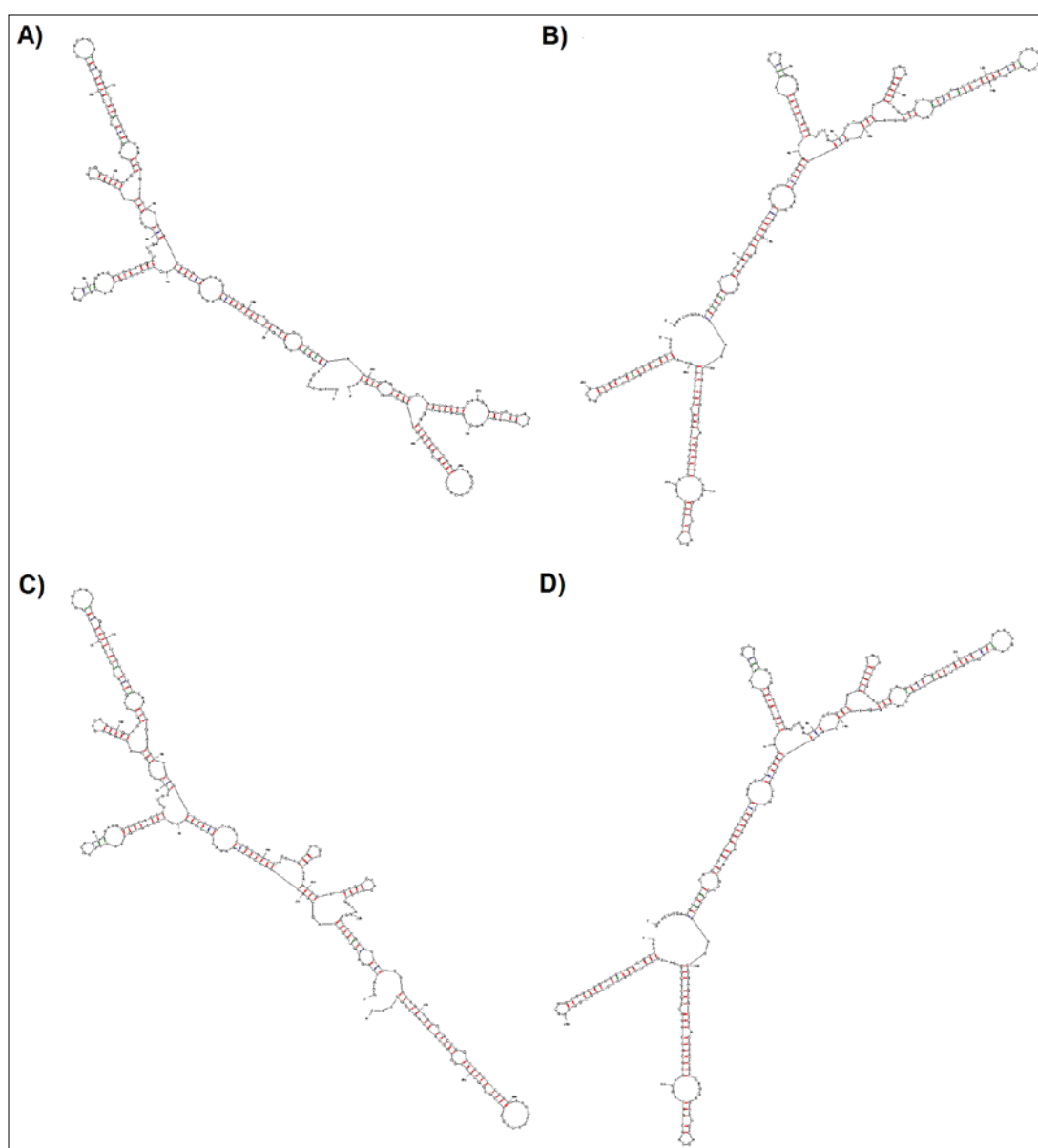


Figure 37. Predicted secondary structures of 300-nucleotide-long *PTCH1b* 5' UTR with **A)** 5, **B)** 6, **C)** 7 and **D)** 8 CGG repeats. One additional CGG triplet on average gives a more stable secondary structure by -2.93 kcal/mol.

4.7. Bicistronic Dual-luciferase Reporter Vectors with Cloned *PTCH1b* 5' UTR

In total, 9 different bicistronic plasmids were constructed using an “empty” pRuF vector as a vector backbone (Figure 38). For 188-nucleotide long 5' UTR we constructed 3 different plasmids, harboring an allele with 5, 7 or 8 CGG repeats, that were named “pRuF PTCH1 188/5”, “pRuF PTCH1 188/7” and “pRuF PTCH1 188/8”, respectively. For 300-nucleotide long 5' UTR we constructed 3 different plasmids harboring an allele with 5, 7 or 8 CGG repeats, and named them “pRuF PTCH1 300/5”, “pRuF PTCH1 300/7” and “pRuF PTCH1 300/8”, respectively. Two additional pRuF-based plasmids were constructed by removing the predicted *PTCH1* IRES motif from the “pRuF PTCH1 188/7” and “pRuF PTCH1 300/7” plasmids (Figure 14B), and they were named “pRuF PTCH1 188 Δ IRES” and “pRuF PTCH1 300 Δ IRES”, respectively. On the other side, plasmid with a DNA insert containing only 76 nucleotides predicted to be an IRES motif (Figure 14A) was named “pRuF PTCH1 IRES”.

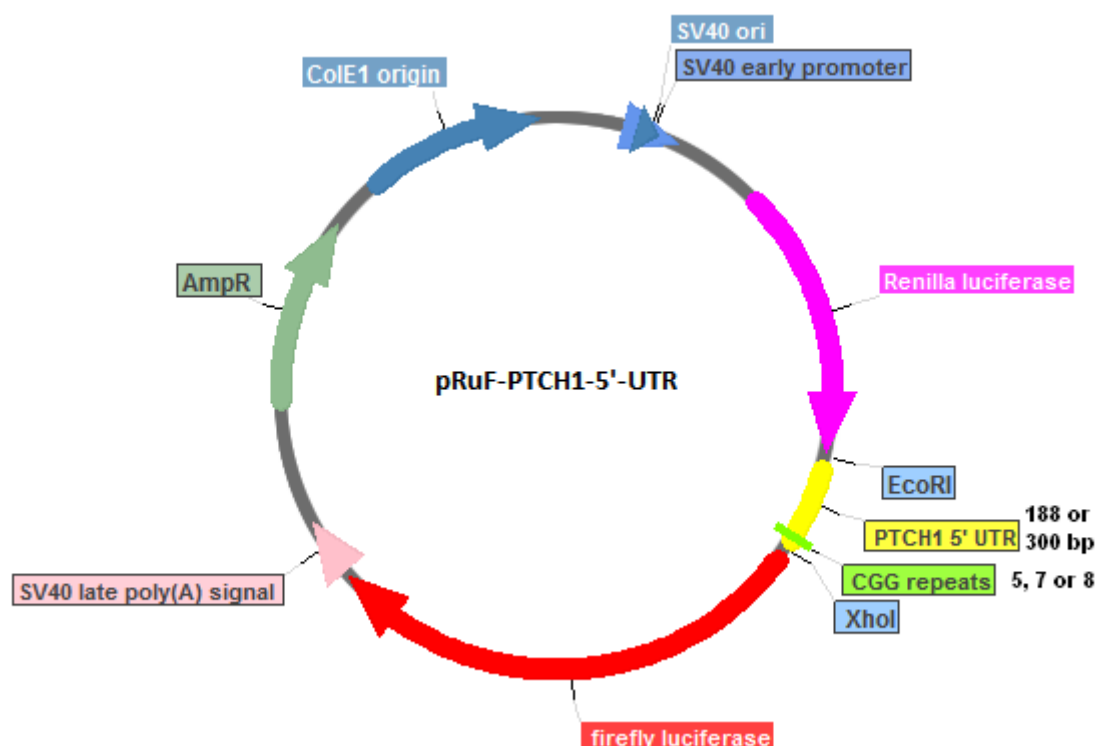


Figure 38. Circular map of bicistronic pRuF-based plasmids with different sized *PTCH1b* 5' UTR harboring different CGG-repeat allele, cloned in the inter-cistronic region between *Renilla* and firefly luciferase gene. If *PTCH1b* 5' UTR contains an internal ribosome entry site (IRES), firefly luciferase would be translated in cap-independent manner.

4.8. Impact of Different *PTCH1b* 5' UTR Size and CGG-repeat Number on Cap-independent Translation of Firefly Luciferase Gene

4.8.1. Results of Dual-Luciferase Reporter Assay in MCF-7 Cell Line

Results of luciferase assay performed in transfected MCF-7 cells showed that cloning of *PTCH1b* 5' UTR into the bicistronic region caused significant increase of firefly luciferase activity compared to the “empty” pRuF plasmid [$F(7, 16) = 36.50, P < 0.0001$] (Figure 39). Cloning of both sized *PTCH1b* 5' UTRs, harboring either (CGG)₅, (CGG)₇ or (CGG)₈ alleles, caused on average 8.5-fold increase in firefly luciferase activity. The results also showed that neither number of CGG repeats nor length of 5' UTR caused any difference on the extent of firefly reporter induction, which could be interpreted as a lack on effect on the extent to which *PTCH1b* 5' UTR affect cap-independent translation of firefly luciferase mRNA. More interestingly, the levels of an increased firefly luciferase activity for all 6 pRuF *PTCH1* plasmids used were similar to the activity of pRuF plasmid with cloned 5' UTR of *c-Myc* gene that is known to harbor an internal ribosome entry site (IRES) (Carter et al, 1999).

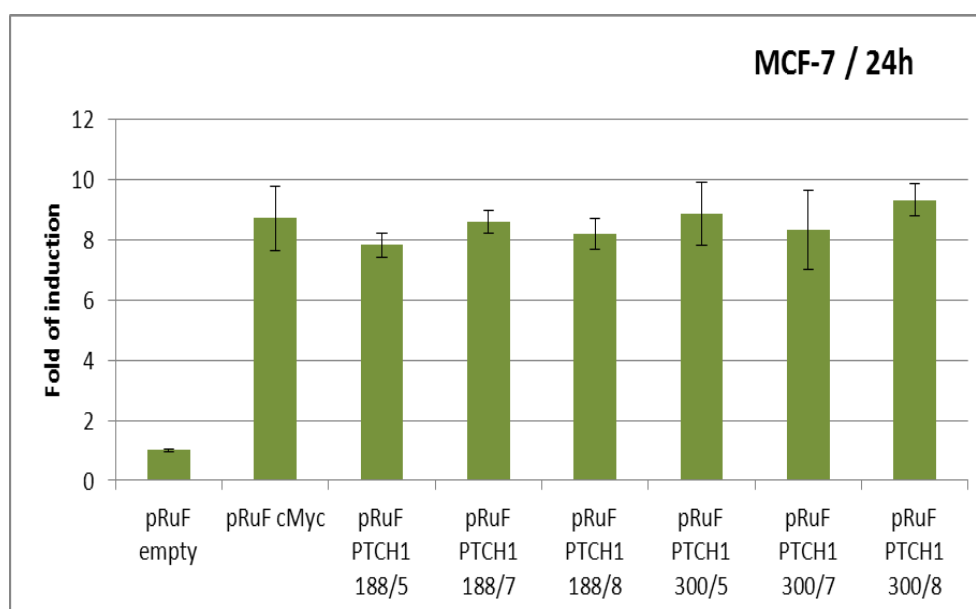


Figure 39. Impact of different *PTCH1b* 5' UTR size and CGG-repeat number on cap-independent translation of firefly luciferase gene in MCF-7 cells. Cloning of both sized *PTCH1b* 5' UTRs, harboring either (CGG)₅, (CGG)₇ or (CGG)₈ allele, caused on average an 8.5-fold increase in firefly luciferase activity, the same as pRuF plasmid harboring 5' UTR of *MYC* gene with known internal ribosome entry site.

4.8.2. Results of Dual-Luciferase Reporter Assay in HEK 293T Cell Line

Results of luciferase assay performed in transfected HEK 293T cells showed that cloning of *PTCH1b* 5' UTR into the bicistronic region caused significant increase in firefly luciferase activity compared to the “empty” pRuF plasmid [$F(7, 15) = 238.5, P < 0.0001$] (Figure 40). Cloning of both sized *PTCH1b* 5' UTRs, harboring either (CGG)₅, (CGG)₇ or (CGG)₈ allele, caused on average 4.5-fold increase in firefly luciferase activity. In this cell line, the activity of pRuF plasmid with c-Myc 5' UTR was significantly higher, causing about 5.5-fold increase in firefly luciferase activity. Regarding the number of CGG repeats, only (CGG)₈ allele in the context of 300-nt-long 5' UTR has shown slight, but significant increase in firefly luciferase activity compared to (CGG)₅ and (CGG)₇ alleles. Visually it seems that higher number of CGG repeats gives a trend for higher activity of firefly luciferase.

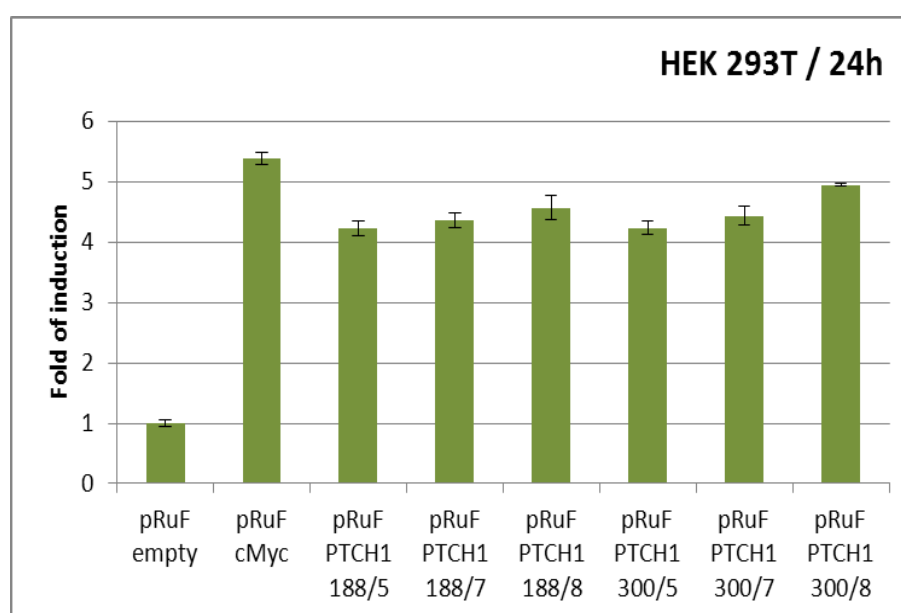


Figure 40. Impact of different *PTCH1b* 5' UTR Size and CGG-repeat number on cap-independent translation of firefly luciferase gene in HEK 293T cells. Cloning of both sized *PTCH1b* 5' UTRs, harboring either (CGG)₅, (CGG)₇ or (CGG)₈ allele, caused on average 4.5-fold increase in firefly luciferase activity. Activity of pRuF plasmid with c-Myc 5' UTR was significantly higher compared to pRuF PTCH1-type plasmids.

4.9. Ruling-out the Presence of Cryptic Promoter within *PTCH1b* 5' UTR

4.9.1. Results of Firefly and *Renilla* Luciferase mRNA Quantification in MCF-7 Cell Line

The *Renilla* and firefly luciferase mRNA quantification performed in transfected MCF-7 cells showed that the relative ratio of firefly to *Renilla* luciferase mRNA for pRuF PTCH1 188/5 and pRuF PTCH1 300/7 plasmids was slightly but significantly higher than 1.0 [F (7, 16) = 11.8, $P < 0.0001$] (Figure 41). This could potentially indicate that for these 2 plasmids there was a cryptic promoter within *PTCH1b* 5' UTR insert, and that higher activity of the firefly reporter gene could arise at least in part from the firefly luciferase translated in a cap-dependent manner from capped firefly luciferase mRNA. However, since the firefly luciferase activity for those two plasmids didn't differ compared to the other pRuF-type PTCH1 plasmids (Figure 39), and that the mRNA quantification showed at best a 40% increase in firefly/*Renilla* mRNA ratio, while the reporter activity increased at least 8 fold, the involvement of cryptic promoter is not likely.

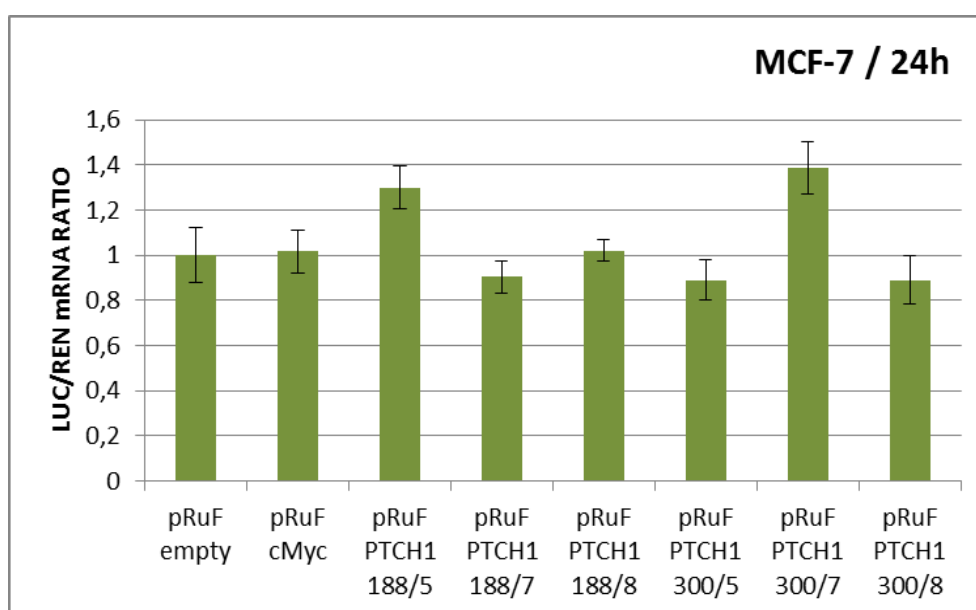


Figure 41. Firefly (LUC) to *Renilla* (REN) luciferase mRNA ratio in transfected MCF-7 cells. The ratio for pRuF PTCH1 188/5 and pRuF PTCH1 300/7 plasmids was higher than 1.0 what could indicate a potential cryptic promoter activity of a DNA insert cloned into these two plasmids.

4.9.2. Results of Firefly and *Renilla* Luciferase mRNA Quantification in HEK 293T Cell Line

The *Renilla* and firefly luciferase mRNA quantification performed in transfected HEK 293T cells showed that the relative ratio of firefly to *Renilla* luciferase mRNA for all pRuF-type PTCH1 plasmids was not significantly different from 1.0 [F (5, 12) = 1.634, $P=0.2249$] (Figure 42). These results ruled-out the presence of a potential cryptic promoter within *PTCH1b* 5' UTR inserts, and indicate that the higher activity of the firefly reporter gene (Figure 40) arose from the firefly luciferase translated from a bicistronic pRuF mRNA in a cap-independent manner.

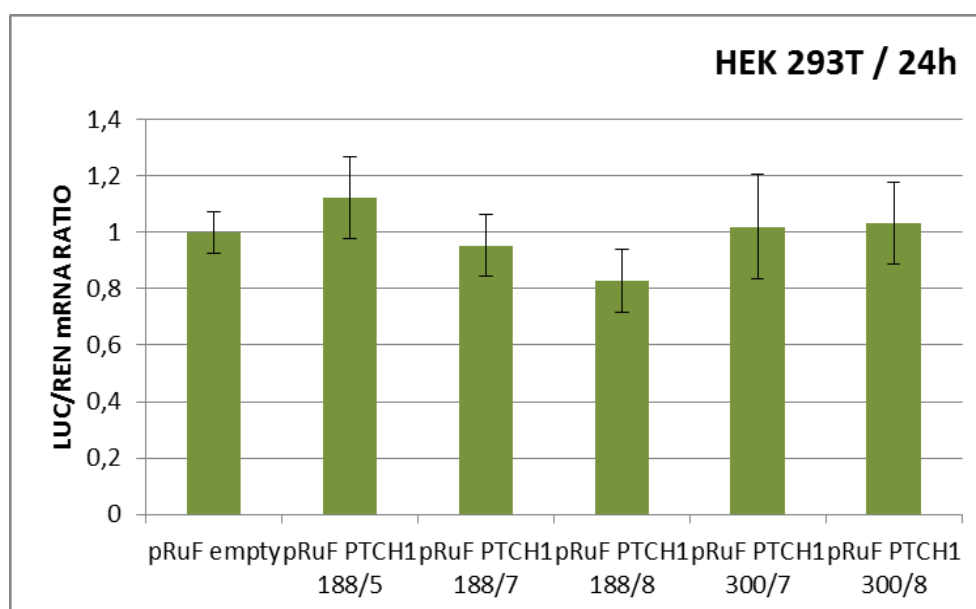


Figure 42. Firefly (LUC) to *Renilla* (REN) luciferase mRNA ratio in HEK 293T cells. The ratio for all pRuF-type PTCH1 plasmids was not significantly different from 1.0 what additionally supported the assumption of IRES motif presence within the *PTCH1b* 5' UTR.

4.10. Precise Localization of IRES Motif within *PTCH1b* 5' UTR

The *UTRscan* software has predicted that the first 76 nucleotides from the 3' part of *PTCH1b* 5' UTR (Figure 43) shares a structural similarity with the common RNA structural motif involved in an internal initiation of translation of cellular mRNAs (Figure 44), as proposed by Le and Maizel (Le and Maizel, 1997).

```

1  gcgcccgcgcg  tgtgagcagc  agcagcggct  ggtctgtcaa  cggagaccgc  agcccgagca
61  gcctgcgggcc  agcagcgtcc  tcgcaagccg  agcgcgccag  cgcgccagga  gccccgcagca
121 gcggcagcag  cgcgccgggc  cgcccgggaa  gcctccgtcc  cgcggcgggc  ggcggcgggc
181 gcggcaac

```

Figure 43. Precise localization of putative internal ribosome entry site (IRES) motif within *PTCH1b* 5' UTR. *UTRscan* software has predicted an IRES element within the first 76 nucleotides from the 3' part of *PTCH1b* 5' UTR.

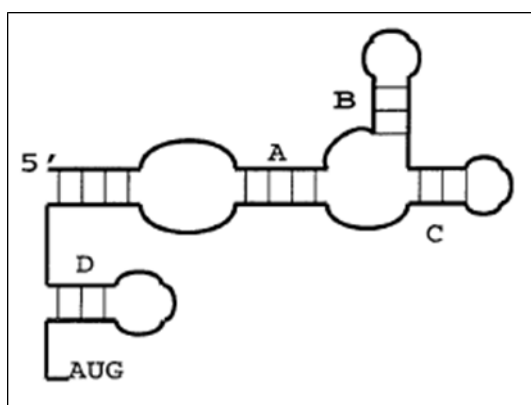


Figure 44. A common RNA structural motif involved in the internal initiation of translation of cellular mRNAs. This motif is used by *UTRscan* software for predicting the putative IRES motifs within the 5' UTR sequences. (figure from: Le and Maizel, 1997)

4.11. Impact of Putative *PTCH1b* IRES Motif on Cap-independent Translation of Firefly Luciferase Gene

4.11.1. Results of Dual-Luciferase Reporter Assay in MCF-7 Cell Line

Results of luciferase assay performed in transfected MCF-7 cells showed that remodeled pRuF-type plasmids, constructed by removing or preserving the putative *PTCH1b* IRES motif, caused significant changes in firefly luciferase activity compared to the complete pRuF *PTCH1* plasmids [$F(6, 13) = 97.28, P < 0.0001$] (Figure 45). Removing 76 nucleotides from pRuF *PTCH1* 188/7 plasmid caused a decrease in firefly luciferase activity by 29%, while removing those nucleotides from pRuF *PTCH1* 300 plasmid caused a decrease by 71%. Plasmid having only putative *PTCH1b* motif cloned within a bicistronic region achieved just 47% of the activity obtained by either pRuF *PTCH1* 188/7 or pRuF *PTCH1* 300/7 plasmid, indicating that those 76 nucleotides alone are not sufficient for the complete IRES activity of intact *PTCH1b* 5' UTRs.

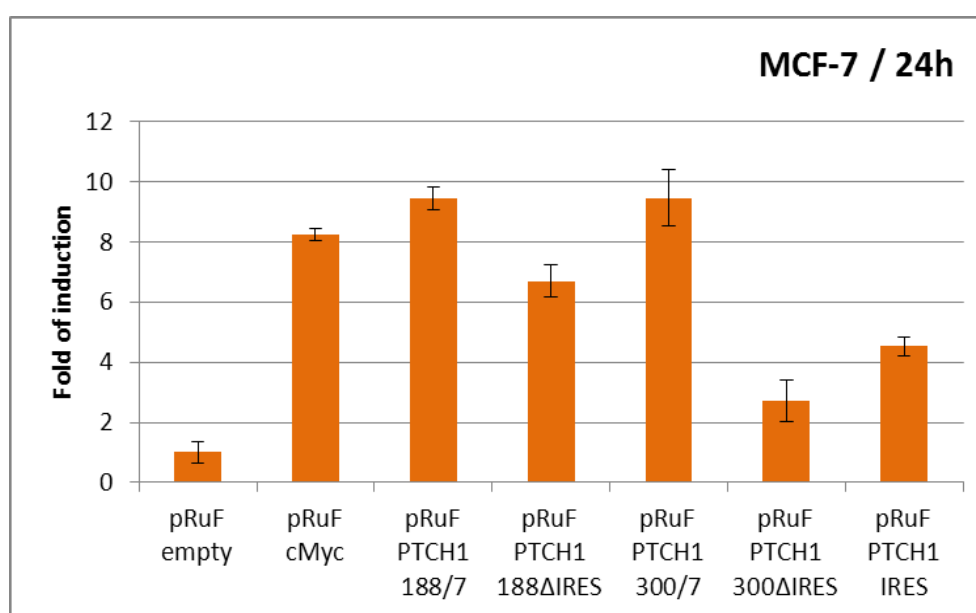


Figure 45. Impact of putative *PTCH1b* IRES motif and the remaining part of *PTCH1b* 5' UTRs on cap-independent translation of firefly luciferase gene in MCF-7 cells. Removing 76 nucleotides from pRuF *PTCH1* 188/7 plasmid caused decrease in firefly luciferase activity by 30%, while removing those nucleotides from pRuF *PTCH1* 300 plasmid caused a decrease by 70%. Those 76 nucleotides alone achieved 47% of activity obtained by complete pRuF *PTCH1* plasmids.

4.11.2. Results of Dual-Luciferase Reporter Assay in HEK 293T Cell Line

Results of luciferase assay performed in transfected HEK 293T cells showed that removing or preserving putative *PTCH1b* IRES motif caused significant change in firefly luciferase activity when compared to the complete pRuF *PTCH1* plasmids [F (6, 13) = 241.6, $P < 0.0001$] (Figure 46). Removing 76 nucleotides from pRuF *PTCH1* 188/7 plasmid caused a decrease in firefly luciferase activity by 66%, while removing those nucleotides from pRuF *PTCH1* 300 plasmid caused a decrease by 87%. Plasmid having only a putative *PTCH1b* IRES motif cloned within a bicistronic region achieved 63% of the activity obtained by the complete pRuF *PTCH1* 188/7 plasmid, and 44% of the activity of the complete pRuF *PTCH1* 300/7 plasmid. These results also indicated that those 76 nucleotides alone are not sufficient for the complete IRES activity of intact *PTCH1b* 5' UTRs. It has to be emphasized that in this experiment the activity of pRuF *PTCH1* 188/7 plasmid was lower compared to either pRuF c-Myc or pRuF *PTCH1* 300/7 plasmid, which hasn't been observed in previous cases.

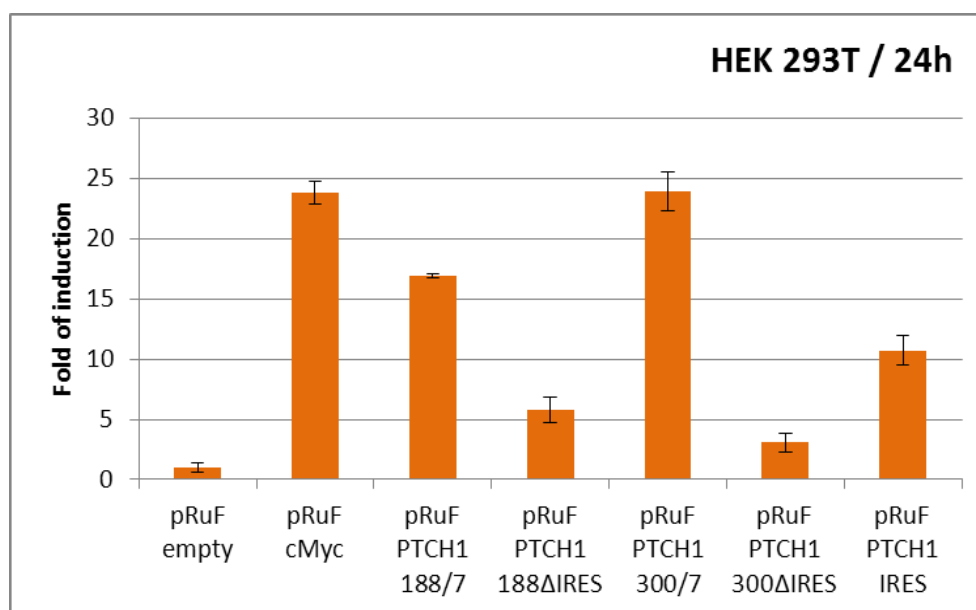


Figure 46. Impact of putative *PTCH1b* IRES motif and the remaining part of *PTCH1b* 5' UTRs on cap-independent translation of firefly luciferase gene in HEK 293T cells. Removing 76 nucleotides from pRuF *PTCH1* 188/7 plasmid caused a decrease in firefly luciferase activity by 66%, while removing those nucleotides from pRuF *PTCH1* 300 plasmid caused a decrease by 87%. Those 76 nucleotides alone achieved 63% and 44% of activity obtained by either complete pRuF *PTCH1* 188/7 or pRuF *PTCH1* 300/7 plasmid, respectively.

4.12. Ruling-out the Presence of Cryptic Promoter within Putative *PTCH1b* IRES Motif4.12.1. Results of Firefly and *Renilla* Luciferase mRNA Quantification in MCF-7 Cell Line

The *Renilla* and firefly luciferase mRNA quantification performed in transfected MCF-7 cells showed that the relative ratio of firefly to *Renilla* luciferase mRNA for all remodeled pRuF-type PTCH1 plasmids was not significantly different from 1.0 [F (5, 12) = 5.285, $P=0.0085$] (Figure 47). These results ruled-out a potential cryptic promoter within remodeled *PTCH1b* 5' UTR inserts, and indicated that a decreased activity of the firefly reporter gene obtained by removing or preserving putative *PTCH1b* IRES motif (Figure 45) arose from reduced IRES-dependent translation of firefly luciferase mRNA.

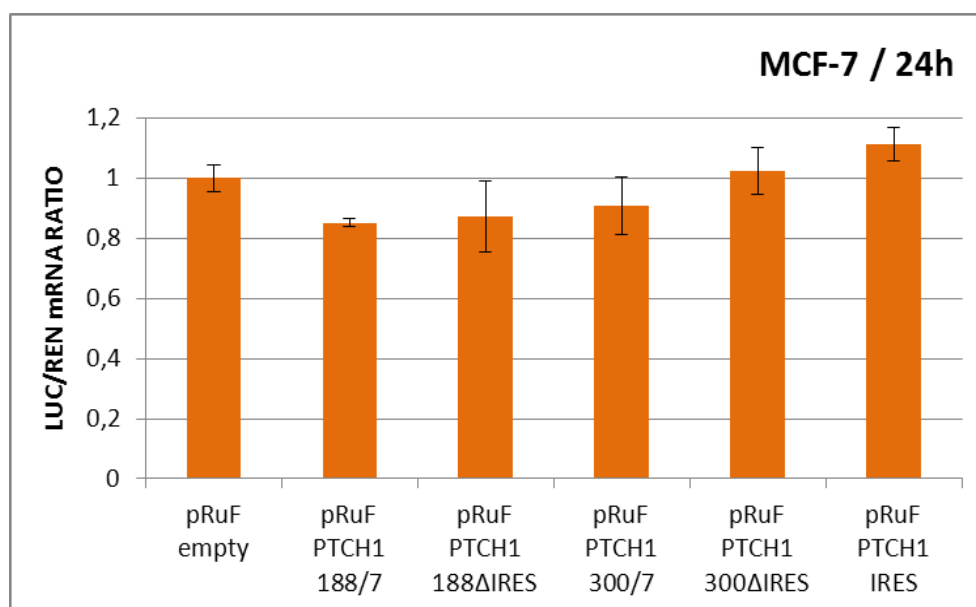


Figure 47. Firefly (LUC) to *Renilla* (REN) luciferase mRNA ratio in transfected MCF-7 cells. The ratio for all remodeled pRuF-type PTCH1 plasmids was not significantly different from 1.0 what was additional conformation of potential IRES motif presence within the *PTCH1b* 5' UTR.

4.12.2. Results of Firefly and *Renilla* Luciferase mRNA Quantification in HEK 293T Cell Line

The *Renilla* and firefly luciferase mRNA quantification performed in transfected HEK 293T cells showed that the relative ratio of firefly to *Renilla* luciferase mRNA for all remodeled pRuF-type PTCH1 plasmids was not significantly different from 1.0 [$F(5, 12) = 3.336$, $P=0.0405$] (Figure 48). These results ruled-out a potential cryptic promoter within remodeled *PTCH1b* 5' UTR inserts, and indicated that a decreased activity of the firefly reporter gene obtained by removing or preserving putative *PTCH1b* IRES motif (Figure 45) arose from reduced IRES-dependent translation of firefly luciferase mRNA.

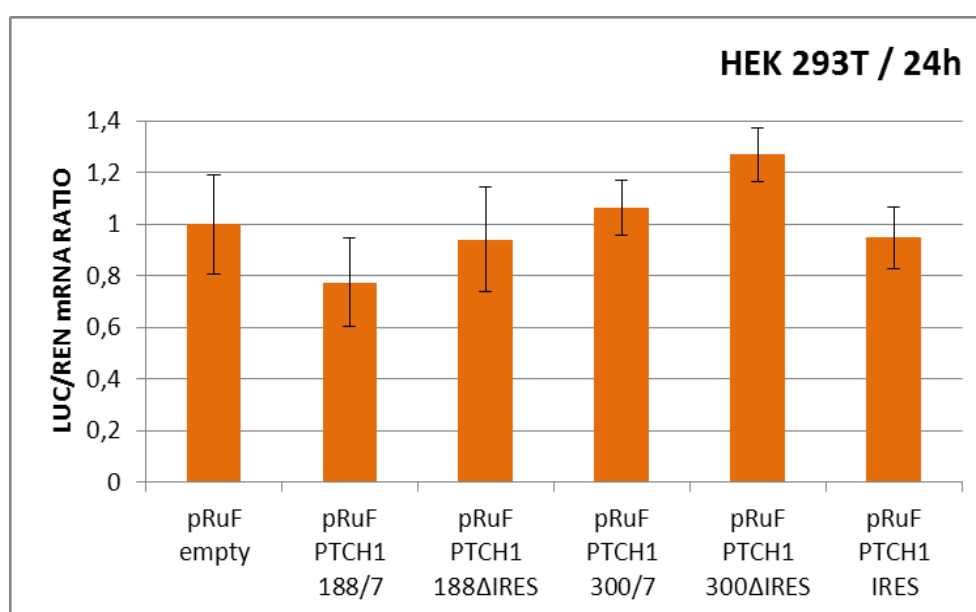


Figure 48. Firefly (LUC) to *Renilla* (REN) luciferase mRNA ratio in transfected HEK 293T cells. The ratio for all remodeled pRuF-type PTCH1 plasmids was not significantly different from 1.0 what was again additional conformation of putative IRES motif presence within the *PTCH1b* 5' UTR.

4.13. Ruling-out an Alternative Splicing of pRuF Bicistronic mRNAs with Different Cloned Fragments

Equal sizes of both *Renilla* (877 bp) and firefly (2,204 bp + DNA insert) luciferase amplicons, regardless the cDNA template used, are proof that there was no alternative splicing of pRuF bicistronic mRNA (Figures 15 and 49). This is also a proof that there is no additional, capped firefly luciferase mRNA transcript which can be cause of an increased firefly luciferase activity seen in dual-luciferase reporter assays (Figures 39, 40, 45 and 46).

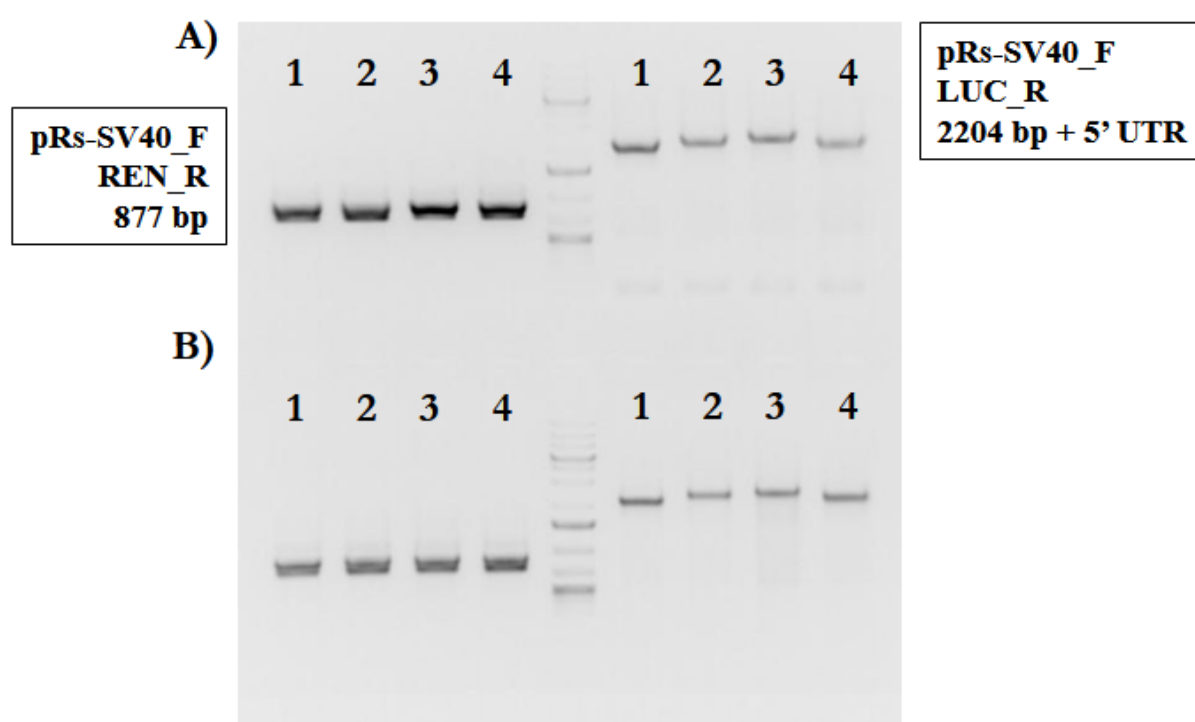


Figure 49. Picture of agarose gel with PCR amplicons amplified from *Renilla* and firefly luciferase cistrons. As a template it was used cDNA extracted from **A)** MCF-7 and **B)** HEK 293T cell line. Both cell lines were transfected with: 1, “empty” pRuF; 2, pRuF PTCH1 188/7; 3, pRuF PTCH1 300/7; and 4, pRuF PTCH1 IRES plasmids. The size of PCR amplicons was estimated according to the GeneRuler 1 kb Plus DNA Ladder standard (Thermo Fisher Scientific, USA) (middle lane).

4.14. Effects of Hypoxia and Rapamycin Treatment on Cap-independent Translation of Firefly Luciferase Gene

4.14.1. Results of Dual-Luciferase Reporter Assay in MCF-7 Cell Line after Treatment with Hypoxia and Rapamycin

Two-way analysis of variance showed that both the treatment [$F(2, 30) = 86.15, P < 0.0001$] and the type of pRuF plasmid used for the transfection of MCF-7 cells [$F(4, 30) = 114.9, P < 0.0001$] showed significant effects on the firefly luciferase activity, also with the significant interaction between the treatments and plasmid types [$F(8, 30) = 14.31, P < 0.0001$]. Among the treatments, only hypoxic conditions caused increased firefly luciferase activity for the plasmids harboring either *MYC* or *PTCH1b* 5' UTR (Figure 50). Plasmid with deleted putative *PTCH1b* IRES motif didn't respond to any treatment.

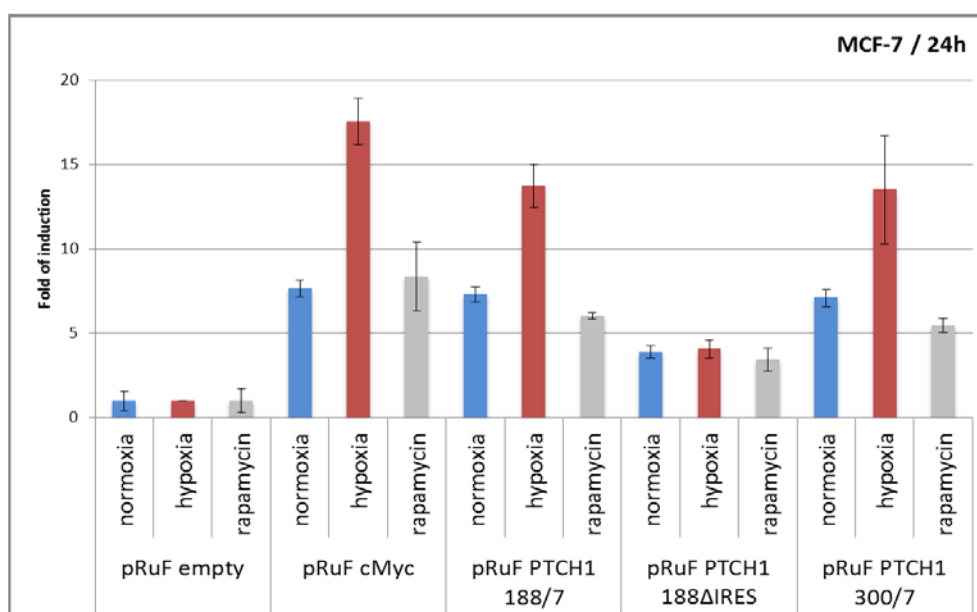


Figure 50. Impact of hypoxia and rapamycin treatment on the activity of *PTCH1b* IRES motif in cap-independent translation of firefly luciferase gene in MCF-7 cells. Only hypoxic conditions caused increased firefly luciferase activity for plasmids harboring either *MYC* or *PTCH1b* 5' UTR, which are assumed to bear internal ribosome entry sites.

4.14.2. Results of Dual-Luciferase Reporter Assay in HEK 293T Cell Line after Treatment with Hypoxia and Rapamycin

Two-way analysis of variance showed that both the treatment [$F(2, 39) = 51.36, P < 0.0001$] and the type of pRuF plasmid used for the transfection of HEK 293T cells [$F(6, 39) = 305.1, P < 0.0001$] showed significant effect on the firefly luciferase activity, also with the significant interaction between the treatments and plasmid types [$F(12, 39) = 6.472, P < 0.0001$].

Surprisingly, both types of treatments caused a decrease in firefly luciferase activity only for plasmids harboring either *MYC* or *PTCH1b* IRES motif (Figure 51). The treatments didn't show any effect on the activity of two plasmids with removed 76 nucleotides assumed to bear the *PTCH1b* IRES motif.

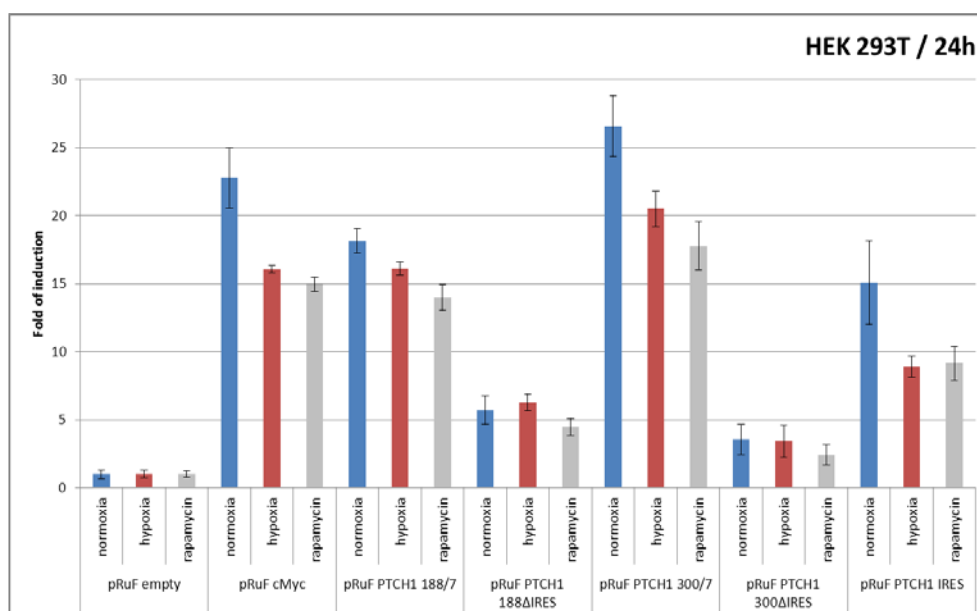


Figure 50. Impact of hypoxia and rapamycin treatment on the activity of *PTCH1b* IRES motif in cap-independent translation of firefly luciferase gene in HEK 293T cells. Both types of treatments caused a decrease in firefly luciferase activity only in plasmids harboring internal ribosome entry site.

4.15. Evolutionary Conservation of *Cis*-regulatory Elements Found in 5' UTR of *PTCH1b* Gene

Figure 52. Multiple alignment of the genomic sequences homologous to the 372-nucleotide-long 5' UTR of human *PTCH1b* gene. Comparative analysis showed that the most conserved *cis*-regulatory elements are three upstream AUG codons, although the STOP codons are not present in all of the species. The number of CCG repeats also varies among the species, and ranges from 3 to 11 repeats.

5. Discussion

PTCH1 tumor suppressor gene codes for a receptor with a negative regulatory role in the Hedgehog signaling pathway (Figure 1). Constitutive activation of Hh-Gli signaling can be induced by inactivation of *PTCH1* gene, which can be caused by means of different genetic and epigenetic mechanisms. *PTCH1* germline mutations cause Gorlin syndrome, disorder characterized by many different developmental abnormalities and tumor susceptibility. Most of the malformations are caused by *PTCH1* haploinsufficiency, meaning that proper amount of Ptch1 protein is needed for performing its tasks in signal transduction (Fodde and Smiths, 2002). This fact provides evidence that fine-tuned elements are prerequisite to properly regulate the Hedgehog-Gli signaling pathway. So far, much is known about the genomic organization of *PTCH1* gene, its transcripts and their protein products (Figures 2 and 3). On the other hand, much less is known about the transcriptional regulation of each known *PTCH1* transcript, and even less is known about the 5' untranslated regions of any known *PTCH1* transcript.

In 2004, a novel polymorphism involving a CGG trinucleotide repeat was discovered in 5' UTR of *PTCH1* gene, transcript 1b (Nagao et al, 2004). It was located 4 nucleotides upstream of the translation initiation site, i.e., separated from AUG codon by CAAC tetranucleotide. The major allele contained 7 repeats, while the minor contained 8 (rs71366293). In our previous research, in patients with different types of ovarian neoplasms and healthy controls, besides (CGG)₇ and (CGG)₈ we identified 2 additional alleles – (CGG)₅, which was found in one healthy control sample, and (CGG)₆ allele, which was found in one ovarian cancer patient (Musani et al, 2012). Since the initial discovery of this trinucleotide repeat variant, its proximity to the AUG codon suggested that this polymorphism, more precisely the number of CGG repeats, could affect the efficacy of 5' UTR in its regulatory role of *PTCH1* expression. To address this issue, Nagao and colleagues also conducted a functional analysis by cloning various (CGG)_nCAAC constructs into the luciferase reporter vector pGV-P2, between the Simian vacuolating virus 40 (SV40) promoter and firefly luciferase gene (Nagao et al, 2004). The results of luciferase assays, performed 24 hours post-transfection in HEK 293 cells, revealed a positive correlation (unfortunately without any statistical proof) between the CGG-repeat number and the luciferase activity, meaning that the reporter gene activity gradually increased with the higher number of CGG repeats (Figure 53A). The quantification of firefly luciferase mRNA showed no significant differences in the reporter gene transcription levels

regarding the CGG-repeat number, leading to the conclusion that the increase in luciferase activity with the expansion of CGG repeats is due to the increased efficiency of firefly luciferase translation (Figure 53B). Consequently, a CGG-repeat number could potentially alter the expression level of Ptc1 protein, which may have an effect on the severity of the disease in which certain CGG-repeat allele was found.

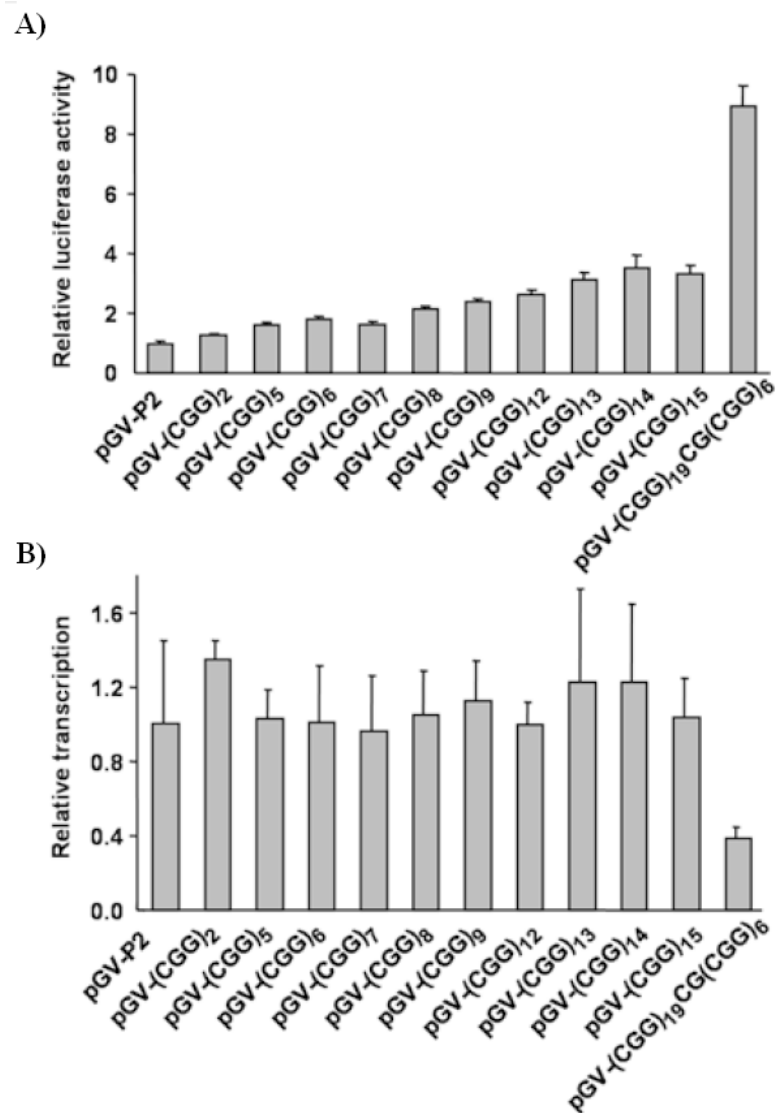


Figure 53. The effect of CGG-repeat number (n) on **A)** firefly luciferase activity and **B)** firefly luciferase transcription, compared to the “empty” pGV-P2 plasmid. Regarding the *PTCH1* 5' UTR, only (CGG)_nCAAC constructs were cloned into the reporter vector backbone. Luciferase assays and total RNA extractions were performed 24 hours post-transfection in/from HEK 293 cells. (figure from: Nagao et al, 2004)

Potentially biggest drawback of Nagao's research was taking the CGG-repeat polymorphism out of the context of the complete *PTCH1b* 5' UTR sequence, concerning the potential existence of different 5' UTR *cis*-regulatory elements that could participate in the *PTCH1b* expression regulation, and whose proper activity could be affected by the CGG-repeat polymorphism. For that reason we wanted to re-evaluate a potential effect of 5' UTR CGG-repeat polymorphism on the transcription and/or translation of downstream mRNA, but this time in more physiological context of the complete *PTCH1b* 5' UTR sequence.

In literature and nucleotide databases, the 5' UTR of the main *PTCH1* transcript is annotated in 3 different lengths – 188, 300 and 372 nucleotides. At the beginning of our study this inconsistency seemed like an experimental artifact or an error in database curation. On the other hand, this was also an additional encouragement for us to re-explore the effects of before mentioned CGG-repeat polymorphism, and also all the other regulatory elements potentially present in 5' UTR of *PTCH1b* gene.

In order to thoroughly examine the eventual impact of varying number of CGG repeats, i.e., alleles which were found in Croatian population, on transcription and/or translation of the *PTCH1b* gene, we decided to apply a methodology previously successfully used for the functional analysis of 5' UTR sequence variants of the *p16* gene (Bisio et al, 2010). Using different luciferase reporter constructs (Figure 21) in assays with 3 established human cell lines – one normal (HEK 293T) and two malignant (HCT116 and MCF-7) – it was shown that the number of CGG repeats has no significant impact on the activity of firefly luciferase. Only the allele with 5 CGG repeats caused slight, but statistically significant, increase in activity of the reporter gene, and this was obtained only in the context of 188-nucleotide-long 5' UTR (Figures 23, 25 and 27). When the activities of all 4 “pGL3-P *PTCH1* 188”-type plasmids were compared, we found quite strong negative correlation between the number of CGG repeats and the luciferase activity, $\rho=-0.76$ and $\rho=-0.67$ for MCF-7 and HEK 293T cell line, respectively (Figures 31 and 33). These results, this time involving the plasmids with the complete sequence of *PTCH1b* 5' UTR, was the first big discordance between ours and the results obtained by Nagao and coworkers (Figure 53A). We must emphasize that pGV-P2 reporter vector used by Nagao and colleagues is in fact the same pGL3-Promoter plasmid used by us, and thus the results are comparable.

Computational prediction of *PTCH1b* 5' UTR secondary structure also confirmed that slight increase in the stability of secondary structure, as the result of the increasing number of CGG repeats, could only have a moderate and not a dramatic impact on the efficiency of the *Ptch1* translation (Figures 36 and 37).

Generally, insertion of the complete *PTCH1b* 5' UTR into the pGL3-Promoter plasmid led to a significant increase in luciferase mRNA transcription (Figures 24, 26, 28, 32 and 34), and this finding was the second big discordance between ours and the results obtained in Nagao's research (Figure 53B). Because of that, it seems that *PTCH1b* 5' UTR could have an *enhancing* influence on the transcription of downstream gene. *RegRNA 2.0* web-server predicted various transcriptional regulatory motifs, mostly located within the 188-nt-long *PTCH1b* 5' UTR sequence. The most abundant motifs were binding sites for BEN, ZF5 and ETF transcription factors, of which the later has a consensus binding site "GCGGCGG" (Kageyama et al, 1989). Similarly, for 5' UTR of the fragile X mental retardation 1 gene (*FMR1*) it was found that CGG repeats enhances the transcription of *FMR1* gene by means of CGGBP-20 transcription factor, coded by the CGG triplet repeat binding protein 1 gene (*CGGBP1*) (Chen et al, 2003; Gulyy et al, 2010).

Although this *PTCH1b* CGG-repeat polymorphism is located only 4 nucleotides upstream of the translation initiation site, our results taken all together showed that the number of CGG repeats, in the context of the complete 5' UTR, has no significant impact on either mRNA or protein expression of *PTCH1b* gene. While only alleles with relatively small number of CGG repeats have been found jet (3 and 5 to 8 repeats), so far there has not been found any unambiguous association of a certain number of CGG repeats with a disease. All these favor the thesis that this *PTCH1* polymorphism could not be a genetic background (a causal mutation) of any trinucleotide repeat disorder-like disease.

On average, 2-fold reduction in firefly luciferase activity compared to the "empty" pGL3-P plasmid was observed for plasmids harboring longer, 300- or 372-nucleotide-long *PTCH1b* (Figures 23, 25, 27, 31 and 33). One plausible explanation for this discovery could be that those longer, already with high GC-content, *PTCH1b* 5' UTRs form more stable secondary structures, which hinder the mRNA unwinding capacity of the translation initiation complex and thus lowering the efficiency of protein synthesis.

When the longest *PTCH1b* 5' UTR sequence was computationally analyzed, there was a prediction of two potential upstream open reading frames (uORFs) and one upstream AUG codon, more significantly, present only within the 300- and 372-nucleotide-long *PTCH1b* 5' UTRs (Figure 29). We have mutated two out of three putative upstream AUG codons, of which one was predicted to create an overlapping open reading frame that could potentially interfere with a translation from the main *PTCH1b* open reading frame and thus reduce the level of Ptch1 protein (Figure 22). Thus mutated "pGL3-P *PTCH1* 300/7"-based plasmid restored luciferase activity to the level that was comparable with the "wild-type" pGL3-P

plasmid with cloned 188-nt-long *PTCH1b* 5' UTR (Figures 30, 31 and 33). Removing those two uAUG codons did not change the levels of luciferase mRNA transcription, indicating that observed difference in the luciferase activity occurs at translational level (Figures 32 and 34). It was also shown that this potentially most damaging, overlapping uORF is evolutionary conserved (Figure 51), although there are no known proteins with amino acid sequences similar to any peptide potentially translated from the predicted *PTCH1b* uORFs. This overlapping uORF may lead to a strong translational inhibition from the main ORF coding for Ptch1 protein.

Quantification of *PTCH1b* mRNA containing either 188- or 300-nucleotide-long 5' UTR, under basal level and endogenously activated Hh-Gli signaling pathway, has shown that in both HCT116 and MCF-7 cells the longer transcript was preferentially expressed after the pathway activation. Additionally, we were also able to observe that an activation of the Hh-Gli pathway caused much higher expression of both sized *PTCH1b* 5' UTRs in MCF-7 breast cancer cells compared to colon carcinoma cells HCT116 (Figure 35). The preference for *PTCH1b* transcripts with longer 5' UTR could be one form of spatio-temporal regulation of translation, utilized when lower and much more tightly regulated level of Ptch1 protein is needed.

When results for pGL3-P-type plasmids harboring 188-nt-long *PTCH1b* 5' UTR, obtained from different cell lines, were compared, we could infer that luciferase activity was the highest in transfected MCF-7 cells (Figure 24), while in both HCT116 and HEK 293T cells an increase was on average only 2-fold higher than for the “empty” reporter vector (Figures 23 and 27). The ratio between luciferase activity and mRNA quantity was around 1.0 for MCF-7 cells, which was again higher than for HCT116 and HEK 293T cells (around 0.6 and 0.4, respectively). This led us to the conclusion that protein translation regulated by 188-nt-long *PTCH1b* 5' UTR is more efficient in MCF-7 cells in comparison to the other two cell lines.

Characteristics such as high GC-content, above the average size, potentially highly structured and presence of uORFs and uAUGs, might lead someone to hypothesize that *PTCH1b* 5' UTR in general affect the efficiency of cap-dependent initiation of Ptch1 translation. This might even anticipate that *PTCH1b* 5' UTR possesses a capability to initiate cap-independent, an internal ribosome entry site-driven translation of Ptch1 protein. To test this assumption, we decided to construct bicistronic dual-luciferase pRuF vectors with *PTCH1b* 5' UTR cloned in between *Renilla* and firefly luciferase gene (Figure 38). Both 188- and 300-nt-long 5' UTRs significantly increased a firefly luciferase activity, but with no differences among the repeat numbers (Figures 39 and 41). Quantification of firefly luciferase mRNA proved that the

increased firefly activity is neither due to a potential cryptic promoter activity of *PTCH1b* 5' UTR (Figures 40 and 42), nor to an alternative splicing event (Figure 48). Thus we were able to conclude that observed higher firefly luciferase activity, with equal amount of both *Renilla* and firefly luciferase mRNA, appears to be a post-transcriptional, translational effect!

The first 76 bp nucleotides from the 3' part of *PTCH1b* 5' UTR (c.-1_-76) were predicted to bear a cellular internal ribosome entry site (IRES) (Figure 43). When this putative *PTCH1* IRES motif was removed from either 188- or 300-nt-long pRuF-based plasmid, the firefly luciferase activity was significantly, albeit not completely, reduced. At the same time, those 76 nucleotides alone were not sufficient to obtain the complete IRES activity of intact 5' UTRs. This could indicate that either putative IRES motif spans larger part of *PTCH1b* 5' UTR, even extending to the coding region, or contiguous part(s) of *PTCH1b* 5' UTR harbor binding sites for IRES *trans*-acting factors (ITAFs), prerequisite for proper folding of the IRES motif itself. Results achieved with remodeled pRuF-based *PTCH1* plasmids were also proven to be due to the translational and not transcriptional processes (Figures 14, 44-48).

Considering all the results observed, our research has presented a strong evidence that *PTCH1b* 5' UTR contains an internal ribosome entry site, and is thus potentially capable to initiate *Ptch1* protein translation in cap-independent manner (Figure 4B). Although there aren't similarities between any known virus IRESes and putative *PTCH1* IRES motif, there are a few eukaryotic genes whose 5' UTRs contain proven cellular IRES motifs and share a similarity with the sequence of putative *PTCH1* IRES motif. More interestingly, the highest similarities lie in the presence of CGG-repeat element! Such genes, having at least 3 CGG repeats within their IRES motif, include previously mentioned fragile X mental retardation 1 (*FMRI*), jun proto-oncogene (*JUN*), ornithine decarboxylase 1 (*ODCI*), B-cell CLL/lymphoma 2 (*BCL2*) and BCL2-associated athanogene (*BAG1*) (Chiang et al, 2001; Sehgal et al, 2000; Pyronnet et al, 2000; Sherrill et al, 2004; Coldwell et al, 2001).

Since it was suggested that hypoxic conditions activate the Hh-Gli signaling pathway (Bijlsma et al, 2009), and it is already known that several genes are being translated under the hypoxia by IRES-dependent mechanism (Thomas and Johannes, 2007), we wanted to explore if putative *PTCH1b* 5' UTR IRES can be activated by oxygen deprivation condition. The increased activity of putative IRES element within the 5' UTR of *PTCH1b* gene has been observed in transfected MCF-7 cells after exposure to hypoxic conditions, while rapamycin treatment did not cause any change in an IRES activity (Figure 50). In HEK 293T cells both treatments did not increase, but in fact decreased, the activity of *PTCH1* IRES element (Figure 51). The presence of an IRES element within the *PTCH1b* 5' UTR could thus allow

Ptch1 protein to be synthesized in conditions when the general level of cellular protein synthesis is decreased, such as in cell conditions of reduced oxygen levels, what is also important in tumor development and metastasis, or for the potential therapeutic role of activated Hh-Gli pathway in acute or chronic ischemic heart disease (Pan and Zhou, 2012). In addition, the activation of the IRES motif can allow overcoming the negative effect of uORFs and uAUG within the 300- or 372-nt-long 5' UTR transcripts (Figures 23, 25, 27, 31, 33, 39 and 40). Coupled to our observation that Gli1 expression can induce the transcription of *PTCH1b* transcript containing the longer version of the 5' UTR, these results could lead to the hypothesis that ensuing negative feedback loop can also be fine-tuned at post-transcriptional levels by the competition between uORFs/uAUG translation inhibition and IRES-dependent translation initiation.

Although the number of reports on cellular IRESes is increasing, their existence still raises skepticism and is often subject of scientific debates, mainly due to concerns about the lack of unambiguous experimental verifications. The fact that there are a growing number of cancer-related genes whose translation regulation can be subjected to cap-independent initiation makes the quest for discovering and testing new putative cellular IRESes even more meaningful (reviewed in Ozretić et al, 2012). Deciphering their sequence, structure, molecular mechanisms of action and requirements for additional trans-acting factors will tell us more about how cancer cells can maintain their growth and sustain their progression in conditions when general protein synthesis is considerably reduced. Actual presence of IRES element within 5' UTR of certain cancer-related genes could also reveal more about their role in cancer etiology. A deeper understanding of the mechanisms underlying cap-independent translation regulation in malignant cells could ultimately lead to novel therapeutic strategies that would not affect protein synthesis of normal cells (Grzmil and Hemmings, 2012).

The achieved results have shown to be considerably more interesting and elaborate than initially expected. The most unexpected positive result was discovery of two additional, so far unknown, levels of regulation of *PTCH1* expression through 5' UTR. First, potential IRES element that would allow a protein product of *PTCH1* transcript 1b to be synthesized using m⁷G-cap-independent translation mechanism in condition when general level of protein synthesis is reduced (e.g., for now, hypoxia is the only confirmed one), and second, the presence of upstream open reading frames in the longer forms of *PTCH1b* 5' UTR, which all together further point to the exceptional significance of 5' UTR in the regulation of *PTCH1* expression.

Post-transcriptional gene expression regulation is generally very complex and for proper functioning it requires fine-tuning by many different regulatory elements (Mathews MB, 2002). It is well known that improper regulation of protein synthesis can lead to many different diseases, one of which is cancer (Rugero et al, 2013). Ever since it became evident that deregulated translation lies behind many diseases, regulation of protein expression became an important therapeutic target and of great interest to the pharmaceutical industry (Grzmil and Hemmings, 2012).

In spite of the absence of a direct association of *PTCH1b* 5' UTR CGG-repeat polymorphism with a disease in which a certain allele was found, this polymorphism and 5' UTR in general, still remains a very interesting topic for further research, especially in the light that many other 5' UTR regulatory elements found in our study are evolutionary conserved and thus considered as probably important (Figure 52). Another unexpected, but potentially very interesting observation was that, besides CGG-repeat polymorphism, the *PTCH1b* 5' UTR shares together some other similarities with the 5' UTR of *FMRI* gene, such as ability to enhance transcription of downstream transcript, presence of IRES motif and similarities in their sequences (Chen et al, 2003; Chiang et al, 2001).

6. Conclusions

- a) The 5' UTR of the main *PTCHI* transcript variant 1b according to the literature and main nucleotide databases is annotated with three different lengths: 188, 300 and 372 nucleotides long.
- b) Regarding the alleles of the *PTCH1b* CGG-repeat polymorphism that were found in Croatian population (5, 6, 7 and 8 repeats), the number of CGG repeats has no significant impact on the efficiency of transcription or translation of downstream gene, although the number of CGG repeats showed a strong negative correlation with the luciferase activity, in the context of 188-nt-long 5' UTR.
- c) Significant reduction in the reporter gene activity was observed with plasmids harboring longer, 300- and 372-nucleotide-long *PTCH1b* 5' UTR.
- d) *In silico* analysis predicts the presence of two upstream open reading frames (uORF) and one upstream AUG codon (uAUG) but only within the longer forms of *PTCH1b* 5' UTR.
- e) Mutagenesis of two uAUGs restored a reporter gene activity to the values that are comparable with the activity of 188-nucleotide long *PTCH1b* 5' UTR. Second uAUG creates potentially the most damaging uORF that overlaps and is out-of-frame with the natural ORF, and is evolutionary conserved.
- f) Existence of an *internal ribosome entry site* (IRES) within the *PTCH1b* 5' UTR was proven by increased activity of firefly luciferase, observed when bicistronic dual-luciferase reporter vectors were used. By ruling-out an alternative splicing of bicistronic mRNA or cryptic promoter within *PTCH1b* 5' UTR we proved that increased activity of firefly luciferase is due to the IRES-dependent translation of luciferase mRNA.
- g) Precise localization of putative IRES motif by removing the first 76 nucleotides from the 3' part of *PTCH1b* 5' UTR (c.-1_-76) leads to a significant reduction in the *PTCHI* IRES activity, although those 76 nucleotides solely are not sufficient to achieve the full IRES activity exhibited by the complete *PTCH1b* 5' UTR.

- h) The presence of an IRES element within the *PTCH1b* 5' UTR could allow Ptch1 protein to be synthesized in conditions when the general level of cellular protein synthesis is decreased, such as in cell conditions of reduced oxygen levels (hypoxia).
- i) All the results of our study have indicated an exceptionally complex and previously unknown role of the 5' UTR in the regulation of *PTCH1b* gene expression, and assumed the coexistence of two or even more alternative *PTCH1b* 5' UTRs.

7. References

- Agren M, Kogerman P, Kleman MI, Wessling M, Toftgård R. Expression of the PTCH1 tumor suppressor gene is regulated by alternative promoters and a single functional Gli-binding site. *Gene*. 2004; 330:101-114.
- Araujo PR, Yoon K, Ko D, Smith AD, Qiao M, Suresh U, Burns SC, Penalva LO. Before It Gets Started: Regulating Translation at the 5' UTR. *Comp Funct Genomics*. 2012; 2012:475731.
- Asano K, Sachs MS. Translation factor control of ribosome conformation during start codon selection. *Genes Dev*. 2007; 21(11):1280-1287.
- Ayers KL, Théron PP. Evaluating Smoothed as a G-protein-coupled receptor for Hedgehog signalling. *Trends Cell Biol*. 2010; 20(5):287-298.
- Baird SD, Turcotte M, Korneluk RG, Holcik M. Searching for IRES. *RNA*. 2006; 12(10):1755-1785.
- Bak M, Hansen C, Friis Henriksen K, Tommerup N. The human hedgehog-interacting protein gene: structure and chromosome mapping to 4q31.21-->q31.3. *Cytogenet Cell Genet*. 2001; 92(3-4):300-303.
- Ballou LM, Lin RZ. Rapamycin and mTOR kinase inhibitors. *J Chem Biol*. 2008; 1(1-4):27-36.
- Banerjee AK. 5'-terminal cap structure in eucaryotic messenger ribonucleic acids. *Microbiol Rev*. 1980; 44(2):175-205.
- Barber RD, Harmer DW, Coleman RA, Clark BJ. GAPDH as a housekeeping gene: analysis of GAPDH mRNA expression in a panel of 72 human tissues. *Physiol Genomics*. 2005; 21(3):389-395.
- Barnes EA, Kong M, Ollendorff V, Donoghue DJ. Patched1 interacts with cyclin B1 to regulate cell cycle progression. *EMBO J*. 2001; 20(9):2214-2223.
- Barrett LW, Fletcher S, Wilton SD. Regulation of eukaryotic gene expression by the untranslated gene regions and other non-coding elements. *Cell Mol Life Sci*. 2012; 69(21):3613-3634.
- Beachy PA, Karhadkar SS, Berman DM. Tissue repair and stem cell renewal in carcinogenesis. *Nature*. 2004; 432(7015):324-331.

- Begnini A, Tessari G, Turco A, Malerba G, Naldi L, Gotti E, Boschiero L, Forni A, Rugiu C, Piaserico S, Fortina AB, Brunello A, Cascone C, Girolomoni G, Gomez Lira M. PTCH1 gene haplotype association with basal cell carcinoma after transplantation. *Br J Dermatol*. 2010; 163(2):364-370.
- Benson DA, Karsch-Mizrachi I, Lipman DJ, Ostell J, Wheeler DL. GenBank. *Nucleic Acids Res*. 2008; 36(Database issue):D25-D30.
- Bert AG, Grépin R, Vadas MA, Goodall GJ. Assessing IRES activity in the HIF-1alpha and other cellular 5' UTRs. *RNA*. 2006; 12(6):1074-1083.
- Bigelow RL, Chari NS, Uden AB, Spurgers KB, Lee S, Roop DR, Toftgard R, McDonnell TJ. Transcriptional regulation of bcl-2 mediated by the sonic hedgehog signaling pathway through gli-1. *J Biol Chem*. 2004; 279(2):1197-1205.
- Bijlsma MF, Groot AP, Oduro JP, Franken RJ, Schoenmakers SH, Peppelenbosch MP, Spek CA. Hypoxia induces a hedgehog response mediated by HIF-1alpha. *J Cell Mol Med*. 2009; 13(8B):2053-2060.
- Bijlsma MF, Spek CA, Zivkovic D, van de Water S, Rezaee F, Peppelenbosch MP. Repression of smoothened by patched-dependent (pro-)vitamin D3 secretion. *PLoS Biol*. 2006; 4(8):e232.
- Birgisdottir V, Stefansson OA, Bodvarsdottir SK, Hilmarsdottir H, Jonasson JG, Eyfjord JE. Epigenetic silencing and deletion of the BRCA1 gene in sporadic breast cancer. *Breast Cancer Res*. 2006; 8(4):R38.
- Bisio A, Nasti S, Jordan JJ, Gargiulo S, Pastorino L, Provenzani A, Quattrone A, Queirolo P, Bianchi-Scarrà G, Ghiorzo P, Inga A. Functional analysis of CDKN2A/p16INK4a 5'-UTR variants predisposing to melanoma. *Hum Mol Genet*. 2010; 19(8):1479-1491.
- Bürglin TR. The Hedgehog protein family. *Genome Biol*. 2008; 9(11):241.
- Calvo SE, Pagliarini DJ, Mootha VK. Upstream open reading frames cause widespread reduction of protein expression and are polymorphic among humans. *Proc Natl Acad Sci U S A*. 2009; 106(18):7507-7512.
- Car D, Sabol M, Musani V, Ozretic P, Levanat S. Epigenetic regulation of the Hedgehog-Gli signaling pathway in cancer. *Periodicum biologorum*. 2010; 112(4):419-423.

- Carpenter D, Stone DM, Brush J, Ryan A, Armanini M, Frantz G, Rosenthal A, de Sauvage FJ. Characterization of two patched receptors for the vertebrate hedgehog protein family. *Proc Natl Acad Sci U S A*. 1998; 95(23):13630-13634.
- Carter PS, Jarquin-Pardo M, De Benedetti A. Differential expression of Myc1 and Myc2 isoforms in cells transformed by eIF4E: evidence for internal ribosome repositioning in the human c-myc 5'UTR. *Oncogene*. 1999; 18(30):4326-4335.
- Chamas F, Sabban EL. Role of the 5' untranslated region (UTR) in the tissue-specific regulation of rat tryptophan hydroxylase gene expression by stress. *J Neurochem*. 2002; 82(3):645-54.
- Chang TH, Huang HY, Hsu JB, Weng SL, Horng JT, Huang HD. An enhanced computational platform for investigating the roles of regulatory RNA and for identifying functional RNA motifs. *BMC Bioinformatics*. 2013; 14 Suppl 2:S4.
- Chang-Claude J, Dunning A, Schnitzbauer U, Galmbacher P, Tee L, Wjst M, Chalmers J, Zemzoum I, Harbeck N, Pharoah PDP, Hahn H. The patched polymorphism Pro1315Leu (C3944T) may modulate the association between use of oral contraceptives and breast cancer risk. *Int J Cancer*. 2003; 103(6):779-783.
- Chatterjee S, Pal JK. Role of 5'- and 3'-untranslated regions of mRNAs in human diseases. *Biol Cell*. 2009; 101(5):251-262.
- Chen LS, Tassone F, Sahota P, Hagerman PJ. The (CGG)_n repeat element within the 5' untranslated region of the FMR1 message provides both positive and negative cis effects on in vivo translation of a downstream reporter. *Hum Mol Genet*. 2003; 12(23):3067-3074.
- Cheng SY, Bishop JM. Suppressor of Fused represses Gli-mediated transcription by recruiting the SAP18-mSin3 corepressor complex. *Proc Natl Acad Sci U S A*. 2002; 99(8):5442-5447.
- Cheng SY, Yue S. Role and regulation of human tumor suppressor SUFU in Hedgehog signaling. *Adv Cancer Res*. 2008; 101:29-43.
- Chiang PW, Carpenter LE, Hagerman PJ. The 5'-untranslated region of the FMR1 message facilitates translation by internal ribosome entry. *J Biol Chem*. 2001; 276(41):37916-37921.
- Coldwell MJ, deSchoolmeester ML, Fraser GA, Pickering BM, Packham G, Willis AE. The p36 isoform of BAG-1 is translated by internal ribosome entry following heat shock. *Oncogene*. 2001; 20(30):4095-4100.

- Corcoran RB, Scott MP. Oxysterols stimulate Sonic hedgehog signal transduction and proliferation of medulloblastoma cells. *Proc Natl Acad Sci U S A*. 2006; 103(22):8408-8413.
- Cretnik M, Musani V, Oreskovic S, Leovic D, Levanat S. The Patched gene is epigenetically regulated in ovarian dermoids and fibromas, but not in basocellular carcinomas. *Int J Mol Med*. 2007; 19(6):875-883.
- Cross SS, Bury JP. The hedgehog signaling pathways in human pathology. *Curr Diag Pathol*. 2004; 10(2):157-168.
- Cvok ML, Cretnik M, Musani V, Ozretic P, Levanat S. New sequence variants in BRCA1 and BRCA2 genes detected by high-resolution melting analysis in an elderly healthy female population in Croatia. *Clin Chem Lab Med*. 2008; 46(10):1376-1383.
- Dasgupta A, Das S, Izumi R, Venkatesan A, Barat B. Targeting internal ribosome entry site (IRES)-mediated translation to block hepatitis C and other RNA viruses. *FEMS Microbiol Lett*. 2004; 234(2):189-199.
- Davuluri RV, Suzuki Y, Sugano S, Zhang MQ. CART classification of human 5' UTR sequences. *Genome Res*. 2000; 10(11):1807-1816.
- de Sousa Abreu R, Penalva LO, Marcotte EM, Vogel C. Global signatures of protein and mRNA expression levels. *Mol Biosyst*. 2009; 5(12):1512-1526.
- Dheda K, Huggett JF, Bustin SA, Johnson MA, Rook G, Zumla A. Validation of housekeeping genes for normalizing RNA expression in real-time PCR. *Biotechniques*. 2004; 37(1):112-119.
- Duman-Scheel M, Weng L, Xin S, Du W. Hedgehog regulates cell growth and proliferation by inducing Cyclin D and Cyclin E. *Nature*. 2002; 417(6886):299-304.
- Edgar RC. MUSCLE: multiple sequence alignment with high accuracy and high throughput. *Nucleic Acids Res*. 2004; 32(5):1792-1797.
- Fan H, Khavari PA. Sonic hedgehog opposes epithelial cell cycle arrest. *J Cell Biol*. 1999; 147(1):71-76.
- Farndon PA, Del Mastro RG, Evans DG, Kilpatrick MW. Location of gene for Gorlin syndrome. *Lancet*. 1992; 339(8793):581-582.
- Flicek P, Amode MR, Barrell D, Beal K, Brent S, Chen Y, Clapham P, Coates G, Fairley S, Fitzgerald S, Gordon L, Hendrix M, Hourlier T, Johnson N, Kähäri A, Keefe D, Keenan S,

- Kinsella R, Kokocinski F, Kulesha E, Larsson P, Longden I, McLaren W, Overduin B, Pritchard B, Riat HS, Rios D, Ritchie GR, Ruffier M, Schuster M, Sobral D, Spudich G, Tang YA, Trevanion S, Vandrovcova J, Vilella AJ, White S, Wilder SP, Zadissa A, Zamora J, Aken BL, Birney E, Cunningham F, Dunham I, Durbin R, Fernández-Suarez XM, Herrero J, Hubbard TJ, Parker A, Proctor G, Vogel J, Searle SM. Ensembl 2011. *Nucleic Acids Res.* 2011; 39(Database issue):D800-D806.
- Fitzgerald KD, Semler BL. Bridging IRES elements in mRNAs to the eukaryotic translation apparatus. *Biochim Biophys Acta.* 2009; 1789(9-10):518-528.
- Fodde R, Smits R. Cancer biology. A matter of dosage. *Science.* 2002; 298(5594):761-763.
- Fossett N. Signal transduction pathways, intrinsic regulators, and the control of cell fate choice. *Biochim Biophys Acta.* 2013; 1830(2):2375-2384.
- Geballe AP, Sachs MS. Translational Control by Upstream Open Reading Frames. In: Sonenberg N, Hershey JWB, Mathews M (Eds.) *Translational Control of Gene Expression.* Cold Spring Harbor Laboratory Press (2nd Ed). Cold Spring Harbor Laboratory Press, New York. 2000; 595-614.
- Ghosh A, Ghosh S, Maiti GP, Mukherjee S, Mukherjee N, Chakraborty J, Roy A, Roychoudhury S, Panda CK. Association of FANCC and PTCH1 with the development of early dysplastic lesions of the head and neck. *Ann Surg Oncol.* 2012; 19 Suppl 3:S528-S538.
- Gingras AC, Raught B, Sonenberg N. Regulation of translation initiation by FRAP/mTOR. *Genes Dev.* 2001; 15(7):807-826.
- Goodrich LV, Johnson RL, Milenkovic L, McMahon JA, Scott MP. Conservation of the hedgehog/patched signaling pathway from flies to mice: induction of a mouse patched gene by Hedgehog. *Genes Dev.* 1996; 10(3):301-312.
- Goodrich LV, Milenković L, Higgins KM, Scott MP. Altered neural cell fates and medulloblastoma in mouse patched mutants. *Science.* 1997; 277(5329):1109-1113.
- Gorlin RJ, Goltz RW. Multiple nevoid basal-cell epithelioma, jaw cysts and bifid rib. A syndrome. *N Engl J Med.* 1960; 262:908-12.
- Goss DJ, Theil EC. Iron responsive mRNAs: a family of Fe²⁺ sensitive riboregulators. *Acc Chem Res.* 2011; 44(12):1320-1328.

- Gould A, Missailidis S. Targeting the hedgehog pathway: the development of cyclopamine and the development of anti-cancer drugs targeting the hedgehog pathway. *Mini Rev Med Chem.* 2011; 11(3):200-213.
- Gray NK, Hentze MW. Regulation of protein synthesis by mRNA structure. *Mol Biol Rep.* 1994; 19(3):195-200.
- Grillo G, Turi A, Licciulli F, Mignone F, Liuni S, Banfi S, Gennarino VA, Horner DS, Pavesi G, Picardi E, Pesole G. UTRdb and UTRsite (RELEASE 2010): a collection of sequences and regulatory motifs of the untranslated regions of eukaryotic mRNAs. *Nucleic Acids Res.* 2010; 38(Database issue):D75-D80.
- Grzmil M, Hemmings BA. Translation regulation as a therapeutic target in cancer. *Cancer Res.* 2012; 72(16):3891-3900.
- Gulyy PV, Orlov SV, Dizhe EB, Kuteikin-Teplyakov KB, Ignatovich IA, Zhuk SV, Perevozchikov AP. Roles of ZF5 and CGGBP-20 transcription factors in regulating expression of human FMR1 gene responsible for fragile X-syndrome. *Cell Tissue Biol.* 2010; 4(1):54-62.
- Hahn H, Christiansen J, Wicking C, Zaphiropoulos PG, Chidambaram A, Gerrard B, Vorechovsky I, Bale AE, Toftgård R, Dean M, Wainwright B. A mammalian patched homolog is expressed in target tissues of sonic hedgehog and maps to a region associated with developmental abnormalities. *J Biol Chem.* 1996; 271(21):12125-12128.
- Hahn H, Wicking C, Zaphiropoulos PG, Gailani MR, Shanley S, Chidambaram A, Vorechovsky I, Holmberg E, Uden AB, Gillies S, Negus K, Smyth I, Pressman C, Leffell DJ, Gerrard B, Goldstein AM, Dean M, Toftgard R, Chenevix-Trench G, Wainwright B, Bale AE. Mutations of the human homolog of *Drosophila* patched in the nevoid basal cell carcinoma syndrome. *Cell* 1996; 85(6):841-851.
- Hall MN, Gabay J, Débarbouillé M, Schwartz M. A role for mRNA secondary structure in the control of translation initiation. *Nature.* 1982; 295(5850):616-618.
- Hall TA. BioEdit: a user-friendly biological sequence alignment editor and analysis program for Windows 95/98/NT. *Nucl Acids Symp Ser.* 1999; 41:95-98.
- Hellen CU, Sarnow P. Internal ribosome entry sites in eukaryotic mRNA molecules. *Genes Dev.* 2001; 15(13):1593-1612.

- Hogan DJ, Riordan DP, Gerber AP, Herschlag D, Brown PO. Diverse RNA-binding proteins interact with functionally related sets of RNAs, suggesting an extensive regulatory system. *PLoS Biol.* 2008; 6(10):e255.
- Holbrook SR. RNA structure: the long and the short of it. *Curr Opin Struct Biol.* 2005; 15(3):302-308.
- Huangfu D, Anderson KV. Signaling from Smo to Ci/Gli: conservation and divergence of Hedgehog pathways from *Drosophila* to vertebrates. *Development.* 2006; 133(1):3-14.
- Hughes TA. Regulation of gene expression by alternative untranslated regions. *Trends Genet.* 2006; 22(3):119-122.
- Iacono M, Mignone F, Pesole G. uAUG and uORFs in human and rodent 5'untranslated mRNAs. *Gene.* 2005; 349:97-105.
- Incardona JP, Eaton S (2000) Cholesterol in signal transduction. *Curr Opin Cell Biol.* 2000; 12(2):193-203.
- Ingham PW, McMahon AP. Hedgehog signaling in animal development: paradigms and principles. *Genes Dev.* 2001; 15(23):3059-3087.
- Ingham PW. How cholesterol modulates the signal. *Curr Biol.* 2000; 10(5):R180-R183.
- Jackson RJ, Hellen CU, Pestova TV. The mechanism of eukaryotic translation initiation and principles of its regulation. *Nat Rev Mol Cell Biol.* 2010; 11(2):113-127.
- Jacobs JL, Dinman JD. Systematic analysis of bicistronic reporter assay data. *Nucleic Acids Res.* 2004; 32(20):e160.
- Jang SK, Kräusslich HG, Nicklin MJ, Duke GM, Palmenberg AC, Wimmer E. A segment of the 5' nontranslated region of encephalomyocarditis virus RNA directs internal entry of ribosomes during in vitro translation. *J Virol.* 1988; 62(8):2636-2643.
- Johnson RL, Rothman AL, Xie J, Goodrich LV, Bare JW, Bonifas JM, Quinn AG, Myers RM, Cox DR, Epstein EH Jr, Scott MP. Human homolog of patched, a candidate gene for the basal cell nevus syndrome. *Science.* 1996; 272(5268):1668-1671.
- Kageyama R, Merlino GT, Pastan I. Nuclear factor ETF specifically stimulates transcription from promoters without a TATA box. *J Biol Chem.* 1989; 264(26):15508-15514.
- Kar S, Deb M, Sengupta D, Shilpi A, Bhutia SK, Patra SK. Intricacies of hedgehog signaling pathways: a perspective in tumorigenesis. *Exp Cell Res.* 2012; 318(16):1959-1972.

- Kasper M, Regl G, Frischauf AM, Aberger F. GLI transcription factors: mediators of oncogenic Hedgehog signalling. *Eur J Cancer*. 2006; 42(4):437-445.
- Katoh Y, Katoh M. Hedgehog target genes: mechanisms of carcinogenesis induced by aberrant hedgehog signaling activation. *Curr Mol Med*. 2009; 9(7):873-886.
- Kawabata T, Takahashi K, Sugai M, Murashima-Suginami A, Ando S, Shimizu A, Kosugi S, Sato T, Nishida M, Murakami K, Iizuka T. Polymorphisms in PTCH1 affect the risk of ameloblastoma. *J Dent Res*. 2005; 84(9):812-816.
- Kawamura S, Hervold K, Ramirez-Weber FA, Kornberg TB. Two patched protein subtypes and a conserved domain of group I proteins that regulates turnover. *J Biol Chem*. 2008; 283(45):30964-30969.
- Kahn AB, Ryan MC, Liu H, Zeeberg BR, Jamison DC, Weinstein JN. SpliceMiner: a high-throughput database implementation of the NCBI Evidence Viewer for microarray splice variant analysis. *BMC Bioinformatics*. 2007; 8:75.
- Kiesslich T, Neureiter D. Advances in targeting the Hedgehog signaling pathway in cancer therapy. *Expert Opin Ther Targets*. 2012; 16(2):151-156.
- Kimonis VE, Goldstein AM, Pastakia B, Yang ML, Kase R, DiGiovanna JJ, Bale AE, Bale SJ. Clinical manifestations in 105 persons with nevoid basal cell carcinoma syndrome. *Am J Med Genet*. 1997; 69(3):299-308.
- King HA, Cobbold LC, Willis AE. The role of IRES trans-acting factors in regulating translation initiation. *Biochem Soc Trans*. 2010; 38(6):1581-1586.
- Kogerman P, Krause D, Rahnema F, Kogerman L, Undén AB, Zaphiropoulos PG, Toftgård R. Alternative first exons of PTCH1 are differentially regulated in vivo and may confer different functions to the PTCH1 protein. *Oncogene*. 2002; 21(39):6007-6016.
- Koromilas AE, Lazaris-Karatzas A, Sonenberg N. mRNAs containing extensive secondary structure in their 5' non-coding region translate efficiently in cells overexpressing initiation factor eIF-4E. *EMBO J*. 1992; 11(11):4153-4158.
- Kozak M. An analysis of 5'-noncoding sequences from 699 vertebrate messenger RNAs. *Nucleic Acids Res*. 1987; 15(20):8125-8148.
- Kozak M. An analysis of vertebrate mRNA sequences: intimations of translational control. *J Cell Biol*. 1991; 115(4):887-903.

- Kozak M. Structural features in eukaryotic mRNAs that modulate the initiation of translation. *J Biol Chem.* 1991; 266(30):19867-19870.
- Kuyumcu-Martinez NM, Van Eden ME, Younan P, Lloyd RE. Cleavage of poly(A)-binding protein by poliovirus 3C protease inhibits host cell translation: a novel mechanism for host translation shutoff. *Mol Cell Biol.* 2004; 24(4):1779-1790.
- Lai K, Robertson MJ, Schaffer DV. The sonic hedgehog signaling system as a bistable genetic switch. *Biophys J.* 2004; 86(5):2748-2757.
- Le Quesne JP, Spriggs KA, Bushell M, Willis AE. Dysregulation of protein synthesis and disease. *J Pathol.* 2010; 220(2):140-151.
- Le SY, Maizel JV Jr. A common RNA structural motif involved in the internal initiation of translation of cellular mRNAs. *Nucleic Acids Res.* 1997; 25(2):362-369.
- Leovic D, Sabol M, Ozretic P, Musani V, Car D, Marjanovic K, Zubcic V, Sabol I, Sikora M, Grce M, Glavas-Obrovac L, Levanat S. Hh-Gli signaling pathway activity in oral and oropharyngeal squamous cell carcinoma. *Head Neck.* 2012; 34(1):104-112.
- Levanat S, Gorlin RJ, Fallet S, Johnson DR, Fantasia JE, Bale AE. A two-hit model for developmental defects in Gorlin syndrome. *Nat Genet.* 1996; 12(1):85-87.
- Levanat S, Musani V, Cvok ML, Susac I, Sabol M, Ozretic P, Car D, Eljuga D, Eljuga L, Eljuga D. Three novel BRCA1/BRCA2 mutations in breast/ovarian cancer families in Croatia. *Gene.* 2012; 498(2):169-176.
- Levanat S, Pavelic B, Crnic I, Situm M, Manojlovic S, Mubrin-Koncar M, Basta-Juzbasic A. Role of PTCH in Cancer and Development. *Periodicum biologorum.* 1998; 100(3):319-324
- Lipinski RJ, Gipp JJ, Zhang J, Doles JD, Bushman W. Unique and complimentary activities of the Gli transcription factors in Hedgehog signaling. *Exp Cell Res.* 2006; 312(11):1925-1938.
- Livak KJ, Schmittgen TD. Analysis of relative gene expression data using real-time quantitative PCR and the $2^{-\Delta\Delta CT}$ Method. *Methods.* 2001; 25(4):402-408.
- Loftus SK, Morris JA, Carstea ED, Gu JZ, Cummings C, Brown A, Ellison J, Ohno K, Rosenfeld MA, Tagle DA, Pentchev PG, Pavan WJ. Murine model of Niemann-Pick C disease: mutation in a cholesterol homeostasis gene. *Science.* 1997; 277(5323):232-235.

- López-Lastra M, Rivas A, Barría MI. Protein synthesis in eukaryotes: the growing biological relevance of cap-independent translation initiation. *Biol Res.* 2005; 38(2-3):121-146.
- Lupberger J, Kreuzer KA, Baskaynak G, Peters UR, le Coutre P, Schmidt CA. Quantitative analysis of beta-actin, beta-2-microglobulin and porphobilinogen deaminase mRNA and their comparison as control transcripts for RT-PCR. *Mol Cell Probes.* 2002; 16(1):25-30.
- MacNicol AM, Wilczynska A, MacNicol MC. Function and regulation of the mammalian Musashi mRNA translational regulator. *Biochem Soc Trans.* 2008; 36(Pt 3):528-530.
- Maier T, Güell M, Serrano L. Correlation of mRNA and protein in complex biological samples. *FEBS Lett.* 2009; 583(24):3966-3973.
- Marigo V, Davey RA, Zuo Y, Cunningham JM, Tabin CJ. Biochemical evidence that patched is the Hedgehog receptor. *Nature.* 1996; 384(6605):176-179.
- Marintchev A, Wagner G. Translation initiation: structures, mechanisms and evolution. *Q Rev Biophys.* 2004; 37(3-4):197-284.
- Martín V, Carrillo G, Torroja C, Guerrero I. The sterol-sensing domain of Patched protein seems to control Smoothed activity through Patched vesicular trafficking. *Curr Biol.* 2001; 11(8):601-607.
- Martínez-Salas E, Piñeiro D, Fernández N. Alternative Mechanisms to Initiate Translation in Eukaryotic mRNAs. *Comp Funct Genomics.* 2012; 2012:391546.
- Mathews DH, Turner DH. Prediction of RNA secondary structure by free energy minimization. *Curr Opin Struct Biol.* 2006; 16(3):270-278.
- Mathews MB. Lost in translation. *Trends Biochem Sci.* 2002; 27(5):267-269.
- Mavrakis KJ, Wendel HG. Translational control and cancer therapy. *Cell Cycle.* 2008; 7(18):2791-2794.
- McGinnis S, Madden TL. BLAST: at the core of a powerful and diverse set of sequence analysis tools. *Nucleic Acids Res.* 2004; 32(Web Server issue):W20-W25.
- McMahon AP, Ingham PW, Tabin CJ. Developmental roles and clinical significance of hedgehog signaling. *Curr Top Dev Biol.* 2003; 53:1-114.
- Meijer HA, Thomas AA. Control of eukaryotic protein synthesis by upstream open reading frames in the 5'-untranslated region of an mRNA. *Biochem J.* 2002; 367(Pt 1):1-11.

- Mendell JT, Dietz HC. When the message goes awry: disease-producing mutations that influence mRNA content and performance. *Cell*. 2001; 107(4):411-414.
- Meng Z, King PH, Nabors LB, Jackson NL, Chen CY, Emanuel PD, Blume SW. The ELAV RNA-stability factor HuR binds the 5'-untranslated region of the human IGF-IR transcript and differentially represses cap-dependent and IRES-mediated translation. *Nucleic Acids Res*. 2005; 33(9):2962-2979.
- Merrick WC. Cap-dependent and cap-independent translation in eukaryotic systems. *Gene*. 2004; 332:1-11.
- Mignone F, Gissi C, Liuni S, Pesole G. Untranslated regions of mRNAs. *Genome Biol*. 2002; 3(3):REVIEWS0004.
- Mitchell SF, Walker SE, Algire MA, Park EH, Hinnebusch AG, Lorsch JR. The 5'-7-methylguanosine cap on eukaryotic mRNAs serves both to stimulate canonical translation initiation and to block an alternative pathway. *Mol Cell*. 2010; 39(6):950-962.
- Mokrejs M, Masek T, Vopálenský V, Hlubucek P, Delbos P, Pospíšek M. IRESite--a tool for the examination of viral and cellular internal ribosome entry sites. *Nucleic Acids Res*. 2010; 38(Database issue): D131-D136.
- Morris DR, Geballe AP. Upstream open reading frames as regulators of mRNA translation. *Mol Cell Biol*. 2000; 20(23):8635-8642.
- Motoyama J, Heng H, Crackower MA, Takabatake T, Takeshima K, Tsui LC, Hui C. Overlapping and non-overlapping Ptch2 expression with Shh during mouse embryogenesis. *Mech Dev*. 1998; 78(1-2):81-84.
- Musani V, Sabol M, Car D, Ozretić P, Kalafatić D, Maurac I, Orešković S, Levanat S. PTCH1 gene polymorphisms in ovarian tumors: Potential protective role of c.3944T allele. *Gene*. 2013; 517(1):55-59.
- Musani V. Mehanizmi regulacije signalnog puta Hedgehog/patched/Gli u tumorima i nasljednim oboljenjima. Doktorska disertacija. Sveučilište u Zagrebu, Prirodoslovno-matematički fakultet. 2008.
- Nagao K, Fujii K, Yamada M, Miyashita T. Identification of a novel polymorphism involving a CGG repeat in the PTCH gene and a genome-wide screening of CGG-containing genes. *J Hum Genet*. 2004; 49(2):97-101.

- Nagao K, Togawa N, Fujii K, Uchikawa H, Kohno Y, Yamada M, Miyashita T. Detecting tissue-specific alternative splicing and disease-associated aberrant splicing of the PTCH gene with exon junction microarrays. *Hum Mol Genet.* 2005a; 14(22):3379-3388.
- Nagao K, Toyoda M, Takeuchi-Inoue K, Fujii K, Yamada M, Miyashita T. Identification and characterization of multiple isoforms of a murine and human tumor suppressor, patched, having distinct first exons. *Genomics.* 2005b; 85(4):462-471.
- Nieuwenhuis E, Hui CC. Hedgehog signaling and congenital malformations. *Clin Genet.* 2005; 67(3):193-208.
- Nieuwenhuis E, Motoyama J, Barnfield PC, Yoshikawa Y, Zhang X, Mo R, Crackower MA, Hui CC. Mice with a targeted mutation of patched2 are viable but develop alopecia and epidermal hyperplasia. *Mol Cell Biol.* 2006; 26(17):6609-6622.
- Nolan T, Hands RE, Bustin SA. Quantification of mRNA using real-time RT-PCR. *Nat Protoc.* 2006; 1(3):1559-1582.
- Nüsslein-Volhard C, Wieschaus E. Mutations affecting segment number and polarity in *Drosophila*. *Nature.* 1980; 287(5785):795-801.
- Orr HT, Zoghbi HY. Trinucleotide repeat disorders. *Annu Rev Neurosci.* 2007; 30:575-621.
- Oyama M, Itagaki C, Hata H, Suzuki Y, Izumi T, Natsume T, Isobe T, Sugano S. Analysis of small human proteins reveals the translation of upstream open reading frames of mRNAs. *Genome Res.* 2004; 14(10B):2048-2052.
- Ozretić P, Bisio A, Inga A, Levanat S. The growing relevance of cap-independent translation initiation in cancer-related genes. *Periodicum biologorum.* 2012; 114(4):471-478.
- Ozretić P, Levačić Cvok M, Musani V, Sabol M, Car D, Levanat S. In silico analysis of potential structural and functional significance of human breast cancer gene BRCA2 sequence variants found in 5' untranslated region. *Periodicum biologorum.* 2010; 112(4):469-474.
- Pan JY, Zhou SH. The hedgehog signaling pathway, a new therapeutic target for treatment of ischemic heart disease. *Pharmazie.* 2012; 67(6):475-481.
- Pastorino L, Cusano R, Nasti S, Faravelli F, Forzano F, Baldo C, Barile M, Gliori S, Muggianu M, Ghigliotti G, Lacaita MG, Lo Muzio L, Bianchi-Scarra G. Molecular characterization of Italian nevoid basal cell carcinoma syndrome patients. *Hum Mutat.* 2005; 25(3):322-323.

- Pedersen AG, Nielsen H. Neural network prediction of translation initiation sites in eukaryotes: perspectives for EST and genome analysis. *Proc Int Conf Intell Syst Mol Biol.* 1997; 5:226-233.
- Pelletier J, Sonenberg N. Internal initiation of translation of eukaryotic mRNA directed by a sequence derived from poliovirus RNA. *Nature.* 1988; 334(6180):320-325.
- Pesole G, Mignone F, Gissi C, Grillo G, Licciulli F, Liuni S. Structural and functional features of eukaryotic mRNA untranslated regions. *Gene.* 2001; 276(1-2):73-81.
- Pickering BM, Willis AE. The implications of structured 5' untranslated regions on translation and disease. *Semin Cell Dev Biol.* 2005; 16(1):39-47.
- Plank TD, Kieft JS. The structures of nonprotein-coding RNAs that drive internal ribosome entry site function. *Wiley Interdiscip Rev RNA.* 2012; 3(2):195-212.
- Pola R, Ling LE, Silver M, Corbley MJ, Kearney M, Blake Pepinsky R, Shapiro R, Taylor FR, Baker DP, Asahara T, Isner JM. The morphogen Sonic hedgehog is an indirect angiogenic agent upregulating two families of angiogenic growth factors. *Nat Med.* 2001; 7(6):706-711.
- Pyronnet S, Pradayrol L, Sonenberg N. A cell cycle-dependent internal ribosome entry site. *Mol Cell.* 2000; 5(4):607-616.
- Recalcati S, Minotti G, Cairo G. Iron regulatory proteins: from molecular mechanisms to drug development. *Antioxid Redox Signal.* 2010; 13(10):1593-1616.
- Resch AM, Ogurtsov AY, Rogozin IB, Shabalina SA, Koonin EV. Evolution of alternative and constitutive regions of mammalian 5'UTRs. *BMC Genomics.* 2009; 10:162.
- Ribes V, Briscoe J. Establishing and interpreting graded Sonic Hedgehog signaling during vertebrate neural tube patterning: the role of negative feedback. *Cold Spring Harb Perspect Biol.* 2009; 1(2):a002014.
- Rohatgi R, Milenkovic L, Corcoran RB, Scott MP. Hedgehog signal transduction by Smoothed: pharmacologic evidence for a 2-step activation process. *Proc Natl Acad Sci U S A.* 2009; 106(9):3196-3201.
- Rozen F, Edery I, Meerovitch K, Dever TE, Merrick WC, Sonenberg N. Bidirectional RNA helicase activity of eucaryotic translation initiation factors 4A and 4F. *Mol Cell Biol.* 1990; 10(3):1134-1144.

- Ruggero D. Translational control in cancer etiology. *Cold Spring Harb Perspect Biol.* 2013; 5(2).
- Ryan KE, Chiang C. Hedgehog secretion and signal transduction in vertebrates. *J Biol Chem.* 2012; 287(22):17905-17913.
- Salamov AA, Nishikawa T, Swindells MB. Assessing protein coding region integrity in cDNA sequencing projects. *Bioinformatics.* 1998; 14(5):384-390.
- Sanger F, Nicklen S, Coulson AR. DNA sequencing with chain-terminating inhibitors. *Proc Natl Acad Sci U S A.* 1977; 74(12):5463-5467.
- Sarnow P. Translation of glucose-regulated protein 78/immunoglobulin heavy-chain binding protein mRNA is increased in poliovirus-infected cells at a time when cap-dependent translation of cellular mRNAs is inhibited. *Proc Natl Acad Sci U S A.* 1989; 86(15):5795-5799.
- Scales SJ, de Sauvage FJ. Mechanisms of Hedgehog pathway activation in cancer and implications for therapy. *Trends Pharmacol Sci.* 2009; 30(6):303-312.
- Scheper GC, van der Knaap MS, Proud CG. Translation matters: protein synthesis defects in inherited disease. *Nat Rev Genet.* 2007; 8(9):711-723.
- Sehgal A, Briggs J, Rinehart-Kim J, Basso J, Bos TJ. The chicken c-Jun 5' untranslated region directs translation by internal initiation. *Oncogene.* 2000; 19(24):2836-2845.
- Sherf BA, Navarro SL, Hannah RR, Wood KV. Dual-luciferase reporter assay: An advanced co-reporter technology integrating firefly and Renilla luciferase assays. *Promega Notes.* 1996; 2-8.
- Sherrill KW, Byrd MP, Van Eden ME, Lloyd RE. BCL-2 translation is mediated via internal ribosome entry during cell stress. *J Biol Chem.* 2004; 279(28):29066-29074.
- Shimokawa T, Rahnema F, Zaphiropoulos PG. A novel first exon of the Patched1 gene is upregulated by Hedgehog signaling resulting in a protein with pathway inhibitory functions. *FEBS Lett.* 2004; 578(1-2):157-162.
- Shimokawa T, Svärd J, Heby-Henricson K, Teglund S, Toftgård R, Zaphiropoulos PG. Distinct roles of first exon variants of the tumor-suppressor Patched1 in Hedgehog signaling. *Oncogene.* 2007; 26(34):4889-4896.

- Signori E, Bagni C, Papa S, Primerano B, Rinaldi M, Amaldi F, Fazio VM. A somatic mutation in the 5'UTR of BRCA1 gene in sporadic breast cancer causes down-modulation of translation efficiency. *Oncogene*. 2001; 20(33):4596-4600.
- Smith L. Post-transcriptional regulation of gene expression by alternative 5'-untranslated regions in carcinogenesis. *Biochem Soc Trans*. 2008; 36(Pt 4):708-711.
- Smyth I, Narang MA, Evans T, Heimann C, Nakamura Y, Chenevix-Trench G, Pietsch T, Wicking C, Wainwright BJ. Isolation and characterization of human patched 2 (PTCH2), a putative tumour suppressor gene in basal cell carcinoma and medulloblastoma on chromosome 1p32. *Hum Mol Genet*. 1999; 8(2):291-297.
- Sobczak K, Krzyzosiak WJ. Structural determinants of BRCA1 translational regulation. *J Biol Chem*. 2002 277(19):17349-17358.
- Sonenberg N, Hinnebusch AG. Regulation of translation initiation in eukaryotes: mechanisms and biological targets. *Cell*. 2009; 136(4):731-745.
- Spriggs KA, Bushell M, Willis AE. Translational regulation of gene expression during conditions of cell stress. *Mol Cell*. 2010; 40(2):228-237.
- Spriggs KA, Stoneley M, Bushell M, Willis AE. Re-programming of translation following cell stress allows IRES-mediated translation to predominate. *Biol Cell*. 2008; 100(1):27-38.
- Strange RC, El-Genidy N, Ramachandran S, Lovatt TJ, Fryer AA, Smith AG, Lear JT, Wong C, Jones PW, Ichii-Jones F, Hoban PR. Susceptibility to basal cell carcinoma: associations with PTCH polymorphisms. *Ann Hum Genet*. 2004; 68(Pt 6):536-545.
- Suzuki M, Hatsuse H, Nagao K, Takayama Y, Kameyama K, Kabasawa Y, Omura K, Yoshida M, Fujii K, Miyashita T. Selective haploinsufficiency of longer isoforms of PTCH1 protein can cause nevoid basal cell carcinoma syndrome. *J Hum Genet*. 2012; 57(7):422-426.
- Tain LS, Whitworth AJ. Translating translation: Regulated protein translation as a biomedical intervention. *Fly (Austin)*. 2009; 3(4).
- Taipale J, Cooper MK, Maiti T, Beachy PA. Patched acts catalytically to suppress the activity of Smoothened. *Nature*. 2002; 418(6900):892-897.
- Talbot LJ, Bhattacharya SD, Kuo PC. Epithelial-mesenchymal transition, the tumor microenvironment, and metastatic behavior of epithelial malignancies. *Int J Biochem Mol Biol*. 2012; 3(2):117-136.

- Thomas JD, Johannes GJ. Identification of mRNAs that continue to associate with polysomes during hypoxia. *RNA*. 2007; 13(7):1116-1131.
- Thompson JD, Higgins DG, Gibson TJ. CLUSTAL W: improving the sensitivity of progressive multiple sequence alignment through sequence weighting, position-specific gap penalties and weight matrix choice. *Nucleic Acids Res*. 1994; 22(22):4673-4680.
- Thompson ME, Jensen RA, Obermiller PS, Page DL, Holt JT. Decreased expression of BRCA1 accelerates growth and is often present during sporadic breast cancer progression. *Nat Genet*. 1995; 9(4):444-450.
- Thompson SR. So you want to know if your message has an IRES? *Wiley Interdiscip Rev RNA*. 2012; 3(5):697-705.
- Thompson SR. Tricks an IRES uses to enslave ribosomes. *Trends Microbiol*. 2012; 20(11):558-566.
- Trinklein ND, Aldred SJ, Saldanha AJ, Myers RM. Identification and functional analysis of human transcriptional promoters. *Genome Res*. 2003; 13(2):308-312.
- Uchikawa H, Toyoda M, Nagao K, Miyauchi H, Nishikawa R, Fujii K, Kohno Y, Yamada M, Miyashita T. Brain- and heart-specific Patched-1 containing exon 12b is a dominant negative isoform and is expressed in medulloblastomas. *Biochem Biophys Res Commun*. 2006; 349(1):277-283.
- van der Velden AW, Thomas AA. The role of the 5' untranslated region of an mRNA in translation regulation during development. *Int J Biochem Cell Biol*. 1999; 31(1):87-106.
- Van Eden ME, Byrd MP, Sherrill KW, Lloyd RE. Demonstrating internal ribosome entry sites in eukaryotic mRNAs using stringent RNA test procedures. *RNA*. 2004; 10(4):720-730.
- Vandesompele J, De Preter K, Pattyn F, Poppe B, Van Roy N, De Paepe A, Speleman F. Accurate normalization of real-time quantitative RT-PCR data by geometric averaging of multiple internal control genes. *Genome Biol*. 2002; 3(7):RESEARCH0034.
- Vega Laso MR, Zhu D, Sogliocco F, Brown AJ, Tuite MF, McCarthy JE. Inhibition of translational initiation in the yeast *Saccharomyces cerevisiae* as a function of the stability and position of hairpin structures in the mRNA leader. *J Biol Chem*. 1993; 268(9):6453-6462.
- Wan Y, Kertesz M, Spitale RC, Segal E, Chang HY. Understanding the transcriptome through RNA structure. *Nat Rev Genet*. 2011; 12(9):641-655.

- Wang J, Lu C, Min D, Wang Z, Ma X. A mutation in the 5' untranslated region of the BRCA1 gene in sporadic breast cancer causes downregulation of translation efficiency. *J Int Med Res.* 2007; 35(4):564-573.
- Wethmar K, Smink JJ, Leutz A. Upstream open reading frames: molecular switches in (patho)physiology. *Bioessays.* 2010; 32(10):885-893.
- Willcocks MM, Carter MJ, Roberts LO. Cleavage of eukaryotic initiation factor eIF4G and inhibition of host-cell protein synthesis during feline calicivirus infection. *J Gen Virol.* 2004; 85(Pt 5):1125-1130.
- Wilson CW, Stainier DY. Vertebrate Hedgehog signaling: cilia rule. *BMC Biol.* 2010; 8:102.
- Wolf I, Bose S, Desmond JC, Lin BT, Williamson EA, Karlan BY, Koeffler HP. Unmasking of epigenetically silenced genes reveals DNA promoter methylation and reduced expression of PTCH in breast cancer. *Breast Cancer Res Treat.* 2007; 105(2):139-155.
- Xu CF, Brown MA, Chambers JA, Griffiths B, Nicolai H, Solomon E. Distinct transcription start sites generate two forms of BRCA1 mRNA. *Hum Mol Genet.* 1995; 4(12):2259-2264.
- Yang L, Xie G, Fan Q, Xie J. Activation of the hedgehog-signaling pathway in human cancer and the clinical implications. *Oncogene.* 2010; 29(4):469-481.
- Zaphiropoulos PG, Undén AB, Rahnama F, Hollingsworth RE, Toftgård R. PTCH2, a novel human patched gene, undergoing alternative splicing and up-regulated in basal cell carcinomas. *Cancer Res.* 1999; 59(4):787-792.
- Zhang T, Haws P, Wu Q. Multiple variable first exons: a mechanism for cell- and tissue-specific gene regulation. *Genome Res.* 2004; 14(1):79-89.
- Zhang Z, Dietrich FS. Identification and characterization of upstream open reading frames (uORF) in the 5' untranslated regions (UTR) of genes in *Saccharomyces cerevisiae*. *Curr Genet.* 2005; 48(2):77-87.
- Zuker M. Mfold web server for nucleic acid folding and hybridization prediction. *Nucleic Acids Res.* 2003; 31(13):3406-3415.

8. Summary

A CGG-repeat polymorphism was found in the 5' untranslated region (5' UTR) of the main transcript of the *PTCH1* tumor suppressor gene (transcript 1b), one of the main members of the Hedgehog-Gli signaling pathway. In Croatian patients suffering from ovarian fibroma, dermoid and ovarian cancer, and healthy controls were found alleles with 5, 6, 7 and 8 repeats, but with no direct association with a certain type of ovarian neoplasm (Musani et al, 2013). Allele harboring 7 repeats is considered as “wild type”, and in the literature *PTCH1b* 5' UTR is annotated in three different lengths: 188, 300 and 372 nucleotides. The main goal of our study was to thoroughly explore the regulatory role of different *cis*-regulatory elements present in the *PTCH1b* 5' UTR.

In order to evaluate the potential impact of varying number of CGG repeat on the transcription and/or the translation of the *PTCH1* gene, we decided to apply methodology previously successfully used for a functional analysis of the 5' UTR of the *p16* gene (Bisio et al, 2010). Using luciferase reporter constructs in assays with three permanent human cell lines (MCF-7, HCT116 and HEK 293T) it was shown that the number of CGG repeats has no significant impact on the efficiency of transcription or translation. Only allele with 5 CGG repeats showed a statistically significant increase in the reporter gene activity, and this was obtained only in the context of 188-nucleotide long 5' UTR. Computationally predicted secondary structure of the 5' UTR also confirmed that the increased stability of secondary structure, as the result of an increased number of CGG repeats, also has no significant impact on the efficiency of *PTCH1* translation.

Significant reduction in the luciferase activity was observed when monocistronic luciferase vectors (pGL3-Promoter-type) with 300- and 372-nucleotide-long cloned *PTCH1b* 5' UTR were used. *In silico* analysis of two longer *PTCH1b* 5' UTRs predicted the presence of two upstream open reading frames (uORF) and one upstream AUG codon (uAUG), what could cause a reduction of Ptch1 protein expression by reducing the translation from the main open reading frame. Mutagenesis of two upstream translation initiation sites (uAUG codons) caused an increase in the reporter gene activity to the values that are comparable with the activity of the 188-nucleotide long 5' UTR. It was also shown that potentially most damaging, overlapping uORF is evolutionary conserved. In addition, the results obtained using different reporter vectors were proved, using qPCR method, not to be due to the differences in reporter gene mRNA levels. Altogether, these results demonstrated that the length of the *PTCH1b* 5' UTR is potentially an important factor in translational regulation.

Usage of bicistronic dual-luciferase reporter vectors (pRuF-type) indicated the existence of *internal ribosome entry site* (IRES) in the *PTCH1b* 5' UTR, whereas *in silico* analysis predicted its localization within the first upstream 76 nucleotides (c.-1_-76). Precise localization of the potential IRES element showed that removal of these 76 nucleotides leads to a significant reduction in the reporter gene activity, although those 76 nucleotides solely are not sufficient to achieve the full IRES activity exhibited by the pRuF plasmids with the complete *PTCH1b* 5' UTR cloned. The presence of an IRES element within the *PTCH1b* 5' UTR could allow Ptch1 protein to be synthesized in conditions when the general level of cellular protein synthesis is decreased, such as in cell conditions of reduced oxygen levels (hypoxia), what is also important in tumor development and metastasis, or for the potential therapeutic role of activated Hh-Gli pathway in acute or chronic ischemic heart disease.

All the results of our study have indicated exceptionally complex and previously unknown role of the 5' UTR in the regulation of *PTCH1b* gene expression. Two or more alternative *PTCH1b* 5' UTRs that differ in length and the presence of uORFs and uAUGs, allow differential expression of Ptch1 protein. What is more interesting, several of features of the *PTCH1b* 5' UTR, such as CGG-repeat polymorphism, IRES motif including CGG repeats, ability to induce transcription of a downstream gene, are shared with the 5' UTR of *FMR1* (fragile X mental retardation 1) gene.

9. Sažetak

Signalni put Hedgehog-Gli (Hh-Gli) evolucijski je visoko konzerviran i ima jednu od fundamentalnih uloga u embriogenezi. Njegovo poremećeno funkcioniranje povezuje se s razvojnim malformacijama a sve je važnija i njegova uloga u etiologiji raka. Npr. tumor-supresorski gen *PTCH1*, jedan od glavnih članova tog signalnog puta, često je mutiran u karcinomima bazalnih stanica, meduloblastomima, rabdomiosarkomim, i dr. Polimorfizam CGG-trinukleotidnog ponavljanja pronađen je u 5' netranslatiranoj regiji (5' UTR) glavnog transkripta gena *PTCH1* (transkript 1b). U hrvatskoj populaciji, kod pacijenata oboljelih od fibroma, dermoida i karcinoma jajnika te zdravih kontrolnih uzoraka, pronađeni su aleli s 5, 6, 7 i 8 CGG ponavljanja, ali bez izravne povezanosti nekog broja ponavljanja s određenim tipom oboljenja (Musani i sur., 2013). Alelom „divljeg tipa“ smatraju se 7 CGG ponavljanja dok je 5' UTR gena *PTCH1* u literaturi anotirana u tri dužine: 188, 300 i 372 nukleotida.

U cilju provjere potencijalnog utjecaja različitog broja CGG ponavljanja na transkripciju i/ili translaciju gena *PTCH1b* korištena je metodologija prethodno uspješno primijenjena za funkcionalnu analizu 5' UTR gena *p16* (Bisio i sur., 2010). Upotreba različitih luciferaznih plazmidnih konstrukta u luciferaznim testovima na trajnim humanim staničnim linijama (MCF-7, HCT116 i HEK 293T) pokazala je da promjena broja CGG ponavljanja nema značajniji utjecaj na učinkovitost transkripcije ili translacije. Jedino alel s 5 CGG ponavljanja pokazuje statistički značajnu povećanu aktivnost reporterskog gena i to samo u kontekstu 5' UTR dužine 188 nukleotida. Računalno predviđanje sekundarne strukture 5' UTR također je potvrdilo da povećanje stabilnosti sekundarne strukture, uzrokovano povećanjem broja CGG ponavljanja, nema značajniji utjecaj na efikasnost translacije gena *PTCH1b*.

Upotrebom monocistronskih luciferaznih reporterskih plazmida (baziranih na pGL3-Promoter vektoru) s ugrađenom 5' UTR dužine 300 ili 372 nukleotida, kod luciferaznih testova došlo je do značajne redukcije u aktivnosti reporterskog proteina. Time se pokazalo da je sama dužina 5' UTR potencijalno značajan čimbenik u regulaciji izražaja gena *PTCH1b*. Računalna analiza tih dviju dužih 5' UTR predvidjela je prisutnost dva uzvodna otvorena okvira čitanja (uORF) i jednog uzvodnog AUG kodona (uAUG), koji bi mogli uzrokovati redukciju količine proteinskog produkta gena *PTCH1b* kao posljedicu smanjene translacije s glavnog okvira čitanja. Mutagenezom promijenjena dva uzvodna mjesta inicijacije translacije (uAUG kodona) doveli su porast aktivnosti reporterskog proteina do vrijednosti koje su usporedive s aktivnošću 5' UTR dužine 188 nukleotida. Također, pokazalo se da je potencijalno

najznačajniji, preklapajući uORF evolucijski konzerviran. Upotrebom metode kvantitativne lančane reakcije polimerazom (qPCR) utvrđeno je da su sve promjene dobivene upotrebom različitih reporterskih vektora nastale zbog razlika u efikasnosti translacije ali ne i transkripcije reporterskog gena.

Upotreba bicistronskih dual-luciferaznih reporterskih vektora (baziranih na pRuF plazmidu) pokazala je postojanje unutarnjeg mjesta vezanja ribosoma (engl. Internal Ribosome Entry Site, IRES) unutar 5' UTR gena *PTCH1b*, dok računalna analiza predviđa njegovu lokalizaciju unutar prvih 76 uzvodnih nukleotida (c.-1_-76). Preciznija lokalizacija potencijalnog IRES elementa pokazala je da uklanjanje tih 76 nukleotida dovodi do znatnog smanjenja aktivnosti reporterskog proteina ali također i da samo tih 76 nukleotida nije dovoljno za postizanje potpune IRES aktivnosti koju pokazuju pRuF plazmidi s kompletnim 5' UTR gena *PTCH1b*. Prisutnost IRES elementa u 5' UTR gena *PTCH1* omogućavala bi sintezu proteina Ptch1 u staničnim uvjetima kada je generalna razina stanične sinteze proteina smanjena, kao npr. u stanjima smanjene količine kisika (hipoksije), što je važno u progresiji i metastaziranju tumora, ali čini se i u terapijskoj ulozi povišene aktivnosti signalnog puta Hh-Gli kod akutne i kronične ishemične bolesti srca.

Svi rezultati ovog istraživanja ukazuju na izuzetno složenu i do sada nepoznatu ulogu 5' UTR u regulaciji izražaja gena *PTCH1b*. Posjedovanje dviju ili više alternativnih 5' netranslatiranih regija, koje se međusobno razlikuju u dužini te prisutnosti uzvodnih otvorenih okvira čitanja i AUG kodona, omogućuje diferenciranu ekspresiju proteina Ptch1, ovisno o tipu stanica i staničnim uvjetima. Posebno zanimljivo je otkriće da, osim polimorfizma CGG ponavljanja, mnogo svojstava svoje 5' netranslatirane regije gen *PTCH1* dijeli s 5' netranslatiranom regijom gena *FMRI*, uzročnika fragilnog X sindroma.

10. Biography

Petar Ozretić was born on December 23, 1976 in Čakovec, Croatia, where he finished his primary and secondary school. On February 8, 2005 he obtained the B. Sc. degree in Molecular Biology from the Faculty of Science, University of Zagreb. Experimental work for his diploma thesis titled “Polymorphisms of Exons 1, 2 and 3 of *p16* Tumor Suppressor Gene” was performed under the supervision of Dr. sc. Sonja Levanat at the Ruđer Bošković Institute. From the academic year 2007/2008 he is enrolled in Doctoral Study of Molecular Biosciences at Josip Juraj Strossmayer University of Osijek.

From November 2006 to April 2007 he worked as a professional associate on the MZOŠ HITRA technological project titled “Developing Method for Detection of Inherited Predisposition to Breast Cancer in Croatia” (project number 5025, principal investigator Dr. sc. Sonja Levanat). From June 2007 he is an assistant in the Laboratory for Hereditary Cancer, Department for Molecular Medicine at Ruđer Bošković Institute, working on the MZOŠ scientific project “Signal Transduction in Tumors: Hh-Gli Pathway, Interactions and Therapeutic Potential” (project number 098-0982464-2461, principal investigator Dr. sc. Sonja Levanat).

Petar Ozretić is a member of the Croatian Society of Biochemistry and Molecular Biology (HDBMB), Croatian Society of Human Genetics (HDHG), International Society for Computational Biology (ISCB), European Association of Cancer Research (EACR) and he is one of the founders of the Croatian Association for Cancer Research (HDIR), where he serves as a secretary since society's founding in 2009.

He has presented his scientific work at 7 domestic and 6 foreign conferences. At the “16th World Congress on Advances in Oncology and 14th International Symposium on Molecular Medicine” in 2011, Rhodes, Greece, he was an invited speaker with a lecture titled “*In silico* methods for assessing potential functional impact of human breast cancer gene *BRCA2* sequence variants found in 5' untranslated region”. For the poster titled “The Role of 5' untranslated region in the regulation of *PTCH1b* gene expression” he won the Best Poster Award at the “HDIR-2: Second Meeting of the Croatian Association for Cancer Research” in 2012, Zagreb, Croatia.

He attended several practical courses and workshops, of which the most notable are “EMBO Practical Course on Computational RNA Biology” at the Institut d'Études Scientifiques de Cargèse, Corsica, France, in 2010; “Joint EMBRACE-EBI workshop: understanding protein

structures” at the Wellcome Trust Genome Campus, Hinxton, UK, in 2009, and “MedILS Summer School 2007 - Workshop on computational biology” at MedILS, Split, Croatia, in 2007.

Petar Ozretić was a member of the Organizing Committee of the “HDIR-1: First Meeting of the Croatian Association for Cancer Research” and the “HDIR-2: Second Meeting of the Croatian Association for Cancer Research”. He has participated in Ruđer Bošković Institute’s “Open Days” in 2008, 2010 and 2013.

In 2011 and 2012 he was awarded with three fellowships (EACR Travel Fellowship, FEBS Collaborative Experimental Scholarships for Central & Eastern Europe, and Croatian Science Foundation’s Fellowship for Doctoral Students) intended for spending 10-month research under the supervision of Prof. dr. sc. Alberto Inga in the Laboratory of Transcriptional Networks at the Centre for Integrative Biology (CIBIO), University of Trento, Trento, Italy.

He is the author of 14 scientific articles, of which 9 are cited in Current Contents Connect database and on two of them (one original and one review paper) he is the first author.

List of publications:

1. Musani V, Sabol M, Car D, Ozretić P, Kalafatić D, Maurac I, Orešković S, Levanat S. PTCH1 gene polymorphisms in ovarian tumors: Potential protective role of c.3944T allele. *Gene*. 2013; 517(1):55-59.
2. Ozretić P, Bisio A, Inga A, Levanat S. The growing relevance of cap-independent translation initiation in cancer-related genes. *Periodicum biologorum*. 2012; 114(4):471-478.
3. Sabol M, Car D, Musani V, Ozretic P, Oreskovic S, Weber I, Levanat S. The Hedgehog signaling pathway in ovarian teratoma is stimulated by Sonic Hedgehog which induces internalization of Patched. *Int J Oncol*. 2012; 41(4):1411-1418.
4. Levanat S, Musani V, Cvok ML, Susac I, Sabol M, Ozretic P, Car D, Eljuga D, Eljuga L, Eljuga D. Three novel BRCA1/BRCA2 mutations in breast/ovarian cancer families in Croatia. *Gene*. 2012; 498(2):169-76.
5. Beketic-Oreskovic L, Maric P, Ozretic P, Oreskovic D, Ajdukovic M, Levanat S. Assessing the clinical significance of tumor markers in common neoplasms. *Frontiers in bioscience. Front Biosci*. 2012; E4:2558-2578.
6. Musani V, Sabol M, Car D, Ozretić P, Orešković S, Leović D, Levanat S. LOH of PTCH1 region in BCC and ovarian carcinoma: microsatellite vs. HRM analysis. *Frontiers in bioscience. Front Biosci*. 2012; E4:1049-1057.

7. Maurac I, Sabol M, Musani V, Car D, Ozretic P, Kalafatic D, Oreskovic S, Babic D, Levanat S. A low grade ovarian carcinoma case with coincident LOH of PTCH1 and BRCA1, and a mutation in BRCA1. *Int J Gynecol Pathol*. 2012. 31(3):264-271.
8. Leovic D, Sabol M, Ozretic P, Musani V, Car D, Marjanovic K, Zubcic V, Sabol I, Sikora M, Grce M, Glavas-Obrovac Lj, Levanat S. Hh-Gli signaling pathway activity in oral and oropharyngeal squamous cell carcinoma. *Head Neck*. 2012. 34(1): 104-12.
9. Beketic-Oreskovic L, Ozretic P, Rabbani ZN, Jackson IL, Sarcevic B, Levanat S, Maric P, Babic, I, Vujaskovic Z. Prognostic significance of carbonic anhydrase IX (CA-IX), endoglin (CD105) and 8-hydroxy-2'-deoxyguanosine (8-OHdG) in breast cancer patients. *Pathol Oncol Res*. 2011; 17(3):593-603.
10. Maric P, Ozretic P, Levanat S, Oreskovic S, Antunac K, Beketic-Oreskovic L. Tumor Markers in Breast Cancer – Evaluation of their Clinical Usefulness. *Coll Antropol*. 2011; 35(1):241-247.
11. Car D, Sabol M, Musani V, Ozretic P, Levanat S. Epigenetic regulation of the Hedgehog-Gli signaling pathway in cancer. *Periodicum biologorum*. 2010; 112(4):419-423.
12. Ozretic P, Levacic Cvok M, Musani V, Sabol M, Car D, Levanat S. *In silico* analysis of potential structural and functional significance of human breast cancer gene BRCA2 sequence variants found in 5' untranslated region. *Periodicum biologorum*. 2010; 112(4):469-474.
13. Cretnik M, Poje G, Musani V, Kruslin B, Ozretic P, Tomas D, Situm M, Levanat S. Involvement of p16 and PTCH in pathogenesis of melanoma and basal cell carcinoma. *Int J Oncol*. 2009; 34(4):1045-1050.
14. Cvok M, Cretnik M, Musani V, Ozretic P, Levanat S. New sequence variants in BRCA1 and BRCA2 genes detected by high-resolution melting analysis in an elderly healthy female population in Croatia. *Clin Chem Lab Med*. 2008; 46(10):1376-1383.